

NACA TN No. 1495

7608



# NATIONAL ADVISORY COMMITTEE FOR AERONAUTICS

TECHNICAL NOTE

No. 1495

ANALYSIS, VERIFICATION, AND APPLICATION OF EQUATIONS  
AND PROCEDURES FOR DESIGN OF  
EXHAUST-PIPE SHROUDS

By Herman H. Ellerbrock, Jr., Chester R. Wcislo,  
and Howard E. Dexter

Langley Memorial Aeronautical Laboratory  
Langley Field, Va.



Washington  
December 1947

AFMDC  
TECHNICAL LIBRARY  
APL 2011

1495 TN-1495

... ..

**ERRATA**

NACA TN No. 1495

**ANALYSIS, VERIFICATION, AND APPLICATION OF EQUATIONS  
AND PROCEDURES FOR DESIGN OF  
EXHAUST-PIPE SHROUDS**

By Herman H. Ellerbrock, Jr., Chester R. Wcislo,  
and Howard E. Dexter

December 1947

Page 4, line 17: Redefine  $\bar{V}$  as follows:

$\bar{V}$  value of velocity such that  $\bar{\rho}\bar{V} = \rho_1 V_1 = \rho_2 V_2$ , feet per second

Page 15, line 23: Delete "velocity and." The line should then read:

If the variation of density with length in the . . .



ANALYSIS, VERIFICATION, AND APPLICATION OF EQUATIONS  
AND PROCEDURES FOR DESIGN OF  
EXHAUST-PIPE SHROUDS

By Herman H. Ellerbrock, Jr., Chester R. Wcislo,  
and Howard E. Dexter

SUMMARY

Results are presented of an investigation to develop simplified methods for designing exhaust-pipe shrouds to provide desired or maximum cooling of exhaust installations in which the dynamic pressure of flight is utilized to force the cooling air through the shroud. Design equations derived from fundamental laws of heat transfer and pressure drop are given for parallel- and counter-flow exhaust-pipe-shroud systems. The only data required for use in the design equations are the upstream temperatures and flow rates of the exhaust gas and cooling air and the upstream pressures of the cooling air. The design equations for the parallel-flow system were verified within the limits of engineering accuracy for one shroud to exhaust-pipe diameter ratio by tests of an experimental exhaust-pipe-shroud setup. The equations have no diameter-ratio limitations provided that cooling-air flow in the annulus is turbulent. The verification of these equations for one diameter ratio lends support to the belief that the equations are applicable to all practical shroud to exhaust-pipe diameter ratios for which the cooling-air flow is expected to be turbulent. Although no tests of counter-flow systems were run, the counter-flow equations are believed to be equally applicable because of their similarity to the parallel-flow equations.

For simplification of the design equations, constant values of 0.24 and 0.30 were used for the specific heats of cooling air and exhaust gas, respectively, and air properties were substituted for exhaust-gas properties in determining the heat-transfer coefficient of the exhaust gas. Calculations showed that these substitutions for the precise terms have a negligible effect on the accuracy of results obtained with the design equations.

Detailed procedures and charts for the design of shrouds are presented for both parallel-flow and counter-flow systems. These

procedures permit the determination of the proportions of an exhaust-pipe shroud that will provide desired cooling of the exhaust installation or, if desired cooling cannot be attained, permit the determination of the proportions of the shroud that will provide the maximum cooling and the values of installation temperatures that will exist with that shroud. The design procedures, based on the derived equations, are complete in themselves as regards shroud design. An example of the use of the shroud-design procedures for a four-engine bomber is included.

The equations and methods of shroud design presented are believed to be directly applicable to the design of shrouds for the tail pipes of jet engines provided that the luminosity of the gases in the tail pipe is negligible and the cooling air exits to the atmosphere. For jet-engine installations in which the luminosity of the gases is not negligible, however, the present analysis must be extended to include the heat transfer to the exhaust pipe by gas radiation. If the cooling-air exit pressure is decreased from atmospheric pressure by means of flaps or ejector pumps, the method of application of the pressure-drop relations to shroud design presented must be modified to account for the departure from atmospheric pressure at the cooling-air exit.

## INTRODUCTION

Shrouded exhaust-pipe systems are generally used in airplanes to reduce the fire hazard, to cool the exhaust pipe, to reduce the heat radiated to other components of the installation, and to cool the exhaust gas flowing to turbines. An illustration of such a system is shown as figure 1. The systems usually consist of an exhaust pipe surrounded by another pipe, with cooling air passing through the annular space formed by the pipes and reducing the temperatures of the exhaust gas and the pipes.

Although many of the necessary fundamental data have been available, the design of shrouded exhaust-pipe systems has been hampered by the lack of a coordinated rational design procedure. This difficulty has undoubtedly been one of the important reasons that shroud system trouble has been so prevalent.

The present paper is divided into two parts. The purpose of part I is to present (a) an analysis of the heat exchange and the pressure drop in parallel-flow and counter-flow exhaust-pipe shroud systems and (b) an experimental verification of the analysis for the parallel-flow system over a representative range of air- and gas-flow rates. Part II presents detailed procedures to facilitate

application of the analysis to shroud design. A summary of the necessary physical properties of air and exhaust gases, extended where necessary, is given in an appendix.

## SYMBOLS

In addition to the following definitions of symbols, a graphical representation is presented in figure 2.

- A duct cross-sectional area, square feet
- a velocity of sound, feet per second
- C constant in equations (26) and (31)
- $c_p$  instantaneous specific heat of fluid at constant pressure, Btu/(lb)(°F)
- $\bar{c}_p$  mean of instantaneous specific heats of fluid at constant pressure, Btu/(lb)(°F)
- D hydraulic diameter of duct, feet  $\left( \frac{4 \times \text{Cross-sectional area}}{\text{Wetted perimeter}} \right)$
- d diameter, feet
- $F_A$  shape modulus in radiation equation
- $F_C$  factor of compressibility  $\left( 1 + \frac{M^2}{4} + \frac{M^4}{40} \dots \right)$
- $F_E$  emissivity modulus in radiation equation
- f friction factor  $\left( \frac{\Delta p_f D}{4 \bar{q} l} \right)$ ; also used for fuel-air ratio
- g ratio of absolute to gravitational unit of mass, pounds per slug, or acceleration due to gravity, feet per second per second
- H mean total pressure, pounds per square foot
- h heat-transfer coefficient, Btu/(sec)(sq ft)(°F)

- J mechanical equivalent of heat, foot pounds per Btu (778)
- k thermal conductivity of fluid flow, Btu/(sec)(sq ft)(°F/ft)
- l length between stations, feet
- M Mach number
- m mass rate of fluid flow, slugs per second
- N any number to be raised to 0.8 and to 1.8
- n an exponent
- p mean static pressure, pounds per square foot absolute
- Q quantity of heat dissipated, Btu per second
- q mean dynamic pressure, pounds per square foot  $\left(\frac{1}{2\rho}\left(\frac{m}{A}\right)^2\right)$
- $\bar{q}$  average of upstream and downstream mean dynamic pressures, pounds per square foot
- S surface area of body through which heat is being transferred
- T mixed mean temperature, °F absolute
- t mixed mean temperature, °F
- V mean fluid velocity, feet per second  $\left(\frac{m}{\rho A}\right)$
- See Errata page in front of Report*  $\bar{V}$  average of upstream and downstream mean fluid velocities, feet per second
- W weight rate of fluid flow, pounds per second
- $Z = \frac{\bar{c}_{pe} W_e}{\bar{c}_{pa} W_a}$
- $\Delta$  denotes difference
- $\epsilon$  emissivity
- $\theta$  temperature difference, °F

- $\mu$  absolute viscosity of fluid, slugs per foot-second
- $\rho$  mean density of fluid, slugs per cubic foot (0.000583 p/T)
- $\bar{\rho}$  average of upstream and downstream mean densities of fluid, slugs per cubic foot
- $\phi$  factor depending on ratio of pipe diameters in heat-transfer equation (See equation (19).)
- $\phi'$  factor depending on ratio of pipe diameters in friction-factor equation (See equation (27).)

$$\psi = \frac{1 - Z}{\bar{c}_{pe} W_e} \left( \frac{\pi d_p^2}{\frac{1}{h_a + h_r} + \frac{1}{h_e}} \right)$$

$$\omega = \frac{1 + Z}{\bar{c}_{pe} W_e} \left( \frac{\pi d_p^2}{\frac{1}{h_a + h_r} + \frac{1}{h_e}} \right)$$

R Reynolds number

Pr Prandtl number

$\sigma$  ratio of density to standard sea-level density ( $\rho/0.002378$ )

Subscripts:

- a cooling air
- b bend
- d diffuser.
- e exhaust gas except when used with  $\Delta H$  when it refers to shroud exit
- f friction pressure drop
- h due to heating of cooling air
- i inlet duct to shroud
- m at manifold

- o free stream
- p exhaust pipe
- r denotes radiation heat transfer
- s shroud
- t total or stagnation conditions
- x refers to any station  $\bar{x}$  feet from shroud entrance
- 1 station 1
- 2 station 2
- 3 station 3
- 0-1 from free stream to station 1
- 1-2 from station 1 to 2
- 1-3 from station 1 to 3

I - ANALYSIS AND VERIFICATION  
ANALYSIS OF HEAT EXCHANGE AND PRESSURE DROP  
IN EXHAUST-PIPE-SHROUD SYSTEMS

An adequate exhaust-pipe-shroud system is one for which all parts of the system and the downstream exhaust-gas are below limiting temperatures and the pressure drop required for forcing air through the system does not exceed the pressure drop available. The analysis of such a system, consequently, requires equations for predicting design temperatures and pressure drop on the cooling-air side of the system. These equations should be in a form such that the desired temperatures and pressure losses will be a function of known conditions. The present analysis derives such equations for the usual straight annular exhaust-pipe-shroud systems for both the case of parallel flow and the case of counter flow. The simplifying assumption of straight flow is made, inasmuch as bends increase the local heat transfer and cooling-air pressure losses and therefore should be avoided. In the present analysis cooling air flows in the annular space around the exhaust pipe, which is the case usually encountered.

## Parallel Flow

Heat-exchange processes in exhaust-pipe-shroud combinations.-

The analysis for parallel flow is for the case of exhaust-gas mixture and cooling air flowing in the same direction. (See fig. 2(a).) For a parallel-flow exhaust-pipe-shroud combination with exhaust gas flowing in the inner pipe and cooling air flowing in the annular space, the mechanism of heat transfer is as follows:

- (a) Heat flows from the exhaust gas to the exhaust pipe by forced convection
- (b) Heat flows from the exhaust gas to the exhaust pipe by thermal radiation
- (c) Heat flows from the exhaust pipe to the cooling air by forced convection
- (d) Heat flows from the exhaust pipe to the shroud by thermal radiation through the cooling air which is a nonabsorbing medium
- (e) Heat is exchanged between the shroud and the cooling air by forced convection
- (f) Heat flows from the shroud to the surrounding atmosphere by natural convection

The thermal radiation from the exhaust gas to the exhaust pipe has been neglected in this analysis. By use of the radiation formulas for nonluminous gases, calculations show that this radiation is small provided that afterburning does not occur. If combustion with a luminous flame does occur, the heat transfer to the pipe will be greatly increased, and the analysis should be extended to include this effect. The heat loss from the shroud by natural convection will also be neglected. It is assumed that the heat given up by the exhaust gas is equal to that picked up by the cooling air. The fluid temperature differences for use in the convection-heat-transfer formulas are determined from the true temperatures, although for preciseness, stagnation temperatures should be used. In well-designed shrouds, however, the cooling-air velocities are low enough to make the error introduced by use of true temperatures negligible.

The design temperatures in an exhaust-pipe-shroud system with parallel flow are the downstream gas temperature  $t_{e2}$  (when a turbosupercharger is used), the exhaust-pipe temperatures  $t_p$ , and the shroud temperatures  $t_s$ . (See fig. 2(a).) In the present paper

equations are given for these design temperatures. Assumptions are made herein, which are thought to be permissible wherever it is advantageous to the simplification of the final results.

Equations for design temperatures.- The heat transfer from a hot gas to a cold gas can be represented by the equation

$$Q = \bar{h}\bar{\theta}S \quad (1)$$

where

$\bar{h}$  mean heat-transfer coefficient

$\bar{\theta}$  mean temperature difference

S surface area of body through which heat is being transferred

For the present case of the parallel-flow exhaust-pipe-shroud system it can be shown by use of information available in standard heat-transfer text books and on the basis of the assumptions given that

$$\bar{h} = \frac{1}{\frac{1}{h_e} + \frac{1}{h_a + h_r}} \quad (2)$$

where  $h_e$  and  $h_a$  are convection-heat-transfer coefficients on the gas and air sides, respectively, and  $h_r$  is the radiant-heat-transfer coefficient from pipe to shroud, and

$$\bar{\theta} = \frac{\theta_1 - \theta_2}{\log_e \frac{\theta_1}{\theta_2}} \quad (3)$$

where

$$\theta_1 = t_{e1} - t_{a1} \quad (4)$$

$$\theta_2 = t_{e2} - t_{a2} \quad (5)$$

The use of the log mean temperature difference (equation (3)) is based on the postulate that  $h_e$ ,  $h_a$ , and  $h_r$  do not vary along the tube length. The area  $S$  for the system is assumed to be

$$S = \pi d_p l \quad (6)$$

The small difference in pipe area on gas and air sides is neglected in the theory presented herein and the outer diameter of the pipe is used.

The heat lost by the exhaust gas and gained by the cooling air can be obtained by means of the following equations:

$$Q = \bar{c}_{p_e} W_e (t_{e1} - t_{e2}) \quad (7)$$

$$Q = \bar{c}_{p_a} W_a (t_{a2} - t_{a1}) \quad (8)$$

In these equations  $\bar{c}_{p_e}$  and  $\bar{c}_{p_a}$  are the integrated mean values of the instantaneous specific heats  $c_{p_e}$  and  $c_{p_a}$ , respectively, between stations 1 and 2.

By use of equations (1) to (8) the following expression can be obtained:

$$t_{e2} - t_{a2} = \frac{t_{e1} - t_{a1}}{e^\omega} \quad (9)$$

where

$$\omega = \frac{1 + Z}{\bar{c}_{p_e} W_e} \left( \frac{\pi d_p^2 l}{\frac{1}{h_a + h_r} + \frac{1}{h_e}} \right) \quad (10)$$

$$Z = \frac{\bar{c}_{p_e} W_e}{\bar{c}_{p_a} W_a} \quad (11)$$

If equation (7) is made equal to equation (8), the following expression is obtained for  $t_{a2}$ :

$$t_{a2} = Z(t_{e1} - t_{e2}) + t_{a1} \quad (12)$$

Substituting for  $t_{a2}$  in equation (9) the equivalent value given by equation (12) and solving the resulting equation for  $t_{e2}$  gives the following equation for the downstream exhaust-gas temperature:

$$t_{e2} = \frac{1}{1 + Z} \left( t_{a1} + Zt_{e1} + \frac{t_{e1} - t_{a1}}{e^{\omega}} \right) \quad (13)$$

The exhaust-pipe temperatures can be obtained with reasonable accuracy from an equation which neglects radiant-heat transfer from the exhaust pipe to the shroud. This equation is obtained by making the heat transferred by convection from the gas to the pipe equal to the heat transferred from the pipe to the cooling air for a differential length  $dl$ . (See fig. 2(a).) At any point  $x$  the equation for pipe temperature becomes

$$t_{px} = \frac{h_e t_{ex} + h_a t_{ax}}{h_e + h_a} \quad (14)$$

Equation (14) is applicable to any station if the appropriate gas and air temperatures are used. The downstream pipe temperature  $t_{p2}$  is determined from the downstream air temperature  $t_{a2}$  and gas temperature  $t_{e2}$  which are obtained from equations (12) and (13).

The shroud metal temperature at each station is assumed to be equal to the corresponding cooling-air temperature at that station in order to avoid the necessity for solving complicated analytical equations for the shroud temperatures. This assumption is conservative, for in the normal case the shroud temperature is slightly lower than the adjacent mean cooling-air temperature.

From equations (12) to (14) and the simplifying assumptions given for shroud temperatures, the design temperatures can be determined from the dimensions of the exhaust-pipe-shroud system, the

upstream temperatures, the air and gas flow rates, the specific heats of air and gas, and the heat-transfer coefficients, all of which will be known in a design problem. The equations for the heat-transfer coefficients are given in the following section.

Fundamental laws for heat-transfer coefficients.- The relation between the convection-heat-transfer coefficient, the exhaust-gas factors, and the exhaust-pipe diameter is shown in the following equation based on the law of heat transfer for turbulent flow in pipes as given in reference 1, page 168:

$$\frac{h_e d_p}{k_e} = 0.023 \left( \frac{V_e \rho_e d_p}{\mu_e} \right)^{0.8} \left( \frac{c_{p_e} \mu_e g}{k_e} \right)^{0.4} \quad (15)$$

The gas properties are determined at the bulk temperature of the fluid which to be precise should be the integrated mean temperature from station 1 to station 2. Actually, however, the bulk temperature can be taken as the temperature at the upstream station with little error in  $h_e$  because the predominating factor affecting  $h_e$ , as shown by equation (15), is the mass flow per unit area. The upstream temperature was used in the present work. If, instead of gas properties at the temperature  $t_{e1}$  being used, air properties determined at the same temperature could be used with little error, the necessity for determining the fuel-air-ratio and the hydrogen-carbon-ratio factors would be avoided and the equations would be somewhat simplified. By substitution of air properties determined at temperature  $t_{e1}$  and the equation

$$V_e \rho_e = \frac{4W_e}{\pi d_p^2 g} \quad (16)$$

in equation (15) the heat-transfer-coefficient equation for exhaust gas then becomes

$$\frac{h_e d_p}{k_a} = 0.023 \left( \frac{4W_e}{\pi d_p^2 \mu_a g} \right)^{0.8} \left( \frac{c_{p_a} \mu_a g}{k_a} \right)^{0.4} \quad (17)$$

or

$$h_e = 0.001735 \frac{k_a (Pr_a)^{0.4}}{\mu_a^{0.8} d_p^{1.8}} W_e^{0.8} \quad (18)$$

An equation similar in form to equation (15) can be used to determine the convection-heat-transfer coefficient  $h_a$  in the annular space. The diameter  $d_p$ , however, must be replaced by the equivalent (or hydraulic) diameter of the annular space  $d_s - d_p$ . (See reference 1, p. 200, and references 2 to 4.) In addition, according to reference 3, the constant 0.023 must be multiplied by a factor dependent upon the ratio of the diameters of the inner and the outer pipes. This factor is

$$\phi = \frac{2 \log_e \frac{d_s}{d_p} - \left(\frac{d_s}{d_p}\right)^2 + 1}{\frac{d_s}{d_p} - \frac{d_p}{d_s} - 2 \frac{d_s}{d_p} \log_e \frac{d_s}{d_p}} \quad (19)$$

References 1 and 2 make no mention of such a factor, but a general review of the literature on annular spaces shows an increase in heat transfer of annular spaces as compared with that of circular pipes. This factor will therefore be included in the present analysis. The Prandtl number for air  $(c_{p_a} \mu_a g / k_a)$  is about constant and equal to approximately 0.73 over a large range of inlet-air temperature. Also,  $10\mu_a$  can be substituted for  $k_a$  with little error. With the foregoing assumptions and the fact that  $V_a \rho_a g$  equals the weight rate of air flow divided by the cross-sectional area of the annular space, the equation for  $h_a$  becomes

$$h_a = 0.01528 \phi \frac{\mu_a^{0.2'}}{(d_s + d_p)^{0.8} (d_s - d_p)} W_a^{0.8} \quad (20)$$

The upstream temperature  $t_{a1}$  was used instead of the bulk temperature of the fluid to determine the air property in equation (20)

because the mass flow per unit area is the predominating factor affecting  $h_a$  and the error involved is therefore negligible.

The expression for the radiant-heat-transfer coefficient  $h_r$  is derived in the following manner: The heat transfer by radiation from the exhaust pipe to the shroud at any point  $x$  and for a differential length  $dl$  (see fig. 2(a)) can be expressed by the equation (reference 5, p. 50)

$$dQ_r = \frac{0.1728}{3600} F_A F_E \left[ \left( \frac{T_{p_x}}{100} \right)^4 - \left( \frac{T_{s_x}}{100} \right)^4 \right] \pi d_p dl \quad (21)$$

The temperatures  $T_{p_x}$  and  $T_{s_x}$  are the appropriate pipe and shroud temperatures. For the usual shroud-design problem it can be shown by means of an equation in reference 5, page 54, that the emissivity modulus  $F_E$  is not much smaller than the pipe emissivity  $\epsilon_p$ . For the simplification of the present analysis the approximation of  $\epsilon_p$  for  $F_E$  will be used hereinafter. The shape modulus  $F_A$  is a factor which allows for the geometrical position of the radiating surfaces and, for the case of an annular space, is equal to unity (reference 5, p. 54). The radiant-heat transfer must be expressed in a form similar to that for convective heat transfer to obtain the coefficient  $h_r$ ; thus

$$dQ_r = h_r (t_{p_x} - t_{a_x}) \pi d_p dl \quad (22)$$

By use of equations (21) and (22) and of factors given for  $F_A$  and  $F_E$ , the following equation for  $h_r$  can be derived:

$$h_r = \frac{0.1728}{3600} \epsilon_p \frac{\left[ \left( \frac{T_{p_x}}{100} \right)^4 - \left( \frac{T_{s_x}}{100} \right)^4 \right]}{t_{p_x} - t_{a_x}} \quad (23)$$

The convection-heat-transfer coefficients  $h_o$  and  $h_a$  have been shown to be little affected by variations of temperatures along the length and consequently were assumed constant along the length. Although the same assumption will cause appreciable inaccuracies in

the coefficient  $h_r$ ; the fact that  $h_r$  is so much smaller than  $h_a$  causes variations in  $h_r$  to affect the over-all coefficient  $\bar{h}$  very little as can be shown by means of equation (2). The assumption has been made that  $h_r$  is also constant along the pipe length. Use of the log-mean-temperature difference is based on the postulate of the constancy of the coefficients in accordance with the statement in reference 2 that the use of this temperature difference will be sufficiently accurate for such systems.

With the assumption that the radiant-heat-transfer coefficient is invariant with the length, the temperatures of the pipe, the shroud, and the air at station 1 can be used in equation (23) to determine  $h_r$ . The use of cooling-air temperature for the shroud temperature can be made as previously recommended. The pipe temperature  $t_{p1}$  is determined by means of equation (14),

Pressure loss in annular passage. The pressure loss through an annular passage consists of the friction drop, the loss due to accelerating the fluid, and the loss at the exit; thus

$$\Delta H = \Delta p_f + \Delta H_a + \Delta H_e \quad (24)$$

The friction pressure drop in an annulus (see references 1 and 5) can be expressed as follows:

$$\Delta p_f = 4f \frac{l}{d_s - d_p} \bar{q} \quad (25)$$

The friction factor  $f$  for smooth pipe varies with Reynolds number in the following manner:

$$f = \frac{C}{R^n} \quad (26)$$

Over a wide range of Reynolds number in the turbulent region for pipes of both circular and annular cross section the value of  $n$  is about 0.2. For pipes of circular cross section, the value of  $C$  is almost constant over this range and various results are in agreement as to the value. (For smooth and commercial pipes, the values of  $C$  are 0.045 and 0.054, respectively.) There is a wide dissimilarity of results for the value of  $C$  for pipes of annular cross

section. In references 1 and 2 the circular-pipe value of  $C$  is used with the Reynolds number based on the equivalent diameter. In references 3 and 4 a much higher value for  $C$  is advocated than that for circular pipes as well as use of Reynolds number based on the equivalent diameter. In reference 3, for instance, it was determined from data that the value for  $C$  of circular pipes should be increased by multiplying by the factor

$$\phi' = \frac{\frac{d_s}{d_p} + \phi}{\frac{d_s}{d_p} + 1} \quad (27)$$

For hot tests, also, no full agreement is reached as to the temperature to use in determining the properties of the fluid. Some investigators use a film temperature and others use the bulk temperature of the fluid. Finally, for pipes that are not smooth an equation in the form of equation (26) is not applicable for some ranges of Reynolds number and, even if it were applicable, the value of  $C$  would depend upon the degree of roughness. Because of the undecided status of results on annular cross-section pipes and inasmuch as the steel generally used in the shroud systems has some roughness, the friction factors in the present tests were determined experimentally in order to provide data which would be generally applicable to exhaust-pipe-shroud systems in airplane installations. The Reynolds numbers used herein were based on the equivalent diameter of the passage  $d_s - d_p$ . *See 2 note in part of Report.*

If the variation of <sup>1</sup>velocity and density with length in the annular space is assumed to be linear, the continuity equation ( $\rho_{a1} V_{a1} = \rho_{a2} V_{a2} = \bar{\rho}_a \bar{V}_a$ ) may be used to show that

$$\bar{q} = \frac{1}{4} (\bar{\rho}_a \bar{V}_a)^2 \left( \frac{1}{\rho_{a1}} + \frac{1}{\rho_{a2}} \right) \quad (28)$$

Now

$$R = \frac{\bar{\rho}_a \bar{V}_a (d_s - d_p)}{\mu_a} \quad (29)$$

and

$$\bar{\rho}_a \bar{V}_a = \frac{4W_a}{\pi(d_s^2 - d_p^2)g} \quad (30)$$

From equations (25), (26), (28), (29), and (30); therefore,

$$\Delta p_f = \left(\frac{4}{\pi g}\right)^{2-n} c \frac{4\mu_a^n W_a^{2-n}}{(d_s + d_p)^{2-n} (d_s - d_p)^3} \left(\frac{1}{\rho_{a1}} + \frac{1}{\rho_{a2}}\right) \quad (31)$$

As in the heat-transfer equation  $\mu_a$  can be determined at the temperature  $t_{a1}$  with little error resulting in  $\Delta p_f$ . This procedure is used herein.

The cooling air is heated in passing through the annular passage. This heating of the air causes a pressure drop to occur due to the expansion of the air in addition to the frictional pressure drop. The pressure drop due to the expansion of the air is a large fraction of the total pressure drop in the annular space.

The loss in total pressure due to acceleration of the air from  $V_{a1}$  to  $V_{a2}$  can be derived from equations in reference 1 as follows:

$$\Delta H_h = q_{a2} - q_{a1} \quad (32)$$

where

$$q_a = \frac{1}{2} \rho_a V_a^2 \quad (33)$$

In the derivation of equation (30), compressibility factors were neglected because they had very little effect on the differences of dynamic pressures used to determine  $\Delta H_h$ . Use of the continuity equation and equations (30), (32), and (33) leads to the following expression for  $\Delta H_h$ :

$$\Delta H_h = \frac{1}{2} \left( \frac{4}{\pi G} \right)^2 \frac{W_a^2}{(d_s + d_p)^2 (d_s - d_p)^2} \left( \frac{1}{\rho_{a2}} - \frac{1}{\rho_{a1}} \right) \quad (34)$$

In equation (34) the constant factors reduce to 0.000781.

An exit loss from the shroud to the free-air stream is also present. Inasmuch as the velocities in the shroud are appreciable, it is assumed that all the velocity pressure is lost at the exit. The assumption is also made that  $p_{a2}$  equals the atmospheric pressure which generally is, or is close to, the existing condition. Then

$$\Delta H_e = q_{a2} = \frac{0.000781 W_a^2}{(d_s + d_p)^2 (d_s - d_p)^2 \rho_{a2}} \quad (35)$$

The sum of the pressure drop due to heating of the air and the pressure drop for the exit loss can be expressed in the following form:

$$\Delta H_h + \Delta H_e = 2q_{a2} - q_{a1} \quad (36)$$

This expression becomes, through use of equations (34) and (35),

$$\Delta H_h + \Delta H_e = \frac{0.3284}{\sigma_{a1}} \frac{W_a^2}{(d_s + d_p)^2 (d_s - d_p)^2} \left( \frac{\rho_{a1}}{\rho_{a2}} - 1 \right) \quad (37)$$

where

$\sigma_{a1}$  ratio of  $\rho_{a1}$  to standard density at sea level

$$\left( \rho_{a1} / 0.002378 \right)$$

The total pressure loss in the exhaust-pipe-shroud system, exclusive of any losses up to the beginning of the annular passage,

will then be the summation of the losses given by equations (31) and (37) as shown by equation (24).

#### Counter Flow

Equations for design temperatures.- In the case of counter flow the downstream exhaust-gas temperature  $t_{e2}$  and the temperatures at station 1 of the exhaust pipe and shroud  $t_{p1}$  and  $t_{s1}$ , respectively, (fig. 2(b)) will be the design temperatures for which an adequate system must be obtained. For counter flow,  $t_{a1}$  is the outgoing-air temperature and  $t_{a2}$  is the incoming-air temperature. (See fig. 2(b).)

Equations (9), (12), and (14) are applicable to the case of counter flow with the following exceptions:

(a) Exponent  $\alpha$  is replaced with  $\psi$  where

$$\psi = \frac{1 - Z}{\bar{c}_{pe} W_e} \frac{\pi d_p l}{\frac{1}{h_a + h_r} + \frac{1}{h_e}} \quad (38)$$

(b) In equation (12),  $t_{a1}$  is interchanged with  $t_{a2}$ . Substitution of the equation for downstream air temperature in equation (9) for counter flow results in the following expression for  $t_{e2}$ :

$$t_{e2} = \frac{t_{a2}(1 - e^\psi) - t_{e1}(1 - Z)}{Z - e^\psi} \quad (39)$$

The design temperature  $t_{p1}$  is obtained by use of equation (14), the upstream gas temperature  $t_{e1}$ , and the downstream air temperature  $t_{a1}$ . To determine the shroud temperature  $t_{s1}$  analytically involves complications similar to those in the case of parallel flow. Consequently, the method of designing for air temperature  $t_{a1}$  in place of shroud temperature  $t_{s1}$  used in parallel flow will also be used in the case of counter flow.

As in the case of parallel flow the following assumptions are made for counter flow:

(a) The heat-transfer coefficients are constant along the pipe length. Equations (18) and (20) are, therefore, applicable for evaluating  $h_e$  and  $h_a$ .

(b) The upstream gas temperature  $t_{e1}$  can be used to evaluate the air properties in equation (18).

(c) The upstream air temperature  $t_{a2}$  can be used to evaluate air viscosity in equation (20).

The radiant-heat-transfer coefficient  $h_r$  is evaluated by use of equation (23), the pipe temperature  $t_{p2}$ , and the temperature  $t_{a2}$  for both the air and shroud temperatures. A trial-and-error solution necessitated by the use of  $t_{e2}$  in equation (14) to evaluate  $t_{p2}$  for use in the  $h_r$  equation is avoided by the substitution of  $t_{e1}$  in place of  $t_{e2}$ . Since the gas temperature drop is small, this substitution will cause little error in the calculated design temperature  $t_{e2}$ .

Pressure drop.- Equations (24), (31), (34), (35), and (37) are applicable for the determination of pressure drop for the counter-flow case with the following exceptions:

(a)  $\sigma_{a1}$  is replaced with  $\sigma_{a2}$ .

(b)  $\mu_a^{0.2}$  is evaluated at temperature  $t_{a2}$ .

(c)  $\rho_{a1}$  is interchanged with  $\rho_{a2}$ .

#### EXPERIMENTAL VERIFICATION OF PARALLEL-FLOW EQUATIONS

Heat-transfer and pressure-drop tests were made with an experimental exhaust-pipe-shroud setup for parallel flow in order to verify the final parallel-flow design equations (12), (13), (14), (31), and (34). A further purpose was to determine the degree of conservatism of using air temperature for shroud temperature.

### Exhaust-Pipe-Shroud Setup

Exhaust-pipe-shroud flow system.- The test equipment consisted essentially of an experimental exhaust-pipe-shroud test section, an aircraft engine, and a source of cooling air. A diagrammatic sketch of the entire system is shown in figure 3.

The test section consisted of two concentric pipes 20 feet long. The outside pipe or shroud was made of black iron with an 11-inch inside diameter; the inner or exhaust pipe was made of stainless steel with a  $6\frac{3}{16}$ -inch outside diameter. The shroud was covered with a 3-inch thickness of rock wool, and the entire test section was then surrounded with a metal shield to protect it from the blast of the propeller on the engine. The pipes were centered at both ends of the test section and were spaced at the midpoint by three small steel fins which were welded radially to the exhaust pipe with enough clearance to provide for expansion of the exhaust pipe and shroud at high temperatures.

An Allison V-3420-11 engine was utilized as the exhaust-gas producer. Expansion between the engine and the test section and engine vibrations were absorbed by four stainless-steel expansion joints welded in the exhaust pipe.

The shroud cooling air was supplied by a centrifugal blower provided with a bell-shaped inlet and a 40-mesh copper screen at the blower outlet to reduce air-flow pulsations to a minimum. A 12-inch radial-vaned flow straightener was placed 1-foot downstream of the discharge as a precaution against whirl in the air flow, and a venturi 10 diameters below the blower outlet measured the cooling-air flow. The cooling air had to be conducted around a bend of about  $135^\circ$  before it entered the test section. In order to reduce the bend loss, the diameter of the pipe from the venturi to the bend was gradually increased. A 40-mesh copper screen placed at the end of the bend and a radial-vaned flow straightener placed in the contracting section were required in order to insure a good distribution of the cooling-air velocity and total pressure at the entrance to the test section. The cooling air was discharged at the end of the test section through a diffuser to decrease the exit loss and consequently to release a larger quantity of the available blower pressure for forcing air through the system.

Instrumentation.- The instrumentation installed in each of the stations is illustrated in figure 4. The three stations were numbered from the upstream end of the test section and spaced as follows: 9.9 feet from station 1 to station 2 and 10 feet from station 2 to

station 3. The relative location of all the thermocouples and pressure tubes at a typical station is shown in figure 5. All instruments at each station were mounted in one plane perpendicular to the axis of the pipes at  $120^\circ$  intervals.

All temperatures were measured with chromel-alumel thermocouples in conjunction with a Brown self-balancing potentiometer. Exhaust-gas temperatures were measured with two radiation-shielded inconel-covered thermocouples per station which were located near the center of the exhaust pipe. Average exhaust-pipe temperatures were measured at each station with two thermocouples spot welded to the outside of the exhaust pipe. These thermocouples were placed radially in line with the exhaust-gas thermocouples to produce a minimum blocking effect in the annular space. Three thermocouples were spot welded to the outside of the shroud at each station, and one thermocouple was placed midway between the stations for an average station temperature and a representative temperature gradient down the pipe. Cooling-air temperatures were measured with three radiation-shielded-traversing thermocouples per station. All thermocouples were calibrated before and after the tests.

Three rakes were installed radially in the annular space at each station. Each rake consisted of four shielded total-pressure tubes, one unshielded total-pressure tube, and one static-pressure tube; the static-pressure tube was nearest the exhaust pipe. The shield had to be removed from the total-pressure tube nearest the static-pressure tube as the shield was responsible for disturbing the air flow over the static-pressure tube. Three wall static-pressure orifices were also installed at each station.

The flow of the exhaust gas was obtained by measuring the engine charge air with a calibrated venturi and by measuring the fuel flow with a rotameter. The gasoline used in the tests was 100-octane grade 130 aromatic fuel, specification AN-F-28 with a hydrogen-carbon ratio of approximately 0.17.

### Tests

Isothermal pressure-drop tests.- One test (test A) was made to determine the pressure drop in the annular space with only air passing through the system. These runs were made to establish the friction formula inasmuch as the measured pressure differences were about equal to the friction losses; the momentum loss due to change in density was negligible with no heat present. The speed of the cooling-air blower was varied so that the range of Reynolds number, based on the equivalent diameter of the annular space, was from about 100,000 to 324,000. Pressure equilibrium was determined for all observations from line plots.

Heat-transfer tests.- Four series of runs were made to include an appreciable range of Reynolds and Prandtl numbers with both cooling air and exhaust gas flowing in the system. A tabulation of approximate values of the variables involved in the isothermal and heat-transfer tests is shown in table 1.

The effect of Prandtl number on the gas and air heat-transfer coefficients was obtained by varying the fuel-air ratio over a range from 0.063 to 0.090 while Reynolds number on the gas and air sides of the exhaust pipe was held constant (test B). This variation of fuel-air ratio gave a large variation in gas temperature.

The effect of exhaust-gas Reynolds number on the heat-transfer coefficient of the exhaust gas was established over a large range of Reynolds number in two tests. While the fuel-air ratio and cooling-air Reynolds number were held constant, the engine power was varied to obtain a variation in exhaust-gas Reynolds number. In one test (test C<sub>1</sub>) the exhaust-gas Reynolds number was varied from approximately 120,000 to 220,000 at a constant cooling-air Reynolds number of 170,000. In the other test (test C<sub>2</sub>, a continuation of C<sub>1</sub>) the exhaust-gas Reynolds number was varied from 215,000 to 360,000 at a constant cooling-air Reynolds number of 250,000.

The effect of the cooling-air Reynolds number on the heat-transfer coefficient of the cooling air was obtained in test D by varying the Reynolds number over a range from 170,000 to 280,000 while the exhaust-gas Reynolds number and the fuel-air ratio were held constant. The cooling-air Reynolds number was varied by varying the air flow by means of the blower.

The cooling-air pressure differences were obtained in each of the four heat-transfer tests to compare these results when an appreciable momentum pressure loss was present with the results of the isothermal tests and to determine the applicability of the friction formula established in the isothermal tests. The extensive range of Reynolds number obtained in test D provided for a large range of pressure drop.

Temperature traverses of the annular space at each station and pressure and temperature equilibrium from line plots were obtained for all observations.

A comparison of exhaust-gas samples upstream and downstream of the test section showed that no afterburning occurred in the exhaust pipe.

#### Methods

Verification of shroud-design equations.- The method of checking the equations for the design temperatures and pressure drops was to

compare the values measured in the tests with the values calculated by means of the equations, the measured values of temperatures at the upstream station, and the flow rates. In the present tests no exit loss was involved and calculated values of  $(\Delta p_f + \Delta H_h)$  were compared with measured values. The degree of conservatism of the method of designing for limiting air temperatures rather than for limiting shroud temperatures was obtained by comparing the measured air temperatures with the measured shroud temperatures.

The calculated values of temperatures required determination of the heat-transfer coefficients  $h_a$ ,  $h_r$ , and  $h_e$ . Equation (20), equation (23), and methods outlined in the section entitled "Fundamental laws for heat-transfer coefficients" were used to calculate the convection coefficient on the air side  $h_a$  and the radiant-heat-transfer coefficient  $h_r$ .

The emissivity of the exhaust pipe, which was required in evaluating  $h_r$ , and the emissivity of the shroud were obtained from reference 5. This reference shows values of 0.79 for oxidized steel and a selected value of 0.70 for stainless steel (8 percent nickel, 18 percent chromium).

For all tests both equations (15) and (18) were used to calculate the convection-heat-transfer coefficient  $h_e$ , and temperatures obtained by use of the values calculated from each equation were compared to determine the effect of using air properties in place of gas properties. The appropriate temperatures used for determining the properties were given in the section on "Fundamental laws for heat-transfer coefficients." The properties were obtained from the appendix. A check was made for a few tests of the error involved in the calculated temperatures by use of 0.30 and 0.24 for  $\bar{c}_{p_e}$  and  $\bar{c}_{p_a}$ , respectively, rather than the integrated mean values of specific heats.

The measured values of air and exhaust-gas temperatures at station 1 and the weight-flow rates of air and gas were substituted in equation (13) in order to calculate the downstream exhaust-gas temperatures. Measured values of air and gas temperatures at station 1 and calculated values of these temperatures at the downstream stations were used to calculate pipe temperatures by means of equation (14). The air temperatures at the downstream stations were calculated from equation (12) and calculated values of downstream-gas temperature.

The friction factors were obtained first for the data of the isothermal tests (table 1) by use of equation (25) and were plotted

against Reynolds number. It was determined from this plot whether the simple exponential variation of equation (26) is valid and, if such were the case, whether the values of  $C$  and  $n$  may be used. Values of the friction factor  $f$  or of  $C$  and  $n$  from the isothermal tests were then available to calculate  $\Delta p_p$  for the heat-transfer tests with either equation (25) or equation (31). Equation (34) was used to calculate  $\Delta T_n$  in the heat-transfer tests. Values of calculated downstream air temperatures were used to calculate downstream air densities for use in the formulas.

Verification of the design formulas was accomplished by comparing the foregoing calculations with the measured values at both station 2 and station 3; station 1 was used as the upstream station in both cases. The appropriate pipe length was used in the formulas in each case.

Integrated mean temperatures and pressures.- As a result of the large temperature gradient of the cooling air in the annular space true mean air temperatures and pressures could only be obtained by integrating the measured pressure- and temperature-distribution curves across the annulus. The integration of all the data obtained in the tests would have involved a vast amount of labor and time which did not seem warranted. Consequently, a method was developed for correcting arithmetic averages. For test D mean values of the measured air temperatures were obtained for the three stations on both an integrated and an arithmetic basis. The arithmetic values were plotted against the integrated values and the resulting straight-line curves were used to correct the arithmetic averages of the measured air temperatures for all of the other tests. In all plots presented for the comparison of calculated and measured values, the results are based on these corrected arithmetic-mean measured air temperatures.

In order to integrate the air temperatures of test D with the individual measured temperatures weighted according to the local weight rate of flow, the static and total pressures as well as the temperatures at each local point must be known. When the pressure and temperature distributions in the annular space were plotted, some doubt arose as to the correct profile for the curves from the tube and thermocouple positions nearest the walls of the pipes to the walls inasmuch as the nearest pressure and temperature readings were about  $\frac{3}{8}$  inch from the walls of the pipes. As a consequence, the pressure-distribution curves in the vicinity of the walls of the annular space for the isothermal tests were obtained by applying methods available in reference 6 for obtaining velocity profiles in pipes and by using a uniform temperature gradient across the space.

In the heat-transfer tests the temperatures in the vicinity of the exhaust-pipe and shroud walls which were required to apply the methods of reference 6 were not available. The pressure-distribution curves were therefore faired approximately like those of the isothermal tests.

In order to determine the effect of this fairing on the integrated temperature average, one run of test D was obtained from another fairing in which the pressure-distribution curve was extended much closer to the pipe walls. The temperatures obtained from a survey nearest a pressure rake (see fig. 5) were used in conjunction with the pressures of that rake to obtain the integrated-temperature averages at the pressure-rake location. The error involved in the integrated air temperatures by using such noncoinciding temperatures was also checked by computing one run of test D by use of temperatures obtained from cross plots of the temperature test data at points coinciding with the pressure-tube locations. The temperature-distribution curves for test D from the point of reading nearest the walls to the walls for any survey were determined by a trial-and-error process by use of information from reference 6 and the pressure-distribution curves obtained as previously explained.

Only the temperatures at the center of the exhaust pipe were obtained at each station because of practical difficulties and also because, in turbulent flow in a circular pipe, the mean temperature is very close to the center temperature. The center values were therefore used for the mean values.

The integrated-pressure averages at each station for test D were obtained by weighting the individual pressure and temperature values according to the local weight rate of flow. The required individual pressure and temperature values were obtained from the distribution curves described in the section entitled "Verification of shroud-design equations." For one run of test D the integrated values for each station were obtained for each of the three types of fairing described in the foregoing paragraphs. Pressure losses were then compared by using both the integrated- and arithmetic-measured pressure averages. For tests other than test D, only arithmetic averages of the measured pressures were used to calculate the losses.

Inasmuch as a few thermocouple failures resulted in the loss of some of the temperature data, the missing temperature values were determined by assuming a heat balance between the gas and the cooling air. The prohibitive time element involved in repeating tests until a complete set of temperature data was obtained was considered to be adequate justification for this procedure.

### Comparison of Experimental and Calculated Values

The comparisons of temperatures and pressures drops calculated by using the theoretical equations with measured values will be given in the following sections. A 45° line is drawn on each part of each figure presented. When the plotted data fall on these lines, perfect agreement between the measured and calculated values is indicated. The results of the calculations to determine the effects of using air properties for gas properties in the equation for gas convection-heat-transfer coefficient  $h_e$ , the constant specific-heat values, the arithmetic pressure averages to determine pressure losses, and the three types of fairing of pressure- and temperature-distribution curves for the annular space are given first inasmuch as they had a direct bearing on the workup of the remaining results.

Effects of approximations and fairing methods. - The effects of the different fairing methods and the approximations to simplify the computations on the calculated design temperatures and pressure losses can be obtained from table 2. In this table the percent difference between the approximate values and precise values or percent difference between the results based on methods of reference 6 and results based on other fairing methods are given.

Comparison of calculated values of downstream exhaust-gas temperatures, cooling-air temperatures, and exhaust-pipe temperatures obtained by use of values of  $h_e$  based on air properties at temperature  $t_{e1}$  with values of temperatures obtained by use of values of  $h_e$  based on gas properties at temperature  $t_{e1}$  showed negligible differences in the gas and air temperatures and only small differences in the pipe temperatures. (See table 2.) The pipe temperatures based on air properties were about 4 percent lower than those based on gas properties. Consequently, comparisons of calculated temperatures and measured values presented hereinafter have used a value of  $h_e$  based on air properties to determine the calculated values.

The calculations to determine the effect of using constant values of specific heats in place of integrated mean values showed that no noticeable error was introduced in the values of calculated design temperatures. (See table 2.) In the following results, constant values of specific heats were therefore used to calculate the temperatures.

The integrated station pressure averages obtained from the three types of fairing differed to some extent, but the resulting station-to-station pressure losses agreed very well. (See table 2.) Also, the pressure losses for test D based on the arithmetic averages

of measured pressures were in excellent agreement with losses based on integrated averages of measured pressures. This agreement was considered sufficient justification for the procedure of using the arithmetic averages of the measured pressures to determine the measured pressure losses.

The three types of fairing resulted in slightly different integrated mean air-station temperatures, but these differences and their consequent effect on the results from the design equations (table 2) were not significant enough to warrant basing the integrated mean air temperatures on any other than the original fairing described in the methods. The original fairing method was consequently used to determine the integrated air temperatures for all of the runs of test D.

With regard to the comparison of arithmetic and integrated average temperatures, the following results of test D may be of interest to other investigators:

(a) Measured air temperatures based on arithmetic averages were about 5 percent higher than those based on integrated averages.

(b) Calculated downstream exhaust-gas temperatures based on arithmetic averages were about 1 percent higher than those based on integrated averages.

(c) Calculated downstream air temperatures based on arithmetic averages were about 4 percent higher than those based on integrated averages.

Downstream exhaust-gas temperatures.- A comparison of the calculated downstream exhaust-gas temperatures with the measured temperatures for stations 2 and 3 is given in figure 6. The calculated temperatures are less than  $1\frac{1}{2}$  percent lower than the measured values.

This small difference probably results either from determining the heat-transfer coefficients for use in equation (13) by the methods outlined or from errors of measurement. A conclusion is drawn that the design equation (13) and the simplified equations for heat-transfer coefficients for determining the downstream exhaust-gas temperature are satisfactorily verified.

Exhaust-pipe temperatures.- The comparison of the calculated exhaust-pipe temperatures with the measured temperatures for the three stations are presented in figure 7. At station 1 the calculated temperatures average about 3 percent lower than the measured values. Corresponding values for stations 2 and 3 are approximately 5 percent and 4 percent lower, respectively. The difference between

the calculated and measured values at station 1 is probably due to the fact that the pipe-temperature equation was derived by assuming that the radiation was negligible, which tends to make the calculated values higher than the measured values. An opposite effect is created by using the heat-transfer coefficient  $h_e$  based on air properties rather than on gas properties; this substitution has a tendency to reduce the pipe temperatures. The difference between the calculated and measured downstream temperatures may be a cumulative effect caused (1) by using calculated exhaust-gas temperatures which are lower than the measured values, (2) by using calculated air temperatures which are higher than the measured values, (3) by neglecting radiation, and (4) by using air properties in the equation for value of  $h_e$ . The first and fourth factors tend to decrease and the second and third factors tend to increase the calculated exhaust-pipe temperatures. From figure 7 it is concluded that exhaust-pipe temperatures, predicted from equations of the type of equation (14) with air properties used throughout in the heat-transfer-coefficient formulas, will be from 3 to 5 percent too low. The verification is still acceptable, however, within the limits of engineering practicability.

Cooling-air temperatures.- The calculated downstream cooling-air temperatures deviate about 3 to 4 percent from the measured values as shown by figure 8. This difference is attributed to the fact that the calculated exhaust-gas temperatures used in equation (12) were about  $1\frac{1}{2}$  percent lower than the measured values. In the lower range of temperatures at station 2 the calculated temperatures are higher than the measured values whereas in the higher range the opposite is true. At station 3 the calculated values are in general higher than the measured values. The use of gas properties instead of air properties would not have appreciably changed the result given in figure 8 because such a substitution had a negligible effect on the calculated downstream exhaust-gas and air temperatures. Although the difference between the calculated and measured air temperatures is rather large, the proposed method apparently leads to the prediction of conservative values of downstream air temperatures. The use of equation (12) and methods given to predict air temperatures are therefore considered satisfactory for shroud design purposes.

Relation of measured shroud temperatures to measured cooling-air temperatures.- Inasmuch as the analysis uses as a design criterion the cooling-air temperature rather than the shroud temperature, these two temperatures should be compared. The results of this comparison are shown in figure 9. The shroud temperature was about 20° F. higher than the corrected arithmetic mean cooling-air temperature at station 1,

about 20° F lower at station 2, and 40° F lower at station 3. The shroud temperature also increased from the upstream station to the downstream stations. Inasmuch as the calculated downstream air temperatures were in general higher than the measured air temperatures, the procedure of using the air temperature as a design criterion will result in a very conservative design for the shroud temperatures.

Determination of constants in friction-pressure-drop equation.-

The friction factors for the isothermal tests were plotted against Reynolds number of the cooling air on logarithmic coordinates (fig. 10) and the values of  $C$  and  $n$  for use in equation (31) were found to be 0.07 and 0.20, respectively. The exponent  $n$  is approximately the value obtained for straight pipes but the value of  $C$  is high as compared with values obtained for smooth and commercial pipes (0.046 and 0.054, respectively, reference 1). Although in references 3 and 4 higher values of  $C$  are advocated for annular spaces than for pipes, the value of  $C$  determined for the diameter ratio of the test setup on the basis of equation (27) was calculated to be 0.058, which is still lower than the value of 0.07 determined experimentally. Consequently, it is believed that indeterminate pipe roughness was probably a factor influencing the value of  $C$ . Inserting the values of  $C$  and  $n$  in equation (31) gives the following expression for  $\Delta p_f$ :

$$\Delta p_f = \frac{0.0879}{\sigma_{a1}} \frac{\mu_a^{0.2}}{(d_s + d_p)^{1.8} (d_s - d_p)^3} \left(1 + \frac{\rho_{a1}}{\rho_{a2}}\right) w_a^{1.8} \quad (40)$$

Cooling-air pressure losses for heat-transfer tests.- The data of figure 11 show the comparison of the calculated and measured cooling-air pressure losses from stations 1 to 2 and stations 1 to 3 for the heat-transfer tests. The isothermal data are also plotted in figure 11 as a check on the calculations. Perfect agreement between the calculated and measured pressure losses is obtained for the isothermal data, as indicated by the plotted points which fall along the 45° lines, because the  $C$  and  $n$  values used to calculate the friction pressure drops were obtained from the measured pressure drops.

The calculated values of the pressure loss averaged about 10 percent higher than the measured values for the heat-transfer tests. This difference is due partly to a slight overestimation of the heating- and friction-pressure losses from equations (34) and (40)

since these equations are very sensitive to downstream air temperatures, which have previously been shown to have been overestimated by about 3 or 4 percent. The difference between the calculated and measured pressure losses for the heat-transfer tests is in the conservative direction, as was the calculated cooling-air temperature, and therefore a design based on the equations will be conservative.

#### GENERAL DISCUSSION

The cooling-air flow rates and the ratios of the cooling-air flow rates to exhaust-gas flow rates used in the experiments were much higher than those usually encountered in flight. These rates and ratios were used because errors in measurement are reduced when larger quantities are involved and because the flow rates in flight are in the turbulent-flow region as were those of the experiments. Moreover, the laws of heat transfer and pressure loss in pipes established in a certain range of the turbulent-flow region are generally applicable with little error to other ranges in the region. For the latter two reasons and because, in general, the design formulas for parallel-flow systems were verified in the experiments, it is believed that the design formulas will be applicable to flight. In a calculation of a shroud design the fact that the pressure loss will be overestimated will result in the calculated temperatures being more nearly equal to the actual temperatures than in the experimental results.

Since the equations have no diameter-ratio limitation provided that the cooling-air flow in the annulus is turbulent, the verification of the parallel-flow equations for one ratio of shroud diameter to exhaust-pipe diameter lends support to the belief that these equations are applicable to all practical values of the ratio of shroud diameter to exhaust pipe diameter for which the cooling-air flow is expected to be turbulent. Although no counter-flow tests were run, the counter-flow equations are believed to be equally as applicable to design problems as the parallel-flow equations because of their similarity. In the analysis the assumption that the downstream shroud temperature would always be a little less than the downstream cooling-air temperature was made for the case of parallel flow and the case of counter flow. The validity of this assumption was verified for parallel flow by experimental data. In the case of counter flow, however, the temperatures of the exhaust gas, the exhaust pipe, and the cooling air are highest at the downstream station of the shroud. It may be possible, therefore, because of radiation from the exhaust pipe and because of the small temperature differential between the cooling air and the shroud that the shroud temperature may be higher than the cooling-air temperature at the downstream

station. Thorough exploration of this possibility would require either a complex analysis or further testing, both of which were outside the scope of the present investigation.

One problem of immediate importance for which the equations derived in this paper should be applicable is the design of shrouds for the tail pipes of jet engines. The design equations will be applicable without modification if the luminosity of the gases is negligible. If luminosity of the gases is appreciable, the analysis will require extension to account for the heat transfer from the exhaust gas to the exhaust pipe by thermal radiation. If flaps or ejector pumps are used, and the cooling-air exit pressure is thus decreased from atmospheric, the application of the pressure-drop relation to shroud design must include methods for determining this cooling-air exit pressure.

Further research is needed to establish definitely the basic laws of heat transfer and pressure losses in annular spaces, especially with respect to the fluid temperatures and constants that should be used. The principal source of difficulty in the determination of such laws is the temperature gradient of the cooling air. In addition, investigation of pressure losses in annular bends would be a great aid in predicting accurately the pressure drops in specific exhaust-pipe-shroud installations. Finally, the extension of the present work to include tests of shrouded tail pipes for jet-engine installations would be desirable.

#### SUMMARY OF RESULTS

The design equations for predicting shrouded exhaust-pipe-installation temperatures for parallel-flow systems were verified within the limits of engineering requirements by tests of an experimental exhaust-pipe-shroud setup for one ratio of shroud diameter to exhaust-pipe diameter. A comparison of measured values with values calculated by use of the design equations based on constant values of specific heats of exhaust gas and cooling air, air properties, and corrected mean air temperatures showed that:

(a) The calculated values of downstream exhaust-gas temperatures generally were never more than  $1\frac{1}{2}$  percent lower than the measured values.

(b) The calculated values of exhaust-pipe temperatures generally were lower than the measured values by not more than 5 percent.

(c) At the downstream stations the calculated cooling-air temperatures were above the measured shroud temperatures.

(d) Conservative values of cooling-air total-pressure losses were obtained with the pressure-drop equation. The calculated values of total-pressure loss were about 10 percent higher than the measured values.

The use of constant values of 0.24 and 0.30 for the specific heats of cooling air and exhaust gas, respectively, and the substitution of air properties for exhaust-gas properties for determining the heat-transfer coefficient for the exhaust-gas in the design equations resulted in a negligible change in the values of calculated exhaust-gas and cooling-air temperatures and only a slight decrease in the values of calculated exhaust-pipe temperature.

## II - PROCEDURES FOR SHROUD DESIGN

### GENERAL DESIGN CONSIDERATIONS

The problem of shroud design requires the determination of the diameter of the shroud for which certain design-installation temperatures will not exceed specified limits when the pressure drop available for forcing air through the system is known. In order to provide satisfactory cooling for all operating conditions, the shroud must be designed for the flight condition in which the cooling requirements are the most difficult to meet; generally, this condition will be maximum power (climb) at rated altitude.

An analytical method for determining the shroud diameter with a minimum of pressure loss in order not to exceed a limiting temperature such as that given in detail for the case of intercooler design in reference 7 could theoretically be developed. Such methods are impractical if not almost impossible with the complex equations which were derived in the analysis, and, consequently, graphical solutions were used.

The general procedure for design is, for a given length of shroud, to use the equations to determine the design temperatures and the cooling-air pressure drop. A value of shroud diameter is assumed and calculations are made for several assumed values of cooling-air-flow rate. These calculations are repeated for other assumed values of shroud diameter. Curves of the significant design temperatures are plotted against cooling-air-flow rate for each shroud diameter assumed. From these curves the value of cooling-air flow rate for each shroud diameter giving a temperature equal to one

of the imposed limit temperatures and lower than all the other limiting values is noted. Each of these combinations of shroud diameter and cooling-air-flow rate for which choking does not occur ( $Ma_2 < 1.0$ ) is then used to calculate the pressure loss in the shroud. A plot of this pressure loss against shroud diameter is made and compared with the pressure available for forcing air through the shroud system. Any shroud diameter for which the pressure loss required is less than that available will give adequate cooling. The diameter to choose will be that diameter which will give the greatest available pressure loss, unless this diameter causes excessive cooling drag. When the latter condition occurs the diameter to choose is that for which cooling drag is a minimum.

When the pressure drop required is greater than that available and augmentation methods fail to increase the available pressure drop sufficiently, the shroud may be divided into shorter segments so that two or more cooling-air entrances and exits are provided as diagrammed in figure 12. The shorter-length segments require less pressure drop than the single-segment design. Due to the complexity of the duct systems involved, no more than two segments will generally be used. If the limits imposed on the design installation temperatures cannot be met with a shroud system of practical size or number of segments for the pressure drop available, some alternatives are available and will be discussed in a section to follow.

The choice of the size of the inlet duct carrying the cooling air from the free stream to the shroud inlet is important and is interrelated with the shroud design, because part of the dynamic pressure of flight is utilized to overcome the losses in this duct and thereby a decrease is caused in the pressure drop available for cooling in the shroud. The choice of size, within practical limits, is such that no appreciable gain in pressure drop available is obtained with further increase in the area of the duct.

Detail step-by-step procedures for the design of a shroud are given for the following systems:

- (a) Single-segment system for parallel flow
- (b) Single-segment system for counter flow
- (c) Multisegment system for parallel or counter flow

In order to expedite use of these procedures methodical calculation forms for parallel flow and counter flow are given in tables 3 and 4, respectively. In addition, table 5 and figures 13 to 16 are given to simplify the calculations. The design procedures are concerned

with step-by-step explanation of how these calculation forms are used to design a shroud for a specific installation. Figure 2 illustrates the symbol notation in the shroud-system sketch.

A typical example has been solved for an installation of a four-engine bomber and results are listed coincidental to the discussion of the procedures. The numerical calculations are included in table 3 and pertinent values are given in the discussion of the procedures. The example uses a straight exhaust-pipe-shroud system for parallel flow with the exhaust gases being delivered to the turbine of the turbosupercharger through a single, straight exhaust pipe. A straight inlet duct of constant cross-sectional area has also been assumed. Temperature limits were specified for all the design installation temperatures for illustrative reasons. In an actual design problem, however, the design installation temperatures for which limits must be specified are peculiar to each installation.

#### SUPPLEMENTARY THEORETICAL CONSIDERATIONS

Certain derivations, other than those given in the analysis presented, are required in the procedures in order to design a shroud system. The methods of determining the cooling-air weight rate of flow at which choking occurs at the shroud exit (designated herein the choke factor), the cooling drag, and the pressure, temperature, and available pressure drop at the shroud entrance must be considered. The discussion of these factors follows.

**Choke factor.**— The method in the parallel-flow design procedures for determining the cooling-air weight rate of flow at which choking occurs in the shroud system is dependent on a relation obtained from compressible-flow theory. With the assumption that no heat is added to the air in the inlet duct and that no friction drop occurs in the annular space of the shroud-pipe system, a relation between the ratio of the air stagnation temperatures at the shroud exit  $T_{a2_t}$  and shroud inlet (assumed equal to  $T_{0t}$ ) and the choke factor

$1.384W_a \frac{\sqrt{T_{0t}}}{(d_s^2 - d_p^2)H_{a1}}$  can be obtained from compressible-flow

theory for Mach numbers at the shroud exit up to 1.0. Data for curves of this relation were calculated for downstream cooling-air Mach numbers of 0.6, 0.7, and 1.0.

The given procedure for design is to determine the cooling-air flow rate for which the choke factor is at its limiting value based

on a downstream cooling-air Mach number of 0.6 instead of 1.0. The value of  $W_a$  so obtained is not the maximum value that will exist in the shroud before choking occurs; however, the use of the choke-factor curve for a Mach number of 0.6 is recommended for the following reasons: (1) The pressure drop will increase with Mach number. (2) The shroud-exit pressure losses are smaller for lower values of  $Ma_2$ , thereby increasing the pressure drop available in the shroud for cooling purposes. (3) The limiting choke factor is overestimated by the stagnation-temperature ratio relation because the latter relation is based on the assumption that no friction occurs in the annulus. (4) The pressure-drop and heat-transfer formulas are more applicable at low cooling-air exit Mach numbers than at high cooling-air exit Mach numbers. At  $Ma_2$  equal to 0.6 or less the assumption of cooling-air exit static pressure equal to the free-stream static pressure, which is used in the pressure-drop formulas, and of the heat-transfer equation being based on true temperatures instead of stagnation temperatures (the latter being the correct temperatures to use) will lead to little error in the results. At the present time some aircraft shrouded exhaust-pipe systems are not cooling satisfactorily, possibly because they are at the choking limit.

Cooling drag.- When more than one shroud diameter will provide adequate cooling of the installation the best selection of the shroud diameter would be the one giving the lowest cooling drag if this drag is appreciable as noted in the foregoing general considerations. The drag power is obtained from the formula

$$\text{Drag power} = \frac{W_a v_o}{g} (v_o - v_2) \quad (41)$$

where the velocity  $v_o$  is that of the free stream, the velocity  $v_2$  is that at the shroud exit, and the value of  $W_a$  corresponds to the value of  $d_s$  selected.

Pressure at shroud entrance.- The total pressure at the shroud entrance is determined by the following equation:

$$H_{a1} = H_o - \Delta H_{o-1} \quad (42)$$

where

$\Delta H_{0-1}$  pressure drop in inlet duct, pounds per square foot

$H_0$  free-stream total pressure, pounds per square foot

The total pressure of the free stream is obtained from altitude tables in reference 8. Standard-air values were used in the present example as it was only given for illustrative purposes. In actual designs probably the summer-air values will be required, which are also given in reference 8. Although summer-air temperatures are higher than standard-air temperatures, a check calculation for the example showed that the use of the summer-air temperatures in place of those for standard air made no appreciable difference in the shroud dimensions necessary for adequate cooling. The details of determining the pressure loss in the inlet duct  $\Delta H_{0-1}$  will be given in step (10) of the procedure for a single-segment shroud with parallel flow.

The static pressure at the shroud entrance  $p_{a1}$  must also be determined. From compressible-flow relations given in reference 10 it can be shown that

$$\frac{\rho_{a1} V_{a1}}{\rho_{alt} a_{alt}} = \sqrt{\frac{2}{\gamma - 1}} \left( \frac{p_{a1}}{H_{a1}} \right)^{\frac{1}{\gamma}} \sqrt{1 - \left( \frac{p_{a1}}{H_{a1}} \right)^{\frac{\gamma-1}{\gamma}}} \quad (43)$$

where  $\rho_{alt}$  and  $a_{alt}$  are the density and velocity of sound of cooling air at station 1 based on stagnation conditions and  $\gamma$  is the ratio of specific heats. Now the stagnation temperature at station 1 is equal to the free-stream stagnation temperature. Then equation (43) reduces to

$$\frac{1.384 W_a \sqrt{T_{0t}}}{(d_s^2 - d_p^2) H_{a1}} = \sqrt{\frac{2}{\gamma - 1}} \left( \frac{p_{a1}}{H_{a1}} \right)^{\frac{1}{\gamma}} \sqrt{1 - \left( \frac{p_{a1}}{H_{a1}} \right)^{\frac{\gamma-1}{\gamma}}} \quad (44)$$

This equation is represented by a curve in figure 16 where the left-hand side of the equation is the ordinate and the abscissa

is  $\frac{H_{a1} - p_{a1}}{H_{a1}}$ . The figure is divided into several parts for different ranges of  $\frac{H_{a1} - p_{a1}}{H_{a1}}$ . If the values of the ordinate and  $H_{a1}$  are known,  $p_{a1}$  may be determined from figure 16.

Temperature at shroud entrance.- The temperature of the cooling air at the shroud entrance is determined from the equation

$$T_a = T_{alt} \left( \frac{p_{a1}}{H_{a1}} \right)^{\frac{\gamma-1}{\gamma}} = T_{ot} \left( \frac{p_{a1}}{H_{a1}} \right)^{0.286} \quad (45)$$

where  $T_{ot}$  is the free-stream stagnation temperature.

Available pressure drop at shroud entrance.- The pressure drop available for forcing the air through the whole system (inlet duct and shroud) is equal to  $H_o - p_o$  with the assumptions that all the velocity head at the shroud exit is lost and that the static pressure at the exit is free-stream static pressure. The pressure drop required by the inlet duct is equal to  $\Delta H_{o-1}$ . The pressure drop available for forcing the air through the shroud is the difference, or

$$\Delta H_{\text{available}} = (H_o - p_o) - \Delta H_{o-1} \quad (46)$$

In the foregoing formulas the subscript 1 has been used to denote shroud entrance. This subscript is for parallel flow. For counter flow all subscripts referring to this station should be changed to 2.

#### SINGLE-SEGMENT SHROUD FOR PARALLEL FLOW

For a parallel-flow system the shroud must be designed so that imposed limiting values of downstream exhaust-gas temperatures  $t_{e2}$ , exhaust-pipe temperatures  $t_p$ , and downstream shroud temperatures  $t_{s2}$  will not be exceeded. (See fig. 2(a).) Values assumed or calculated for this example are given in the following steps:

Step 1 - Exhaust-gas flow rate  $W_e$ :

From manufacturer's data or the following approximate formula, obtain

$$W_e = \frac{7.5 \text{bhp}(1 + f)}{3600} \quad (47)$$

where

$f$  fuel-air ratio

bhp brake horsepower

Then, for the illustrative example,

$$W_e = 4.84 \text{ pounds per second}$$

Step 2 - Inlet exhaust-gas temperature  $t_{e1}$ :

The value of  $t_{e1}$  may be obtained from the equation

$$t_{e1} = t_m - xl \quad (48)$$

where

$t_m$  exhaust-gas temperature at manifold obtained from manufacturer's data or by analytical methods

$x$  cooling rate of gas in exposed exhaust pipe, approximately  $2^\circ$  per foot

$l$  length of exposed exhaust pipe between manifold and shroud entrance

For illustrative purposes, a value of  $t_{e1}$  is assumed, as

$$t_{e1} = 1800^\circ \text{ F}$$

Step 3 - Exhaust-pipe diameter  $d_p$ :

The outside diameter of the exhaust pipe  $d_p$  is obtained from manufacturer's data or installation drawings.

## Step 4 - Airplane and altitude conditions:

Airplane altitude and velocity are secured from manufacturer's data for the design flight condition. Free-stream conditions  $p_0$ ,  $T_0$ , and  $\rho_0$  are obtained from altitude tables for standard air. (See reference 8.)

Step 5 - Design downstream exhaust-gas temperature  $t_{e2}$ :

Obtain  $t_{e2}$  from manufacturer's data on the safe operating temperatures of the turbine or, if a turbine is not used, the value selected by the designer for reasons peculiar to the installation. Decrease this design imposed maximum value of  $t_{e2}$  by approximately  $1\frac{1}{2}$  percent in the design procedure to correct for the slight underestimation of downstream exhaust-gas temperature by equation (13). For the example, the design maximum temperature is  $1675^\circ\text{F}$  and, therefore,

$$t_{e2} = 1650^\circ\text{F}$$

Step 6 - Design exhaust-pipe temperature  $t_p$ :

Obtain from available data or estimate from experience the maximum temperature at which the exhaust pipe can operate without danger of failure. Approximate limits to use if no data are available are from  $1200^\circ\text{F}$  to  $1450^\circ\text{F}$ . Decrease this design imposed maximum value of  $t_p$  by approximately 4 percent in the design procedure to correct for the slight underestimation of downstream exhaust-gas temperature by equation (14). For an imposed maximum pipe temperature of  $1450^\circ\text{F}$ ,

$$t_p = 1400^\circ\text{F}$$

Step 7 - Design shroud temperature  $t_s$ :

Obtain from the geometry and location of components of the installation the maximum shroud temperature that will not produce adverse effects of heat radiation. Limits to use, if none are specified by the airplane or engine manufacturer, are between  $500^\circ\text{F}$  and  $800^\circ\text{F}$ . If the shroud touches or passes close to rubber, neoprene, or other organic materials, use a lower limit of  $500^\circ\text{F}$  and shield the shroud at these points. This value of  $t_s$  is used for the critical downstream

cooling-air temperature  $t_{a2}$  because, as brought out in the section entitled "Relation of measured shroud temperatures to measured cooling-air temperatures," a conservative design procedure to meet a limiting shroud temperature is to design for a limiting cooling-air temperature of the same value as the shroud-temperature limit. For the present illustration,

$$t_s = t_a = 800^\circ \text{F}$$

Step 8 - Emissivity of exhaust pipe  $\epsilon_p$ :

The emissivity  $\epsilon_p$  for the most commonly used exhaust-pipe material, stainless steel, is about 0.70, and this value can be used inasmuch as small errors in the absolute value of  $\epsilon_p$  will have a negligible effect on the design. If another material is used, refer to a standard heat-transfer test for values. The value used in the example is

$$\epsilon_p = 0.70$$

Step 9 - Cooling-air-flow rate  $W_a$ :

Assume a large range of values of cooling-air-flow rate (approximately 1/8 to 1/2 of value of  $W_e$ ) and use with each assumed value of shroud diameter. Assumed values used for  $W_a$  are 0.50, 1.00, 1.50, 2.00, 2.50 pounds per second.

Step 10 - Selection of shroud-air-inlet duct size:

Assume an inlet duct cross-sectional area. For the values of cooling-air-flow rate  $W_a$ , use the equation for the pressure drop in the inlet duct

$$\Delta H_{0-1} = \underbrace{0.05q_{c0}}_{\text{Inlet loss}} + \underbrace{\sum \frac{z_1}{D_1} q_1 f}_{\text{Sum of straight-section losses}} + \underbrace{\sum K_b q_{1b}}_{\text{Sum of bend losses}} + \underbrace{\sum K_d \left(1 - \frac{A_{d\text{inlet}}}{A_{d\text{exit}}}\right)^2 q_{1d}}_{\text{Sum of diffuser losses}}$$

and the methods and data of reference 9 to calculate the pressure drop available at the shroud entrance. (All or part of the equation is used depending on duct geometry.) Repeat these calculations for other assumed values of duct size. Plot  $\Delta H_{\text{available}}$  against  $W_a$  for each duct size. (Fig. 17(a).) Select the inlet-duct area that shows no appreciable gain in pressure drop with further increase in duct area. When space limitations restrict the size of the inlet duct, use the largest area possible to get maximum  $\Delta H_{\text{available}}$ . From figure 17(a), the values selected for duct size are:

$$A_1 = 0.2376 \text{ square foot}$$

$$d_1 = 0.550 \text{ foot}$$

Step 11 - Length of shroud  $l$ :

Obtain  $l$  from installation geometry and purpose of shroud. The initial choice should be a single-segment shroud. The value of  $l$  for the present example is:

$$l = 18 \text{ feet}$$

Step 12 - Diameter of shroud  $d_s$ :

Assume a large range of practical shroud diameters, such as, for the present problem,

$$d_s = 0.542, 0.583, 0.625, 0.667, 0.710, 0.752 \text{ foot}$$

Step 13 - Curves of cooling-air static pressure at shroud inlet  $p_{a1}$ :

Determine the value of  $p_{a1}$  by computing items (30) to (36) of table 3 with values of  $W_a$  assumed in step 9. The calculations cannot be continued for any combination of  $d_s$  and  $W_a$  that causes item (34) to exceed 0.5907, for at this value choking occurs in the inlet duct to the shroud. Plot the choke factor (item (34)) against  $W_a$  for each  $d_s$ . (Shown, for the present examples, as the radial lines of figure 17(b).) The cooling-air-flow rate for each  $d_s$  is further limited by choking in the shroud due to heat addition to the air. Thus, the limiting value of choke factor (item (34)) must be obtained for the actual value of downstream cooling-air temperature that will result with each  $W_a$ . These temperatures are not yet known;

therefore, the calculations must be continued so that  $t_{a2}$  can be determined for all the assumed  $W_a$  values for each  $d_s$  that will not cause the inlet duct to choke. Plot  $P_{a1}$  against  $W_a$  for each  $d_s$  as in figure 17(c).

Step 14 - Curves of cooling-air temperature at shroud inlet  $t_{a1}$ :

Determine value of  $t_{a1}$  by computing item (37) of table 3. Plot  $t_{a1}$  against  $W_a$  for each  $d_s$  as in figure 17(d).

Step 15 - Curves of upstream exhaust-pipe temperature  $t_{p1}$ :

Determine value of  $t_{p1}$  by computing items (38) to (50) of table 3. Plot  $t_{p1}$  against  $W_a$  for each  $d_s$  (fig. 17(e)).

Step 16 - Curves of downstream exhaust-gas temperature  $t_{e2}$ :

Determine value of  $t_{e2}$  by computing items (52) to (64) of table 3. Plot  $t_{e2}$  against  $W_a$  for each  $d_s$  (fig. 17(f)).

Step 17 - Curves of downstream cooling-air temperature  $t_{a2}$ :

Determine value of  $t_{a2}$  by computing item (65) of table 3. Plot  $t_{a2}$  against  $W_a$  for each  $d_s$  (fig. 17(g)).

Step 18 - Curves of downstream exhaust-pipe temperature  $t_{p2}$ :

Determine  $t_{p2}$  by computing items (66) and (67) of table 3. Plot  $t_{p2}$  against  $W_a$  for each  $d_s$  (fig. 17(h)).

Step 19 - Design  $d_s$  and  $W_a$  combinations:

Select from the plots obtained in steps 15 to 18 (figs. 17(e) to 17(h)) the value of  $W_a$  needed for each  $d_s$  to make every installation temperature equal to its specified limiting value. (See steps 5 to 7.) All installation temperatures considered, the maximum value of  $W_a$  obtained for each  $d_s$  is the cooling-air-flow rate required to maintain all installation temperatures below specified limits. Plot these maximum values of  $W_a$  on the radial  $d_s$  lines of the plot obtained in step 13 (fig. 17(b)) to obtain the choke-factor curve for required cooling-air-flow rate. Select the value of  $t_{a2}$  for these same  $W_a$  and  $d_s$  combinations from the plot obtained in step 17 (fig. 17(g)).

Use these values of  $t_{a2}$  to determine the cooling-air downstream stagnation temperature from the equation

$$T_{a2t} = T_{a2} + 0.2361 \left( \frac{W_a T_{a2}}{A_a p_{a2}} \right)^2$$

where  $p_{a2}$  is cooling-air downstream static pressure assumed equal to free-stream static pressure. Determine  $T_{a2t}/T_{0t}$  for each  $d_s$  and  $W_a$  combination. Obtain the value of the limiting approximate choke factor for each  $T_{a2t}/T_{0t}$  from the curve for  $M_{a2} = 0.6$  of figure 17(i). (Recommended design procedure is to limit  $M_{a2}$  to a value of 0.6.) Plot these values of choke factor on the radial  $d_s$  lines of plot obtained in step 13 (fig. 17(b)) to obtain the choke-factor curve for the recommended design limit. Select from this plot the values of  $d_s$  for which the choke factors for required cooling-air-flow rate are less than the choke factors for the recommended design limit. (For the illustrative example, values of  $d_s$  selected from figure 17(b) were 0.667, 0.710, and 0.752.) Use these values of  $d_s$  and the corresponding values of required cooling-air-flow rate  $W_a$  in the shroud pressure-drop calculations (items (68) and (69) of table 3). For the  $d_s$  and required  $W_a$  combinations for which choke factors for required cooling-air-flow rate are greater than the recommended design limit choke factors, it is possible to determine the Mach number at the shroud exit. Those combinations for which  $M_{a2}$  is less than 1.0 may possibly provide satisfactory cooling if sufficient pressure is available to force the air through the system. Such designs, however, are not recommended.

Step 20 - Curve of cooling-air pressure drop through shroud  $\Delta H$ :

Determine the pressure drop for each  $d_s$  and  $W_a$  combination finally obtained in step 19 by computing items (70) to (88) of table 3. Select values of  $p_{a1}$ ,  $t_{a1}$ , and  $t_{a2}$  needed for this calculation from the plots obtained in steps 13, 14, and 17 (figs. 17(c), 17(d), and 17(g)). Plot the  $\Delta H_{\text{required}}$  so obtained, the  $\Delta H_{\text{available}}$  for the inlet-duct size previously selected (step 10), and  $d_s$  against  $W_a$  on the same curve.

The  $d_g$  values are plotted against their corresponding combination values of  $W_a$  that meet imposed limiting temperatures as obtained in step 19. The plot for the illustrative examples is given in figure 17(j).

Step 21 - Selection of shroud diameter  $d_g$ :

Compare the pressure-drop-required curve with the pressure-drop-available curve (from step 20). Three situations are possible:

(1) All of the pressure-drop-required curve is lower than the pressure-drop-available curve. For this case select the value of  $d_g$  corresponding to the value of  $W_a$  having the greatest excess available pressure drop or, if appreciable, the lowest cooling drag. Any shroud diameter will give adequate cooling.

(2) Only a part of the pressure-drop-required curve is lower than that available. For this case select the value of  $d_g$  in the range of the value of  $W_a$  for which the pressure-drop-required curve is lower than the available-pressure-drop curve. The best diameter to use in this range is determined as in the preceding case 1.

(3) All of the pressure-drop-required curve is higher than that available. For this case no single-segment shroud of any diameter used will provide satisfactory cooling. In order to obtain the required cooling the shroud must be divided into segments of shorter length. The design procedure for this case is continued in the section on multisegment shrouds.

The sample problem fell into the category of case 3 in step 21. (See fig. 17(j).) A two-segment shroud was assumed and the design continued as explained in a subsequent section on multisegment shrouds. The inlet ducts for both segments were assumed identical. The design procedure, calculations, and curves for the multisegment shroud are similar to those for the single-segment shroud; therefore, they are not given for the sample problem. A shroud divided into two segments of equal length, 9 feet long and 0.752 feet in diameter, was found to provide satisfactory cooling for the subject installation. Pertinent values are listed in the following table:

Segment	Value of $W_a$ to provide required cooling (lb/sec)	$\Delta H$ in shroud for required cooling (lb/sq ft)	$\Delta H_{\text{available}}$ for required $W_a$ value (lb/sq ft)	Cooling-air-exit Mach number
First	1.92	85.6	91.5	0.32
Second	2.00	88.1	91.0	.31

The exit Mach number for both segments is noted to be far below the recommended design value of 0.6. The drag power for the two-segment shroud was less than  $\frac{1}{2}$  percent of the brake horsepower of the engine. This drag power is an inappreciable power requirement and will have a very small effect on the airplane performance.

#### SINGLE-SEGMENT SHROUD FOR COUNTER FLOW

The design of a shroud for counter flow proceeds exactly as for parallel flow using, however, the calculation form given in table 4. For a counter-flow system the shroud must be designed to meet limiting values of downstream exhaust-gas temperature (in the exhaust-gas-flow direction)  $t_{e2}$ , downstream cooling-air temperature (in the cooling-air-flow direction)  $t_{a1}$ , and upstream exhaust-pipe temperature (in the exhaust-gas-flow direction)  $t_{p1}$  illustrated in figure 2(b). This condition constitutes the only appreciable difference between the design for counter flow and parallel flow.

Steps 1 to 14 - Factors and curves required for shroud design:

The factors and curves required for shroud design are determined exactly as in parallel flow, steps 1 to 14, respectively. In steps 10, 13, and 14, station 1 is replaced by station 2.

Step 15 - Curves of downstream exhaust-gas temperature  $t_{e2}$ :

Determine  $t_{e2}$  by computing items (38) to (64) of table 4.  
Plot  $t_{e2}$  against  $W_a$  for each  $d_s$ .

Step 16 - Curves of downstream cooling-air temperature  $t_{a1}$ :

Determine  $t_{a1}$  by computing item (65) of table 4. Plot  $t_{a1}$  against  $W_a$  for each  $d_s$ .

Step 17 - Curves of upstream exhaust-pipe temperature  $t_{p1}$ :

Determine  $t_{p1}$  by computing items (66) and (67) of table 4.  
Plot  $t_{p1}$  against  $W_a$  for each  $d_s$ .

### Step 18 - Design $d_s$ and $W_a$ combinations:

Select from the preceding plots of installation temperature (steps 15 to 17) the value of  $W_a$  for each  $d_s$  giving a temperature equal to the limiting temperature. After all installation temperatures are considered, note the value of  $W_a$  which gives a temperature equal to one of the limiting values and lower than all the other limiting values for each  $d_s$ . The procedure given in step 19 of parallel flow is used to determine the  $d_s$  and  $W_a$  combinations that will not exceed the recommended limiting choke factor. These combinations of  $d_s$  and  $W_a$  are used in the pressure-drop calculation, (Items (68) and (69) of table 4.)

### Step 19 - Curve of cooling-air pressure drop through shroud $\Delta H$ :

Determine the pressure drop for each  $d_s$  and  $W_a$  combination obtained in step 18 by computing items (70) to (88) of table 4. Select values of  $P_{a2}$ ,  $t_{a2}$ , and  $t_{a1}$  needed for this calculation from the previously drawn plots of these values against  $W_a$  (steps 13, 14, and 16). Plot the  $\Delta H_{\text{required}}$  so obtained, the  $\Delta H_{\text{available}}$  for the inlet duct size previously selected (step 10), and  $d_s$  against  $W_a$  on the same curve. The  $d_s$  values are plotted against their corresponding combination values of  $W_a$  that meet imposed limiting temperatures as obtained in step 18.

### Step 20 - Selection of shroud diameter $d_s$ :

Selection of shroud diameter is exactly the same as for parallel flow (step 21). Similarly, if no single-segment shroud of any diameter used will provide satisfactory cooling, the shroud must be divided into segments of shorter length. The design procedure for this case is continued in the following section on multisegment shrouds.

## MULTISEGMENT SHROUD FOR PARALLEL OR COUNTER FLOW

The design of a multisegment shroud proceeds in much the same manner as that of the single-segment shroud for either parallel flow or counter flow, because each segment is treated as an individual shroud and is dependent only on the preceding segment for the inlet exhaust-gas temperature.

**Step 1 - Diameter of shroud  $d_s$ :**

Select the shroud diameter from the pressure-drop curve, obtained for the single-segment shroud, which requires the smallest pressure drop for adequate cooling. This value of  $d_s$  is used for all the shroud segments.

**Step 2 - Segment inlet-exhaust-gas temperature  $t_{e1}$ :**

Determine the inlet-exhaust-gas temperature for each shroud segment by assuming linear gradient of exhaust-gas temperature. The exhaust-gas temperature at the shroud entrance and at the turbine inlet are the inlet-exhaust-gas temperature and the design downstream exhaust-gas temperature, respectively, obtained for a single-segment shroud from steps 2 and 5 of the parallel-flow or counter-flow design procedures.

**Step 3 - Segment design downstream exhaust-gas temperature  $t_{e2}$ :**

The segment inlet temperatures obtained in step 2 are used as the limiting exhaust-gas temperatures to be met at the exit of the adjacent upstream segment; that is,  $t_{e2}$  of first segment equals  $t_{e1}$  of second segment, and so forth. (See fig. 12.)

**Step 4 - Determination of shroud diameter  $d_s$ :**

The design then proceeds exactly as explained previously, with table 3 used for parallel flow or table 4 for counter flow; each segment is treated as an individual shroud. The pressure drop in each shroud segment is calculated only for the value of  $d_s$  from step 1 and the value of  $W_a$  that gives the required cooling and for which the recommended limiting choke factor is not exceeded. The shroud diameter selected in step 1 will provide satisfactory cooling if the pressure drop in each shroud segment is less than the pressure drop available for that segment.

It is unlikely that more than two segments with two entrances and two exits will ever be used because of the complexity of the duct system, the additional weight, and the possible attendant drag increases.

## DESIGN PROCEDURE WHEN MULTISEGMENT SHROUD SYSTEMS

## PROVIDE UNSATISFACTORY COOLING

When the pressure drop available for cooling is less than the pressure drop required for adequate cooling, the available pressure drop can be increased by several methods: (1) locate the intake of the inlet duct in a region of higher dynamic pressure, (2) locate the shroud exit in a region of lower pressure, (3) use a fan or ejector pump, and (4) install diffuser at the shroud exit to recover some of the exit dynamic pressure. If such improvements are impossible or the resulting gain in available pressure drop is insufficient to provide the additional cooling required, the only alternative left is to select the most favorable shroud geometry based on the criterions set up in the foregoing procedure, to determine the cooling-air-flow rate and design temperatures that will be obtained for the pressure drop available, and then to adapt the installation by relocating components of the installation and selecting materials that can withstand these temperatures.

## DISCUSSION OF DESIGN PROCEDURES

For this investigation the heat transfer from the exhaust gas to the cooling air was determined to be more greatly affected by the cooling-air-flow rate than by any other variable that may change with flight condition. Since the cooling-air-flow rate varies approximately as the square root of the density at the shroud inlet and the pressure drop available and since the density decreases so rapidly with altitude, in the usual case the most critical flight condition for design is maximum-power flight for the slowest speed (climb) at rated altitude.

In the procedures given herein all of the exhaust gas was assumed to flow through one exhaust pipe. In the cases in which two exhaust pipes carry the gases from the engine to the turbine or to the atmosphere, the exhaust-gas-flow rate for each pipe is assumed equal to one-half the exhaust-gas-flow rate through the engine.

In the design procedure a wide range of practical shroud diameter is assumed, as was illustrated when the sample problem was discussed. Since increasing the shroud diameter relative to the exhaust pipe decreases the downstream cooling-air temperatures and the cooling-air pressure drop for a shroud of constant length, (see figs. 17(g) and 17(j)) it would seem desirable to assume large

values of shroud diameter. The exhaust-pipe temperatures and the exhaust-gas temperatures, however, increase with increase of shroud diameter. (See figs. 17(e), 17(f), and 17(h).) The shroud diameter, therefore, is limited by the allowable exhaust-pipe and exhaust-gas temperatures and the weight and space limitations of the installation.

Analytical methods for determining the upstream exhaust-gas temperature  $t_{e1}$  are not well developed and constitute another problem which is not considered herein. In the present work the manufacturer's data are assumed to exist. The flight condition for which the shroud is being designed will set the engine-operating conditions that will enable the designer to determine from the engine data the gas temperature at the exhaust manifold. The exhaust-gas temperature at the inlet to the shroud system can then be assumed equal to or slightly less than the temperature at the exhaust manifold, depending on the length of exposed pipe from the exhaust manifold to the shroud system entrance. The temperature drop in the uncooled length will probably be not more than a few degrees per foot of length.

For the case of a design in which a single-segment shroud does not provide satisfactory cooling it has been proposed that a multi-segment shroud be used. Another proposal for those cases in which shroud temperature is exceeded in a single-segment system would be to use a double shroud around the hot inner pipe. No calculations were made for such a system but it has definite possibilities provided that space is available. Again for those cases in which the shroud-temperature limit is exceeded, local heat shields may provide satisfactory protection of the installation at the critical points of the shroud system.

#### CONCLUDING REMARKS

The equations for predicting installation temperatures and cooling-air pressure loss for shrouded exhaust-pipe systems for parallel flow are considered to be verified within the limits of engineering requirements for one ratio of shroud diameter to exhaust-pipe diameter by experimental data. Since the equations have no diameter-ratio limitations, provided that turbulent cooling-air flow exists in the annulus, the verification of the equations for one diameter ratio lends support to the belief that the equations are applicable to all practical ratios of shroud diameter to exhaust-pipe diameter for which the cooling-air flow is expected to be turbulent. No experimental data were obtained for counter-flow systems. The counter-flow equations, however, are believed to be equally applicable because of their similarity to the parallel-flow equations.

The application of the equations to the design of shrouds has been considerably simplified by the use of constant values of 0.24 and 0.30 for the specific heats of the cooling air and the exhaust gas, respectively, and by the use of air properties in place of exhaust-gas properties for determining the heat-transfer coefficient of the exhaust gas. Calculations showed that these substitutions have a negligible effect on the accuracy of the results.

The detailed procedures and charts, based on the derived equations, permit the determination of the proportions of an exhaust-pipe shroud that provides desired or maximum cooling of an exhaust installation for both parallel-flow and counter-flow systems. The procedures for the initial choice of a single-segment shroud are extended to multisegment shrouds for the case in which desired cooling cannot be realized with a single-segment shroud. These procedures are further extended to include the case in which desired cooling cannot be attained with a multisegment shroud of practical proportions. For this situation the procedures permit the determination of the shroud proportions that provide the maximum possible cooling and the determination of the value of installation temperatures that exist with that shroud. The results of the design example, which is included to illustrate the use of the design procedures, indicate that in well-designed shrouds adequate cooling can be obtained with inappreciable cooling drag.

One problem of immediate significance for which the equations and methods of shroud design are believed to be directly applicable is the design of shrouds for the tail pipes of jet engines provided that the luminosity of the gases in the tail pipe is negligible and the cooling air exits to the atmosphere. If the luminosity of the gases is not negligible for jet-engine installations, however, the analysis presented in this paper must be extended to include the heat transfer to the exhaust pipe by gas radiation. For installations in which flaps or ejector pumps are used the method of application of the pressure-drop relations to shroud design must be modified from that of the present method to account for the departure of the cooling-air exit pressure from atmospheric pressure.

Langley Memorial Aeronautical Laboratory  
National Advisory Committee for Aeronautics  
Langley Field, Va., June 19, 1947

## A P P E N D I X

## PROPERTIES OF EXHAUST-GAS MIXTURES AND AIR

## Status of Data on Properties

During the present investigation which led to the development and verification by experiments of equations for the design of exhaust-pipe shrouds and the development of shroud-design procedures based on the equations, certain properties of air and exhaust-gas mixtures for temperatures as high as  $2300^{\circ}\text{F}$  were required. These properties were the enthalpy, instantaneous specific heat, viscosity, and thermal conductivity.

Data existed on the enthalpy and instantaneous specific heat of air from  $80^{\circ}\text{F}$  to  $2240^{\circ}\text{F}$  in reference 11 and on the instantaneous specific heat, viscosity, and thermal conductivity of air from  $-100^{\circ}\text{F}$  to  $1600^{\circ}\text{F}$  in reference 12. Equations were also given in reference 12 for the determination of viscosity and thermal conductivity. Some data on the properties of mixtures of two gases are given in the literature, but only a small amount of data on viscosity is available on mixtures of gases with as many constituents as exist in exhaust gas from engines. Equations for the instantaneous specific heat and enthalpy of exhaust-gas mixtures, however, were derived in reference 11 based on classical thermodynamics and tables of constants included for use in the equations. The data of both references 11 and 12 were based on the work of many experimenters over a long period of years.

In order to meet the foregoing requirement for the shroud design investigation values of viscosity and thermal conductivity of air from  $1600^{\circ}\text{F}$  to  $2300^{\circ}\text{F}$  and values of instantaneous specific heat and enthalpy of exhaust-gas mixtures from  $500^{\circ}\text{F}$  to  $2300^{\circ}\text{F}$  had to be calculated by use of the equations of references 11 and 12. In addition, formulas had to be derived for the viscosity and thermal conductivity of exhaust-gas mixtures in a manner similar to the derivation of the formulas for instantaneous specific heat and enthalpy of exhaust-gas mixtures in reference 11, and values of the properties had to be calculated with use of these newly derived formulas over the same range of temperature as the other exhaust-gas-mixture properties were calculated. The exhaust-gas-mixture properties involved properties of individual gases such as carbon monoxide which were obtained for the most part from reference 12.

The purpose of this appendix is to give tables or charts of the foregoing properties and also the Prandtl numbers of air and exhaust-gas mixtures over the range of temperature indicated and based on the

foregoing calculations and data. Details of methods for obtaining the properties and the derivation of the formulas for the viscosity and the thermal conductivity of exhaust-gas mixtures are included herein. Although some of the results have been given in other papers, these results have been replotted so that all results will be in convenient form in one paper.

The accuracy of the calculated results is uncertain in most cases because of the nonexistence of experimental data. Some indication of the accuracy can be obtained by noting the accuracy of the properties of the individual gases in the references from which they were obtained and the manner in which calculated data fair into the experimental data. As far as the properties of exhaust-gas mixtures are concerned, regardless of the accuracy of the individual gas properties, the accuracy depends on the exactness of the classical thermodynamic theory (presumably the best theory to date) which was used in reference 11 and in the present paper. Until experimental data are available, the calculated results presented herein are considered to be the most accurate available.

#### Symbols

$$a_1 = \frac{\mu_{H_2O} - \frac{\mu_{O_2}}{2}}{2.016}$$

$$a_2 = \frac{k_{H_2O} - \frac{k_{O_2}}{2}}{2.016}$$

$$b_1 = \frac{\mu_{CO_2} - \mu_{O_2}}{12}$$

$$b_2 = \frac{k_{CO_2} - k_{O_2}}{12}$$

$$c_1 = \mu_{O_2} + 2\mu_{CO} - 2\mu_{CO_2}$$

$$C_2 = k_{O_2} + 2k_{CO} - 2k_{CO_2}$$

$c_1, c_2$  constants in formula for viscosity of air

$c_{Pa}$  instantaneous specific heat of air at constant pressure, Btu/lb/°F

$c_{Pe}$  instantaneous specific heat of exhaust gas at constant pressure, Btu/lb/°F

$c_{Va}$  instantaneous specific heat of air at constant volume, Btu/lb/°F

$c_{vH_2O}$  instantaneous specific heat of water vapor at constant volume, Btu/lb/°F

$$D_1 = \frac{2\mu_{CO} - \mu_{CO_2}}{12}$$

$$D_2 = \frac{2k_{CO} - k_{CO_2}}{12}$$

$$E_1 = \frac{\mu_{H_2O} + \mu_{CO} - \mu_{CO_2}}{2.016}$$

$$E_2 = \frac{k_{H_2O} + k_{CO} - k_{CO_2}}{2.016}$$

$f$  fuel-air ratio

$g$  ratio of absolute to gravitational unit of mass, lb/slug, or acceleration due to gravity, ft/sec<sup>2</sup>

$i_a$  heat content (enthalpy) of cooling air, Btu/lb (referred to 0° absolute)

$i_e$  heat content (enthalpy) of exhaust gas, Btu/lb (referred to 0° absolute)

$K$  constant in equation (A23)

$K_1$  constant in equation for  $k_a$  determined from  $\mu_a$  and  $c_{Va}$

$K_2$	constant in equation for $k_{H_2O}$
$k_a$	thermal conductivity of cooling air, Btu/sec/sq ft/°F/ft
$k_e$	thermal conductivity of exhaust gas, Btu/sec/sq ft/°F/ft
$k_{H_2O}, k_{N_2}, \dots$	thermal conductivity of exhaust-gas constituents (designated by subscripts), Btu/sec/sq ft/°F/ft
$M_a$	molecular weight of air (29)
$m$	hydrogen-carbon ratio
$S$	Sutherland constant in viscosity equation
$T$	temperature, °C absolute or °F absolute
$T_e$	exhaust-gas temperature, °F absolute
$t$	temperature, °F
$x$	mols of exhaust gas per mol of air
$\mu_a$	absolute viscosity of air, slugs/sec/ft
$\mu_e$	absolute viscosity of exhaust gas, slugs/sec/ft
$\mu_{H_2O}, \mu_{N_2}, \dots$	absolute viscosity of exhaust-gas constituents (designated by subscripts), slugs/sec/ft
$\phi_1 = \mu_{CO_2} + \mu_{H_2} - \mu_{CO} - \mu_{H_2O}$	
$\phi_2 = k_{CO_2} + k_{H_2} - k_{CO} - k_{H_2O}$	
$Pr_a$	Prandtl number of air $(c_{p_a} \mu_a / k_a)$
$Pr_e$	Prandtl number of exhaust gas $(c_{p_e} \mu_e / k_e)$

## Chemical Symbols

CO mols of carbon monoxide in exhaust gas per mol of air burned

$$(CO)' = CO + H_2$$

CO<sub>2</sub> mols of carbon dioxide in exhaust gas per mol of air burned

$$(CO_2)' = CO_2 - H_2$$

H<sub>2</sub> mols of hydrogen in exhaust gas per mol of air burned

H<sub>2</sub>O mols of water vapor in exhaust gas per mol of air burned

$$(H_2O)' = H_2O + H_2$$

(H<sub>2</sub>O)<sub>a</sub> mols of water vapor in air per mol of air burned

N<sub>2</sub> mols of nitrogen in exhaust gas per mol of air burned

O<sub>2</sub> mols of oxygen required for combustion per mol of air burned

O<sub>2</sub>' mols of excess oxygen in exhaust gas per mol of air burned

(O<sub>2</sub>)<sub>a</sub> mols of oxygen in air per mol of air burned (0.2098)

## Methods of Obtaining Properties of Air

Enthalpy  $i_a$ . - The enthalpy for air over a range of temperature from 0° to 2240° F has been reported in table II of reference 11. All enthalpy values were referred to a temperature of 0° absolute. The values given were based on information published in chemical journals from 1933 to 1939; the complete bibliography containing the information is given in reference 11. These values were plotted against temperature for use in the present paper in order that all of the data compiled herein would be available in one paper in a convenient manner.

Instantaneous specific heat  $c_{p_a}$ .— The instantaneous specific heats of air based on the same information as that for the enthalpy of air and over the same range of temperature are also given in table II of reference 11. In reference 12 the instantaneous specific heats of air are also given from  $-100^\circ\text{F}$  to  $1600^\circ\text{F}$ . The results of references 11 and 12 are in excellent agreement for the overlapping range of temperature. A curve of instantaneous specific heat of air over a range of temperature from  $-100^\circ\text{F}$  to  $2240^\circ\text{F}$  was then drawn based on the data of the two references. Further comparison of the data of references 11 and 12 with data on instantaneous specific heat in reference 13 up to  $1600^\circ\text{F}$  showed the latter data also agreed very well with the other values.

Viscosity  $\mu_a$ .— Values of viscosity of air for a temperature range from  $-100^\circ\text{F}$  to  $1600^\circ\text{F}$  have been reported in reference 12 in a table and a figure. These values were based on the work of many experimenters and a bibliography in reference 12 gives the reports used. The viscosity values given in reference 12 were replotted for presentation herein. At temperatures between  $1600^\circ\text{F}$  and  $2300^\circ\text{F}$  the following formula given in reference 12 was used to calculate the viscosity values which were also plotted on the curve of viscosity against temperature:

$$\mu_a = c_1 \frac{T_a^{\frac{3}{2}}}{T_a + c_2} \quad (A1)$$

where

$T_a$  temperature of air,  $^\circ\text{F}$  absolute

$c_1$  a constant

$c_2$  a constant

The constants in the formula were obtained from the data given for temperatures below  $1600^\circ\text{F}$ .

Conductivity  $k_a$ .— Values of conductivity of air are also given in reference 12 over a temperature range from  $-100^\circ\text{F}$  to  $1600^\circ\text{F}$ . As for the viscosity  $\mu_a$  these values of conductivity are based on

the work of many experimenters whose reports are listed in reference 12. The conductivity of air values given in this reference were replotted for use in the present paper. For temperatures between 1600° F and 2300° F the conductivity values were calculated by use of the following formula given in reference 12:

$$k_a = K_1 \mu_a c_{v_a} \quad (A2)$$

The constant  $K_1$  was calculated from the data on  $\mu_a$  and  $k_a$  for temperatures below 1600° F in reference 12 and from values of  $c_{v_a}$ , the instantaneous specific heat at constant volume, calculated by means of the following formula given on page 178 of reference 13:

$$c_{v_a} = 0.1509 + 0.0000342T_a - 0.00000000293T_a^2 \quad (A3)$$

where  $T_a$  is air temperature in °F absolute. Values of the conductivity of air for temperatures above 1600° F were then calculated by use of equations (A2) and (A3), the value of  $K_1$  calculated by the method given, and the calculated values of  $\mu_a$  for temperatures above 1600° F. The  $k_a$  values above 1600° F were then plotted with the values below 1600° F.

Prandtl number  $Pr_a$ .— The Prandtl number for air  $c_{p_a} \mu_a g / k_a$  was calculated for a range of temperature from -100° F to 2300° F by use of the values of  $c_{p_a}$ ,  $\mu_a$ , and  $k_a$  that had been determined for this range of temperature.

#### Methods of Obtaining Exhaust-Gas Mixture Properties

Enthalpy  $i_e$  and instantaneous specific heat  $c_{p_e}$ .— Equations for the calculation of the enthalpy  $i_e$  and the instantaneous specific heat  $c_{p_e}$  of exhaust-gas mixtures for any fuel-air ratio and hydrogen-carbon ratio of the fuel are given in reference 11. The equations are based on classical thermodynamics and complete details of their derivation are given in the reference. Tables of constants to be used in the equations are included in the reference. The energy of combustion of CO and  $H_2$  (carbon monoxide and hydrogen, respectively) at the absolute zero of temperature was

included in the constants to be used in the enthalpy equations of reference 11. These constants were recalculated for the present paper without this energy. The result is that the enthalpy calculated with the new constants will be  $\int c_{p_e} dT_e$  above the absolute zero of temperature. Calculations of the enthalpy and instantaneous specific heat were then made with the equations, the constants of reference 11 for  $c_{p_e}$ , and the new constants for  $i_e$  over a range of fuel-air ratio from 0.01 to 0.12, hydrogen-carbon ratios from 0.10 to 0.20, and exhaust-gas temperatures from 500° F to 2300° F.

It was intended to present paired curves based on these calculations for the entire ranges of exhaust-gas temperatures, fuel-air ratios, and hydrogen-carbon ratios. It was possible to do so for the instantaneous specific heat and these curves are shown herein. Since the hydrogen-carbon ratio is a constant for each fuel, these curves and all the rest of the curves for exhaust-gas-mixture properties are presented in families of constant hydrogen-carbon ratio. The accuracy of interpolation for variables between the given curves is limited only by the accuracy of the curves themselves. Inasmuch as the fuel-air ratio for the stoichiometric mixture varies with hydrogen-carbon ratio between the limits 0.06 and 0.08, the range of fuel-air ratio over which appropriate equations were applicable was indefinite. Consequently lean-mixture equations were applied up to a fuel-air ratio of 0.06 and rich-mixture equations down to a fuel-air ratio of 0.08, and the values for a fuel-air ratio of 0.07 were obtained by cross plotting the calculated values against fuel-air ratio and interpolating in the range between 0.06 and 0.08. In order to present paired curves of enthalpy of sufficient accuracy for use, the curves would have required a greatly expanded scale and consequently a very large figure. In order to avoid this large plot, the calculated values of the enthalpy of exhaust gas for the ranges of temperatures, fuel-air ratios, and hydrogen-carbon ratios are presented in a table. One figure is given simply as an illustrative curve of enthalpy for one hydrogen-carbon ratio to show the variation of enthalpy with temperature and fuel-air ratio.

Viscosity  $\mu_g$ .— Data on viscosity over only a limited range of conditions (reference 14) were available for mixtures of gases with a large number of constituents such as are found in exhaust-gas mixtures. Mixtures of two constituents are about the only gas mixtures usually reported in the literature. An equation was therefore derived for the viscosity  $\mu_g$  by methods which were similar to those used to arrive at the equations for  $i_e$  and  $c_{p_e}$  in

reference 11. This equation was then used to calculate  $\mu_e$  over a range of exhaust-gas temperature, fuel-air ratio, and hydrogen-carbon ratio. The derivation of this equation is given herein.

Discussions in references 15 and 16 on the viscosity and thermal conductivity of mixed gases may be summarized as follows: For exhaust gases containing no hydrogen the viscosity of the mixture is very nearly the average of that of the components, weighted in proportion to their partial volumes. The absolute viscosity must be used for this calculation. When hydrogen is present, the averaging process yields too low a viscosity. The average viscosity computed by excluding hydrogen from the average is probably a little too large. The thermal conductivity is obtained by an averaging process similar to that for viscosity. The result is more nearly correct for thermal conductivity than for viscosity, particularly, when hydrogen is present. Then, approximately,

$$x\mu_e = (\text{CO}_2)\mu_{\text{CO}_2} + (\text{H}_2)\mu_{\text{H}_2} + \dots \quad (\text{A4})$$

$$xk_e = (\text{CO}_2)k_{\text{CO}_2} + (\text{H}_2)k_{\text{H}_2} + \dots \quad (\text{A5})$$

where

$x$  mols of exhaust gas per mol of air  
 $\text{CO}_2, \text{H}_2, \dots$  mols of exhaust-gas constituents per mol of air  
 $\mu_{\text{CO}_2}, k_{\text{H}_2}, \dots$  physical properties of exhaust-gas constituents

The equation involving  $k_e$  has been included at this point to show its similarity to the equation for  $\mu_e$ . The conductivity, however, will be taken up in the next section.

The first part of the problem is the determination of the mols of constituents per mol of air and exhaust-gas mixture in terms of fuel-air and hydrogen-carbon ratios. These values are then substituted in an equation similar to equation (A4) and a formula derived for  $\mu_e$  in terms of the fuel-air ratio  $f$ , the hydrogen-carbon ratio  $m$ , and the viscosities of the individual gases. Finally, values of  $\mu$  for the individual gases are obtained and substituted in the equation for  $\mu_e$ .

Formulas are given in reference 11 for the masses of exhaust-gas constituents formed when 1 mol of air is burned for ranges of mixtures leaner than the stoichiometric and richer than the stoichiometric. The masses of the constituents are functions of the fuel-air and hydrogen-carbon ratios. Various assumptions are made in reference 11 in order to determine these formulas. One assumption is that, in the range of mixtures leaner than stoichiometric, the fuel is completely converted to carbon dioxide  $\text{CO}_2$  and water  $\text{H}_2\text{O}$ . A further assumption made is that the amount of water vapor in the combustion air is negligible and can be disregarded for both the lean and rich mixtures. The formula for  $\mu_e$  in the lean-mixture range is

$$x\mu_e = (\text{CO}_2)\mu_{\text{CO}_2} + (\text{H}_2\text{O})\mu_{\text{H}_2\text{O}} + (\text{N}_2)\mu_{\text{N}_2} + (\text{O}_2')\mu_{\text{O}_2} \quad (\text{A6})$$

where

$\text{O}_2'$  mols of excess oxygen in exhaust gas per mol of air after combustion

$\text{N}_2$  mols of nitrogen in exhaust gas per mol of air

Now

$$\mu_a = (\text{N}_2)\mu_{\text{N}_2} + (\text{O}_2')\mu_{\text{O}_2} + (\text{O}_2)\mu_{\text{O}_2}$$

where

$\text{O}_2$  mols of oxygen required for combustion per mol of air

or

$$(\text{N}_2)\mu_{\text{N}_2} + (\text{O}_2')\mu_{\text{O}_2} = \mu_a - (\text{O}_2)\mu_{\text{O}_2} \quad (\text{A7})$$

Substituting equation (A7) in equation (A6) gives

$$x\mu_e = \mu_a + (\text{CO}_2)\mu_{\text{CO}_2} + (\text{H}_2\text{O})\mu_{\text{H}_2\text{O}} - (\text{O}_2)\mu_{\text{O}_2} \quad (\text{A8})$$

From the formulas in reference 11 the following formulas were derived:

$$\text{CO}_2 = \frac{fM_a}{12(m+1)} \quad (A9)$$

$$\text{H}_2\text{O} = \frac{fM_a m}{2.016(m+1)} \quad (A10)$$

$$O_2 = \frac{fM_a \left( \frac{1}{12} + \frac{m}{2 \times 2.016} \right)}{(m+1)} \quad (A11)$$

$$x = 1 + \left[ \frac{fM_a m}{2 \times 2.016(m+1)} \right] \quad (A12)$$

where

$f$  fuel-air ratio

$m$  hydrogen-carbon ratio

$M_a$  molecular weight of air (29)

If equations (A9) to (A12) are substituted in equation (A8), the viscosity of the exhaust gas becomes

$$\mu_e = \frac{\frac{\mu_a}{M_a} + \frac{f(a_1 m + b_1)}{m+1}}{\frac{1}{M_a} + \frac{f m}{2 \times 2.016(m+1)}} \quad (A13)$$

where

$$a_1 = \frac{\mu_{\text{H}_2\text{O}} - \frac{\mu_{\text{O}_2}}{2}}{2.016} \quad (A14)$$

$$b_1 = \frac{\mu_{\text{CO}_2} - \mu_{\text{O}_2}}{12} \quad (A15)$$

In the range of mixtures richer than stoichiometric one of the assumptions made is that the constituents of the exhaust gas are  $\text{CO}_2$ ,  $\text{H}_2\text{O}$ ,  $\text{H}_2$ ,  $\text{CO}$ , and  $\text{N}_2$ . (See reference 11.) Then,

$$x\mu_e = (\text{CO}_2)\mu_{\text{CO}_2} + (\text{H}_2\text{O})\mu_{\text{H}_2\text{O}} + (\text{H}_2)\mu_{\text{H}_2} + (\text{CO})\mu_{\text{CO}} + (\text{N}_2)\mu_{\text{N}_2} \quad (\text{A16})$$

Now

$$(\text{N}_2)\mu_{\text{N}_2} = \mu_a - (\text{O}_2)_a \mu_{\text{O}_2} \quad (\text{A17})$$

where

$$(\text{O}_2)_a \quad \text{mols of oxygen in air per mol of air (0.2098)}$$

Equation (A16) then becomes

$$x\mu_e = (\text{CO}_2)\mu_{\text{CO}_2} + (\text{H}_2\text{O})\mu_{\text{H}_2\text{O}} + (\text{H}_2)\mu_{\text{H}_2} + (\text{CO})\mu_{\text{CO}} + \mu_a - (\text{O}_2)_a \mu_{\text{O}_2} \quad (\text{A18})$$

From reference 11 the following equations for the mols of exhaust gas and constituents were derived:

$$\text{CO}_2 = 2(\text{O}_2)_a - \frac{fM_a}{12(m+1)} - \frac{fM_{a,m}}{2.016(m+1)} + H_a \quad (\text{A19})$$

$$\text{H}_2\text{O} = \frac{fM_a}{2.016(m+1)} - H_2 \quad (\text{A20})$$

$$\text{CO} = \frac{fM_{a,m}}{2.016(m+1)} + \frac{fM_a}{6(m+1)} - 2(\text{O}_2)_a - H_2 \quad (\text{A21})$$

$$\text{N}_2 = 1 - (\text{O}_2)_a \quad (\text{A22})$$

$$H_2 = \frac{\sqrt{[K(CO_2)' + (CO)' + (H_2O)']^2 + 4(K-1)(CO)'(H_2O)'}}{2(K-1)}$$

$$= \frac{K(CO_2)' + (CO)' + (H_2O)'}{2(K-1)} \tag{A23}$$

where

$$K = 3.8$$

$$(CO_2)' = (CO_2) - (H_2) \tag{A24}$$

$$(CO)' = (CO) + (H_2) \tag{A25}$$

$$(H_2O)' = (H_2O) + (H_2) \tag{A26}$$

$$x = 1 - (O_2)_a + \frac{fM_a}{12(m+1)} + \frac{fM_a m}{2.016(m+1)} \tag{A27}$$

Substitution of equations (A19) to (A27) in equation (A18) leads to the following expression for  $\mu_e$  in the mixture range richer than stoichiometric:

$$\mu_e = \frac{\left[ \frac{\mu_a}{M_a} - \frac{(O_2)_a C_1}{M_a} + \frac{f}{1+m} (D_1 + mE_1) + \frac{H_2}{M_a} \right]}{\left[ \frac{1}{M_a} - \frac{(O_2)_a}{M_a} + \frac{f}{1+m} \left( \frac{1}{12} + \frac{m}{2.016} \right) \right]} \tag{A28}$$

where

$$G_1 = \mu_{O_2} + 2\mu_{CO} - 2\mu_{CO_2} \quad (A29)$$

$$D_1 = \frac{(2\mu_{CO} - \mu_{CO_2})}{12} \quad (A30)$$

$$E_1 = \frac{(\mu_{H_2O} + \mu_{CO} - \mu_{CO_2})}{2.016} \quad (A31)$$

$$\phi_1 = (\mu_{CO_2} + \mu_{H_2} - \mu_{CO} - \mu_{H_2O}) \quad (A32)$$

The viscosities of the individual gases were next determined for use in finding the constants  $a_1$ ,  $b_1$ , and so forth in the equations for  $\mu_e$ . The viscosities of  $H_2$ ,  $N_2$ ,  $O_2$ ,  $CO_2$ , and  $CO$  were obtained by means of formulas and values given in tables in reference 12. The viscosity of  $H_2O$  was calculated by use of the Sutherland equation obtained from reference 17, page 1. This equation is

$$\frac{(\mu_{H_2O})_T}{(\mu_{H_2O})_{0^\circ C}} = \left(\frac{T}{273.1}\right)^{\frac{3}{2}} \left(\frac{273.1 + S}{T + S}\right) \quad (A33)$$

where

T temperature,  $0^\circ C$  absolute

S Sutherland constant (from reference 17, table 1, p. 4,  
S for  $H_2O = 650$ )

The viscosity of  $H_2O$  at  $100^\circ C$  is  $0.2527 \times 10^{-6}$  slugs per second-foot. (See reference 15, p. 180, units changed to British engineering.) This value and the value of S were used in equation (A33) to calculate the viscosity of water at  $0^\circ C$ . Since the value of  $(\mu_{H_2O})_{0^\circ C}$

was known, values of the viscosity over a large range of temperature were calculated by use of equation (A33).

The constants in the equations for  $\mu_e$  were then calculated by use of the viscosities of the individual gases and equations (A14), (A15), (A29), (A30), (A31), and (A32). These constants were then used to calculate  $\mu_e$  over ranges of fuel-air and hydrogen-carbon ratios and temperatures by use of equations (A13) and (A28).

Conductivity  $k_g$ .— No data on the conductivity of mixtures of gases with a large number of constituents were available. Consequently, derivations of equations for  $k_g$  in a manner identical to that used for the equations of  $\mu_e$ , on the basis of equations (A4) and (A5), were made. The derivations led to equations, for the range of mixtures leaner than stoichiometric, identical to equations (A13) to (A15) and for the range of mixtures richer than stoichiometric to equations identical to equations (A28) to (A32), with the exception that every value of  $\mu$  in the foregoing equations is replaced with a  $k$ . The constants in the equations for  $k_g$  are denoted  $a_2$ ,  $b_2$ ,  $C_2$ ,  $D_2$ ,  $E_2$ , and  $\phi_2$  which correspond to the constants in the equations containing  $\mu_e$ .

The conductivities of the individual gases were then determined. The conductivities of  $\text{CO}_2$ ,  $\text{N}_2$ ,  $\text{CO}$ ,  $\text{O}_2$ , and  $\text{H}_2$  were determined in the same manner that was used to determine the conductivity of air, which has already been described, by use of the data on the conductivities of the individual gases at temperatures below  $1600^\circ \text{F}$  in reference 12, the data on the viscosities of the individual gases calculated in the manner given in the preceding section of this paper, and equations for instantaneous specific heat at constant volume given in reference 13 for the individual gases. The conductivity of  $\text{H}_2\text{O}$  was calculated from the formula

$$k_{\text{H}_2\text{O}} = K_2 \mu_{\text{H}_2\text{O}} c_{v\text{H}_2\text{O}} \quad (\text{A34})$$

where  $K_2$  was obtained from reference 15, p. 180, and values of  $c_{v\text{H}_2\text{O}}$  were calculated from an equation given in reference 13. The values of viscosity  $\mu_{\text{H}_2\text{O}}$  already described were also used.

The constants in the equations for  $k_g$  were then calculated by use of the conductivities of the individual gases and equations similar to equations (A14), (A15), (A29) to (A32) with the term  $\mu$

replaced with  $k$  in all instances. These constants were then used to calculate  $k_e$  over ranges of fuel-air ratios, hydrogen-carbon ratios, and temperatures from equations similar to equations (A13) and (A28). The thermal-conductivity curves were extrapolated between the fuel-air ratios of 0.06 and 0.08; the curves are dashed in this range.

Prandtl number,  $Pr_e$ . The Prandtl number  $c_{pe}\mu_e/k_e$  for the gas mixtures was calculated by use of the values of instantaneous specific heat, viscosity, and conductivity that were read from paired curves of these properties. Because of the excessive overlapping and crossing of paired curves of the calculated Prandtl numbers of exhaust gases that were plotted for a range of temperature, fuel-air ratio, and hydrogen-carbon ratio, the data are presented in a table. One plot of Prandtl number for one hydrogen-carbon ratio was prepared to illustrate the variation of Prandtl number with fuel-air ratio and temperature. Values at the fuel-air ratio of 0.07 were calculated from the interpolated values of specific heat, viscosity, and thermal conductivity.

#### Properties of Exhaust-Gas Mixtures and Air

Air properties. The instantaneous specific heat and enthalpy of air over a range of temperature up to 2300° F are given in figure 18 and the viscosity, conductivity, and Prandtl number of air up to the same temperature are given in figure 19. The calculated values of viscosity and conductivity above 1600° F fair very well into the values below 1600° F (fig. 19); thus, confidence is provided in the formulas used in the calculations.

The instantaneous specific heat (fig. 18) varied from about 0.24 at room temperature to 0.29 at 2300° F. Consequently, the value of 0.24 usually used may be in error as much as 15 percent.

The Prandtl number is also usually assumed a constant with a value of about 0.73. Figure 19 shows that use of this value at room temperatures will lead to little error, but its use at high temperatures will lead to some error because the Prandtl number falls to a value of about 0.62.

Exhaust-gas-mixture properties. Values of the enthalpy  $i_e$  of exhaust-gas mixtures are given in table 6. Figure 20 illustrates the type of variation obtained with fuel-air ratio and temperature for a hydrogen-carbon ratio of 0.10. From table 6 and figure 20 it is apparent that the main change in enthalpy occurs because of temperature change.

The variation of the specific heat of exhaust-gas mixtures with temperature, fuel-air ratio, and hydrogen-carbon ratio is given in figures 21(a) and 21(b). An appreciable change in  $c_{p_e}$  occurs for a wide variation in temperature and fuel-air ratio, but the change with hydrogen-carbon ratio is much less. Appreciable error could possibly be introduced in a problem dealing with exhaust-gas mixtures if a constant value of  $c_{p_e}$  such as 0.30, which is sometimes assumed, is used.

Curves similar to those of figure 21 for  $c_{p_e}$  are given in figure 22 for the viscosity  $\mu_e$ . Values of  $\mu_e$  and of the constants to be used in the exhaust-gas-mixture viscosity equations are given in table 7 for a temperature range from 500° F to 2300° F. Only the values of  $\mu_e$  for the extreme ranges of hydrogen-carbon ratio, 0.10 and 0.20, are given in figure 22 because the change in  $\mu_e$  was small enough such that interpolation between the values given for other ratios will result in good estimates of viscosity.

As stated previously, some data on the viscosity of exhaust-gas mixtures are given in reference 14. The ranges of conditions for which these data were obtained were from 75° F to 890° F and fuel-air ratios from 0.0625 to 0.167. The hydrogen-carbon ratio of the fuel used was not given. For the ranges tested the viscosity was found to be nearly independent of the fuel-air ratio used. No mention is made in reference 14 of the effect of hydrogen-carbon ratio on the viscosity  $\mu_e$ . Figure 22 shows that the viscosity is affected to some extent by both fuel-air ratio and hydrogen-carbon-ratio variations. In order to compare the results of reference 14 with those of figure 22 it was assumed that gasoline with a hydrogen-carbon ratio of 0.17, a normal value for aviation gasoline, was used in the tests of reference 14. The comparison showed that the average differences between the two sets of results varied from about 3 percent to 4 percent; the experimental values are higher than the calculated values. Inasmuch as reference 14 states that the experimental values can be as much as 2 percent too high because of experimental errors and also because the hydrogen-carbon ratio had to be assumed, the agreement is very good.

Curves of exhaust-gas-mixture conductivity  $k_e$  against fuel-air ratio for several constant temperatures are given in figure 23(a) for a hydrogen-carbon ratio of 0.10 and in figure 23(b) for a ratio of 0.20. Only results for the two H/C ratios are given for the same reason that only curves of  $\mu_e$  for these two ratios were given. Values for any intermediate hydrogen-carbon ratio obtained by interpolation will differ from the calculated values by less than  $\frac{1}{2}$  percent.

Constants and values of conductivity of air  $k_a$  used in the  $k_e$  formulas are given in table 8 for a range of temperatures from 500° F to 2300° F. In the range of fuel-air ratio leaner than the stoichiometric from 0.01 to 0.06, the conductivity changed very little with fuel-air-ratio change. (See figs. 23(a) and 23(b).) Above the range of the stoichiometric mixture the conductivity increased rapidly with increases of fuel-air ratio. The increase of conductivity with temperature was rapid in both the lean and rich fuel-air-ratio ranges.

Values of Prandtl number for exhaust-gas mixtures, for a temperature range from 500° F to 2300° F and a fuel-air ratio range from 0.01 to 0.12, at a hydrogen-carbon ratio of 0.10 are given in figure 24 to illustrate the type of curves obtained. Values for other hydrogen-carbon ratios are given in table 9.

A summary table is given below for easy reference to the figures and tables for obtaining the properties.

Property	Symbol	Units	Location
Enthalpy of air	$i_a$	Btu/lb.	Fig. 18
Instantaneous specific heat of air	$c_{p_a}$	Btu/(lb)(°F)	Fig. 18
Viscosity of air	$\mu_a$	slugs/(sec)(ft)	Fig. 19
Conductivity of air	$k_a$	Btu/(sec)(ft <sup>2</sup> )(°F/ft)	Fig. 19
Prandtl number of air	$Pr_a$	-----	Fig. 19
Enthalpy of exhaust gas	$i_e$	Btu/lb	Table 6
Instantaneous specific heat of exhaust gas	$c_{p_e}$	Btu/(lb)(°F)	Fig. 21
Viscosity of exhaust gas	$\mu_e$	slugs/(sec)(ft)	Fig. 22
Conductivity of exhaust gas	$k_e$	Btu/(sec)(ft <sup>2</sup> )(°F/ft)	Fig. 23
Prandtl number of exhaust gas	$Pr_e$	-----	Table 9

## REFERENCES

1. McAdams, William H.: Heat Transmission. Second ed., McGraw-Hill Book Co., Inc., 1942.
2. Martinelli, R. C., Weinberg, E. B., Morrin, E. H., and Boelter, L. M. K.: An Investigation of Aircraft Heaters. III - Measured and Predicted Performance of Double Tube Heat Exchangers. NACA ARR, Oct. 1942.
3. Monrad, G. C., and Pelton, J. F.: Heat Transfer by Convection in Annular Spaces. Trans. American Inst. Chem. Eng., vol. 38, sec. A, no. 3, June 25, 1942, pp. 593-611.
4. Wiegand, J. H., and Baker, E. M.: Transfer Processes in Annuli. Trans. American Inst. Chem. Eng., vol. 38, sec. A, no. 3, June 25, 1942, pp. 569-592.
5. McAdams, William H.: Heat Transmission. First ed., McGraw-Hill Book Co., Inc., 1933.
6. Bakmeteff, Boris A.: The Mechanics of Turbulent Flow. Princeton Univ. Press, 1941.
7. Joyner, Upshur T.: Mathematical Analysis of Aircraft Intercooler Design. NACA TN No. 781, 1940.
8. Silverstein, Abe: High-Altitude Cooling. I - Résumé of the Cooling Problem. NACA ARR No. L4111, 1944.
9. Henry, John R.: Design of Power-Plant Installations. Pressure-Loss Characteristics of Duct Components. NACA ARR No. L4F26, 1944.
10. Taylor, G. I., and Maccoll, J. W.: The Mechanics of Compressible Fluids. Steady Flow through Channels. Vol. III of Aerodynamic Theory, div. H, ch. II, secs. 2 and 3, W. F. Durand, ed., Julius Springer (Berlin), 1935, pp. 222-226.
11. Pinkel, Benjamin, and Turner, L. Richard: Thermodynamic Data for the Computation of the Performance of Exhaust-Gas Turbines. NACA ARR No. 4B25, 1944.
12. Tribus, Myron, and Boelter, L. M. K.: An Investigation of Aircraft Heaters. II - Properties of Gases. NACA ARR, Oct. 1942.

13. Faires, Virgil Moring: Applied Thermodynamics. The Macmillan Co., 1943.
14. Boelter, L. M. K., and Sharp, W. H.: An Investigation of Aircraft Heaters. XVI - Determination of the Viscosity of Exhaust Gases from a Gasoline Engine. NACA ARR No. 4F24, 1944.
15. Kennard, Earle H.: Kinetic Theory of Gases. McGraw-Hill Book Co., Inc., 1938.
16. Chapman, Sydney, and Cowling, T. G.: The Mathematical Theory of Non-Uniform Gases. Cambridge Univ. Press, 1939.
17. National Research Council: International Critical Tables. Vol. V. McGraw-Hill Book Co., Inc., 1929.

TABLE 1  
APPROXIMATE VALUES OF VARIABLES INVOLVED IN ISOTHERMAL  
AND HEAT-TRANSFER TESTS

Test	Type of test	Range of variables					Fuel-air ratio
		Cooling-air Reynolds number, $\rho V(d_n - d_p)/\mu$	Exhaust-gas Reynolds number, $\rho V d/\mu$	Exhaust-gas Prandtl number, $\mu g/k$	Exhaust-gas temperature, $^{\circ}F$	Exhaust-gas temperature, $^{\circ}C$	
A	Isothermal	100,000 to 300,000	-----	-----	-----	-----	-----
B	Heat transfer	265,000	220,000	0.59 to 0.66	1160 to 1500	0.063 to 0.090	
C <sub>1</sub>	Heat transfer	170,000	180,000 to 220,000	0.64 to 0.65	920 to 1270	0.078	
C <sub>2</sub>	Heat transfer	250,000	215,000 to 360,000	0.58 to 0.61	1150 to 1420	0.089	
D	Heat transfer	170,000 to 260,000	189,000	0.64	1170	0.078	

TABLE 2

EFFECTS OF APPROXIMATIONS AND FAIRING METHODS ON  
DESIGN TEMPERATURES AND PRESSURE LOSSES

(a) Effect of using air properties in place of gas properties				
Design temperatures	Station	Percent error due to use of air properties		
Exhaust gas, $t_e$	2	0.2		
	3	0.2		
Cooling air, $t_a$	2	-1.0		
	3	-1.5		
Exhaust pipe, $t_p$	1	-4.5		
	2	-3.5		
	3	-3.0		
(b) Effect of using constant values of specific heat in place of integrated mean values				
Design temperatures	Station	Percent error due to use of constant values of specific heats		
Exhaust gas, $t_e$	2	-0.3 to 0.0		
	3	-0.4 to 0.2		
Cooling air, $t_a$	2	-0.3 to 0.8		
	3	-0.6 to 0.5		
Exhaust pipe, $t_p$	1	-0.3 to 0.3		
	2	-0.5 to 0.3		
	3	-0.6 to 0.5		
(c) Effect of fairing method on measured pressure losses				
Shroud-segment length		Percent deviation from results on original fairing - methods of reference 6		
		Arithmetic mean	Extreme fairing	Coinciding rake fairing
$\Delta H_{1-2}$		$\pm 2.0$	1.1	-2.0
$\Delta H_{1-3}$		$\pm 3.0$	-1.3	-0.3
(d) Effect of fairing method on design temperatures				
Design temperatures	Station	Percent deviation from results on original fairing - methods of reference 6		
		Arithmetic mean	Extreme fairing	Coinciding rake fairing
Exhaust gas, $t_e$	2	1.3	-0.3	-1.0
	3	1.0	-0.3	-1.0
Cooling air, $t_a$	2	3.0	0.8	2.0
	3	3.5	0.6	1.4
Exhaust pipe, $t_p$	1	0.3	-1.0	-0.7
	2	1.3	-0.8	-1.2
	3	1.1	-0.4	-0.8

TABLE 3  
CALCULATION FORM FOR SHROUD DESIGN - PARALLEL FLOW

Step	Item <sup>1</sup>	Quantity	Source	Symbol	Units
Factors for design					
	(1)	Brake horsepower	Manufacturer	bhp	hp
	(2)	Fuel-air ratio	Manufacturer	f	
1	(3)	Exhaust-gas-flow rate through engine	Manufacturer's data or equation (47)	$\dot{W}_o$	lb/sec
2	(4)	Exhaust-gas temperature at shroud entrance	Manufacturer's data and equation (48) or analytical method	$t_{e1}$	$^{\circ}F$
3	(5)	Exhaust-pipe diameter (outer)	Manufacturer	$d_p$	in
4	(6)	Velocity of airframe	Performance data	$V_o$	ft/sec
	(7)	Altitude	Performance data		ft
5	(8)	Exhaust-pipe material	Manufacturer		18-8 stainless steel
	(9)	Design exhaust-gas temperature	Manufacturer	$t_{e2}$	$^{\circ}F$
6	(10)	Design exhaust-pipe temperature	Manufacturer	$t_p$	$^{\circ}F$
7	(11)	Design shroud temperature	Manufacturer	$t_{e2}$	$^{\circ}F$
Pressure drop available at shroud entrance					
4	(12)	Free-stream static pressure	(7) and reference 8	$P_o$	lb/ft <sup>2</sup>
	(13)	Free-stream temperature	(7) and reference 8	$T_o$	$^{\circ}F$ abs.
	(14)	Free-stream density	(7) and reference 8	$\rho_o$	slugs/ft <sup>3</sup>
	(15)	Free-stream dynamic pressure	(14) $\times$ (6) <sup>2</sup> $\times V_{co}$ <sup>2</sup> /2	$q_o$	lb/ft <sup>2</sup>

<sup>1</sup>Items are carried in parentheses to indicate row used in calculations.

TABLE 3 - Continued  
 CALCULATION FORM FOR BOUND LINES - FLOWING FLOW - Continued

Step	Item	Quantity	Source	Symbol	Units														
Pressure drop available at throat entrance																			
9	(16)	Flowing-air-flow rate	Assumed (approximately 1/8 to 1/4 of (3))	$W_a$	lb/sec	1.00	1.00	1.00	1.00	1.00	1.00	1.00	1.00	1.00	1.00	1.00	1.00	1.00	
	(17)	Cross-sectional area of inlet duct straight section	Area of straight section of assumed inlet duct	$A_1$	$ft^2$	0.1847													0.1864
	(18)	Length of inlet duct straight section	Length of straight section of assumed inlet duct	$L_1$	ft	6													6
	(19)	Hydraulic diameter of inlet duct straight section	$4 \times (\pi r^2) / \text{Perimeter of inlet duct straight section}$	$D_1$	ft	0.498													0.50
	(20)	Dynamic pressure in straight section	$0.0048 \times [(W_a / (\pi r^2))^2 / (2g)]$	$q_1$	lb/ft <sup>2</sup>	4.98	29.90	14.779	79.68	184.41	3.70	14.00	31.49	70.99	87.49				
	(21)	$K_{b0}$	$[(13) - 460]$ and figure 19	$K_{b0}$	$\frac{\text{slugs}}{(\text{sec})^2 (ft)}$	0.317 x 10 <sup>-6</sup>													0.317 x 10 <sup>-6</sup>
10	(22)	$Z_1$	$0.001 \times (25) \times (29) / [(\pi r^2) \times (21)]$	$Z_1$		139.970	871.940	427.930	243.880	679.800	129.440	848.960	373.440	471.980	682.400				
	(23)	Friction factor	(26) and reference 9	$f_1$		0.00218	0.00445	0.00432	0.00332	0.00377	0.00221	0.00428	0.00461	0.00398	0.00385				
	(24)	Friction pressure loss in straight-section inlet duct	$4 \times (28) \times (20) \times (23) / (19)$	$\Delta P_1$	lb/ft <sup>2</sup>	1.33	4.68	9.60	16.10	84.07	0.87	3.03	6.30	10.27	19.79				
Where the inlet duct contains more than one straight section, the calculations of items (16) to (24) are repeated to determine the pressure loss in each straight section. If the inlet duct contains bends and/or diffusers supplementary calculations must be made to calculate the pressure losses in each bend and/or diffuser as given by the equation and method of step 10 of the single-segment design procedure.																			
	(25)	Total pressure drop in inlet duct	$0.05 \times (15) + \sum (24) + \sum \frac{\text{Bend and diffuser losses}}{\text{Losses}}$	$\Delta P_{T-1}$	lb/ft <sup>2</sup>	6.47	9.76	14.79	21.84	89.01	6.01	8.17	11.44	15.71	60.93				
	(26)	Pressure drop available at throat entrance	(15) - (25)	$\Delta P_{\text{available}}$	lb/ft <sup>2</sup>	96.33	93.04	86.06	81.95	71.59	96.79	94.65	91.36	87.09	81.87				

Values are carried in parentheses to indicate row used in calculations.

NATIONAL ADVISORY  
 COMMITTEE FOR AERONAUTICS

TABLE 3 - Continued  
 CALCULATIONS FROM THE HEAT EXCHANGER - MAINLINE FLOW - Continued

Step Item <sup>1</sup>	Quantity	Source	Symbol	Units														
Pressure drop available at axial entrance																		
9	(16)	Cooling-air-flow rate	$\dot{V}_a$	lb/sec														
	(17)	Cross-sectional area of inlet duct straight section	$A_1$	ft <sup>2</sup>														
	(18)	Length of inlet duct straight section	$L_1$	ft														
	(19)	Hydraulic diameter of inlet duct straight section	$D_1$	ft														
	(20)	Dynamic pressure in straight section	$q_1$	lb/ft <sup>2</sup>														
	(21)	$P_{a0}$	$P_{a0}$	lb/ft <sup>2</sup>														
30	(22)	$P_1$	$P_1$	lb/ft <sup>2</sup>														
	(23)	Friction factor	$f_1$															
	(24)	Friction pressure loss in straight-section inlet duct	$\Delta P_1$	lb/ft <sup>2</sup>														
<p>Where the inlet duct contains more than one straight section the calculations of items (16) to (24) are repeated to determine the pressure loss in each straight section. If the inlet duct contains bends and/or diffusers supplementary calculation forms will be needed to calculate the pressure losses in each bend and/or diffuser as given by the equation and method of step 10 of the single-segment design procedure.</p>																		
	(25)	Total pressure drop in inlet duct	$\Delta P_{0-1}$	lb/ft <sup>2</sup>														
	(26)	Pressure drop available at axial entrance	$\Delta P_{available}$	lb/ft <sup>2</sup>														

<sup>1</sup>Items are carried in parentheses to indicate row used in calculations.

TABLE 3 - Continued  
 CALCULATED FROM THE DESIGN TABLES - SUBCATEGORIES 7, 8, 9 - Continued

Design Variable	Quantity	Formula	Units	Table						
11 (17)	Length of thermal segment	As usual	ft	18	18	18	18	18	18	18
12 (18)	Segment diameter	As usual	in	0.001	0.001	0.001	0.001	0.001	0.001	0.001
13 (19)	Sealing-air flow rate	As usual	lb/min	0.001	0.001	0.001	0.001	0.001	0.001	0.001
Cooling-air conditions at axial stations										
(20)	Exhaust-air stagnation temperature	(13) + 0.0005(17) <sup>2</sup>	°R	149.6	149.6	149.6	149.6	149.6	149.6	149.6
(21)	Exhaust-air static pressure at axial station	(16) and (17) and figure 16	lb/in <sup>2</sup>	97.11	97.11	97.11	97.11	97.11	97.11	97.11
(22)	Exhaust-air static pressure at axial station	(16) + (13)	lb/in <sup>2</sup>	785.81	785.81	785.81	785.81	785.81	785.81	785.81
(23)	$(h_2 - h_1)$	(16) - (17)	°R	0.3859	0.3859	0.3859	0.3859	0.3859	0.3859	0.3859
(24)	$\frac{2.378h_1 \sqrt{h_2}}{(h_2 - h_1)^{1/2}} \times 10^3$	$2.378h_1 \sqrt{h_2} / [(h_2 - h_1)^{1/2}] \times 10^3$		0.2203	0.2203	0.2203	0.2203	0.2203	0.2203	0.2203
(25)	$(h_2 - h_1) / h_1$	(14) and figure 16		0.00080	0.00080	0.00080	0.00080	0.00080	0.00080	0.00080
(26)	Exhaust-air static pressure at axial station	(18) [1 - (25)]	lb/in <sup>2</sup>	773.1	773.1	773.1	773.1	773.1	773.1	773.1
(27)	Exhaust-air temperature at axial station	(20) [(26)/(20)] <sup>0.488 - 1.60</sup>	°R	781.1	781.1	781.1	781.1	781.1	781.1	781.1
Exhaust-subsonic temperature										
(28)	$T_{0.8}$	(3) and table 5	°R	3.271	3.271	3.271	3.271	3.271	3.271	3.271
(29)	$T_{0.4}$	(2) and table 5	°R	0.4958	0.4958	0.4958	0.4958	0.4958	0.4958	0.4958
(30)	$\frac{1}{2} (T_{0.8} + T_{0.4}) / h_1$	(1) and figure 16	°R	0.775	0.775	0.775	0.775	0.775	0.775	0.775
(31)	Heat-transfer coefficient on air side	0.00225 x (30) x (16)/(18)	lb/in <sup>2</sup>	0.00225	0.00225	0.00225	0.00225	0.00225	0.00225	0.00225
(32)	Factor depending on ratio of pipe diameters	(16)/(15) and figure 20		1.008	1.008	1.008	1.008	1.008	1.008	1.008
(33)	$h_2$	(17) and figure 13		0.0003	0.0003	0.0003	0.0003	0.0003	0.0003	0.0003
(34)	$T_{0.8}$	(2) and table 5	°R	0.374	0.374	0.374	0.374	0.374	0.374	0.374
(35)	$(h_2 - h_1) / h_1$	(16) - (17)		0.0003	0.0003	0.0003	0.0003	0.0003	0.0003	0.0003
(36)	Heat-transfer coefficient on air side	0.00225 x (34) x (33) x (34)	lb/in <sup>2</sup>	0.00225	0.00225	0.00225	0.00225	0.00225	0.00225	0.00225
(37)	$h_2$	(1) x (31) + (17) x (17)	°R	33.28	33.28	33.28	33.28	33.28	33.28	33.28
(38)	$h_2$	(13) + (17)	°R	314.8	314.8	314.8	314.8	314.8	314.8	314.8
(39)	Exhaust-subsonic temperature	(16)/(16)	°R	314.8	314.8	314.8	314.8	314.8	314.8	314.8

\*Values are corrected in parentheses to include air used in calculations.

TABLE 3 - Continued  
 CALCULATION FORM FOR HEATED TUBES - HEATED FLOW - Continued

Step No.	Quantity	Source	Symbol	Units	Range variables													
11	(17) Length of heated segment	Assumed	L	ft.	18													
12	(18) Internal diameter	Assumed	$d_i$	in.	0.750													
13	(19) Heating-air-flow rate	Assumed	$\dot{m}_a$	lb/min	0.50	1.00	1.50	2.00	2.50	3.00	3.50	4.00	4.50	5.00	5.50	6.00	6.50	7.00
Cooling-air conditions at inlet entrance																		
(20)	Free-stream stagnation temperature	(23) + 0.000029( $\dot{m}_a$ ) <sup>2</sup>	$T_{01}$	°R	109.6													
(21)	Pressure drop available for static air at inlet entrance	(16) and curve of Figure 10 for static air at inlet entrance substituted by step 13	$\Delta p_{s1}$	lb/ft <sup>2</sup>	97.11	95.74	94.37	93.00	91.63	90.26	88.89	87.52	86.15	84.78	83.41	82.04	80.67	79.30
(22)	Total pressure at inlet entrance	(21) + (24)	$p_{t1}$	lb/ft <sup>2</sup>	705.81	703.48	701.15	698.82	696.49	694.16	691.83	689.50	687.17	684.84	682.51	680.18	677.85	675.52
(23)	$(p_{t1}^2 - p_{t2}^2) / \rho_1$	(16) <sup>2</sup> - (21) <sup>2</sup>			0.0941													
(24)	$\frac{2.3324 \sqrt{p_{t1}}}{\sqrt{(p_{t1}^2 - p_{t2}^2) / \rho_1} + 2.00}$	1.0544 (16) / (21) + (23)			0.0673	0.1942	0.0009	0.0725	0.3432	0.0297	0.1113	0.1596	0.0297	0.0297	0.0297	0.0297	0.0297	0.0297
(25)	Cooling-air static pressure at inlet entrance	(24) and Figure 22	$p_{s1}$	lb/ft <sup>2</sup>	0.0024	0.0024	0.0024	0.0024	0.0024	0.0024	0.0024	0.0024	0.0024	0.0024	0.0024	0.0024	0.0024	0.0024
(26)	Cooling-air static pressure at inlet entrance	(24) [(20) / (25)] <sup>0.05</sup> - 140	$p_{s1}$	°R	90.18	90.18	90.18	90.18	90.18	90.18	90.18	90.18	90.18	90.18	90.18	90.18	90.18	90.18
Uniform coolant-gas temperature																		
(27)	$T_{01}$	(23) and table 5			3.521													
(28)	$T_{02}$	(5) and table 5			0.0496													
(29)	$\frac{h_c (T_{01} - T_{02}) / \rho_1 \Delta p_{s1}}{h_c (T_{01} - T_{02}) / \rho_1 \Delta p_{s1}}$	(4) and Figure 24			0.728													
(30)	Static-pressure coefficient on gas side	0.00225 x (29) x (10) / (27)	$\lambda_0$	$\frac{p_{s1}}{(\rho_1 \Delta p_{s1}) / \rho_1}$	0.0189													
(31)	Factor depending on ratio of Reynolds numbers	(16) / (25) and Figure 25	$\phi$		1.118													
(32)	$\lambda_0 \phi$	(27) and Figure 13			0.0024	0.0024	0.0024	0.0024	0.0024	0.0024	0.0024	0.0024	0.0024	0.0024	0.0024	0.0024	0.0024	0.0024
(33)	$\lambda_0 \phi$	(29) and table 5			0.074	1.000	1.325	1.741	2.157	2.573	2.989	3.405	3.821	4.237	4.653	5.069	5.485	5.901
(34)	$(\lambda_0 \phi + \lambda_0)^{0.8}$	(33) + (29)			1.113													
(35)	$(\lambda_0 \phi - \lambda_0)$	(16) - (29)			0.0217													
(36)	Heat-transfer coefficient on air side	0.00225 x (16) x (10) x (34) / (27) x (16)	$h_c$	$\frac{p_{s1}}{(\rho_1 \Delta p_{s1}) / \rho_1}$	0.0016	0.0016	0.0016	0.0016	0.0016	0.0016	0.0016	0.0016	0.0016	0.0016	0.0016	0.0016	0.0016	0.0016
(37)	$h_c \lambda_0 + h_c \lambda_0$	(1) x (33) + (27) x (17)			33.98	33.94	33.89	33.84	33.79	33.74	33.69	33.64	33.59	33.54	33.49	33.44	33.39	33.34
(38)	$h_c + h_c$	(33) + (17)			15.1	15.0	14.9	14.8	14.7	14.6	14.5	14.4	14.3	14.2	14.1	14.0	13.9	13.8
(39)	Uniform coolant-gas temperature	(16) / (16)	$T_{02}$	°R	15.1	15.0	14.9	14.8	14.7	14.6	14.5	14.4	14.3	14.2	14.1	14.0	13.9	13.8

Values are carried 20 parentheses to indicate use need 5x underlines.

TABLE 3 - Continued

CALCULATIONS FOR THE MIXED BROWNE - MORGAN STAY - Continued

Step	Item	Quantity	Source	Symbol	Units	Densities column-gas temperatures												
8	(51)	Molecular weight of column gas	(9) and 21 numbers	$M_p$		0.70												
	(52)	$(\frac{p_{21}}{p_{22}} - \frac{p_{21}}{p_{23}})$	(20) - (27)			2039	1971	2061	1928	1968	1943	2085	1933	2060	1937	1939	1904	
	(53)	$(\frac{p_{21}}{p_{22}}) \frac{p_{21}}{p_{23}}$	$\left\{ \frac{[(20) + (46)]}{(200)} \right\}^2$			146,980	202,650	71,040	168,170	186,890	100,570	82,540	68,038	185,580	145,340	110,710	102,000	85,200
	(54)	$(\frac{p_{21}}{p_{22}}) \frac{p_{21}}{p_{23}}$	$\left\{ \frac{[(27) + (46)]}{(200)} \right\}^2$			394	318	963	337	327	305	876	824	339	328	301	306	284
	(55)	Reduced heat-conductivity coefficient	$0.00049 \times (21) \times \left\{ \frac{[(23) - (54)]}{(200)} \right\}^2$		$\frac{21 \times 10^6}{(200)^2 \times (27)}$	0.00088	0.00031	0.00044	0.00090	0.00087	0.00080	0.00087	0.00087	0.00086	0.00075	0.00079	0.00084	0.00081
	(56)	$\left( \frac{2}{p_{21}} + \frac{2}{p_{22}} \right)$	$\frac{2}{(27) + (26)} + \frac{2}{(41)}$			196.9	164.8	244.4	811.5	168.3	168.5	246.5	246.4	811.0	252.6	277.0	168.6	238.8
	(57)	$\frac{21 \times 10^6}{p_{21} p_{22} p_{23}}$	$20.47 \times (2) \times \frac{(27)}{(27) \times (41)}$			37.86												
	(58)	$\frac{p_{21} p_{22}}{p_{21} p_{22} p_{23}}$	$1.49 \times (3) / (29)$		$\Sigma$	28.18	6.05	4.033	22.30	6.05	4.033	3.092	8.42	18.1	6.05	4.033	3.092	8.42
	(59)	$\frac{p_{21}}{p_{22}}$	$(27) \left[ 1 + \frac{(28)}{(29)} \right] / (26)$			1.1290	0.7021	0.6889	1.1063	0.6906	0.6931	0.4993	0.4433	1.0285	0.6438	0.5970	0.4427	0.4028
	(60)	$\frac{p_{21}}{p_{22}}$	$\frac{p_{21}}{p_{22}}$			3.0838	0.4395	1.8636	3.084	1.992	1.739	1.485	1.225	8.088	1.924	1.668	1.277	1.494
(61)	$(\frac{p_{21}}{p_{22}} - \frac{p_{21}}{p_{23}}) \frac{p_{21}}{p_{23}}$	$(4) - (27)$			183	150	1977	189	183	184	198	187	181	183	187	184	187	
(62)	$(\frac{p_{21}}{p_{22}} - \frac{p_{21}}{p_{23}}) \frac{p_{21}}{p_{23}}$	$(61) / (60)$			58	84	977	66	80	202	130	208	69	93	129	118	203	
(63)	$\frac{p_{21}}{p_{22}} + \frac{p_{21}}{p_{23}}$	$(4) \times (28) + (27)$			21,720	10,820	7880	21,748	10,800	7817	5402	4278	24,750	20,827	7883	5438	4699	
(64)	Densities column-gas temperatures	$[(61) + (62)] / [1 + (58)]$		$\rho_{p_2}$	170	266	1689	3706	1670	1645	1683	1684	1683	1677	1685	1686	1681	
Densities cooling-air temperatures												Densities column-gas temperatures						
10	(65)	$\frac{p_{21} p_{22}}{p_{21} p_{22} p_{23}}$	$(58) [(4) - (61)] + (27)$	$\rho_{p_2}$		1141	627	628	1106	728	588	424	379	2070	711	548	495	397
	(66)	Densities column-gas temperatures	$(41) \times (64) + (47) \times (63)$	$\rho_{p_2}$		3645	3642	3542	3532	3540	3459	3474	3481	3478	3467	3448	3438	3426
(67)	Densities column-gas temperatures	$(65) / (46)$		$\rho_{p_2}$	1680	1448	1310	1689	1448	1469	1683	1675	1681	1683	1684	1686	1686	

\*Values are omitted in parentheses to indicate they were used in calculations.

RESEARCH AIR FORCE  
COMMISSION FOR AERONAUTICS

TABLE 3 - Continued

CALCULATIONS FROM FOR ENGINE DESIGN - REGULATED FLOW - Continued

Step	Symbol	Quantity	Source	Units	Downstream exhaust-gas temperature											
8	(21)	Exhaustivity of exhaust pipe	(8) and 14	$\epsilon_p$	0.70											
	(24)	$(h_{p1} - h_{p2})$	(9) - (37)		1678	1772	1867	1971	1694	1535	1475	1493				
	(23)	$(h_{p1} - h_{p2}) / 100$	$\frac{[(9) + 162] / 100}{h_p}$		16.78	17.72	18.67	19.71	16.94	15.35	14.75	14.93				
	(24)	$(h_{p1} - h_{p2}) / 100$	$\frac{[(37) + 162] / 100}{h_p}$		139	136	139	144	140	137	133	137				
	(25)	Radial heat-transfer coefficient	$0.00048 \times (21) \times [(23) - (24)] / (22)$	$h_r$	0.00221	0.00341	0.00475	0.00620	0.00768	0.00928	0.01098	0.01273				
	(26)	$\left( \frac{1}{h_p} + \frac{1}{h_r} \right)$	$\frac{1}{(47) + (25)} + (11)$		288.0	295.7	304.6	314.0	323.0	331.7	340.8	349.6				
	(27)	$\frac{h_p}{(h_p + h_r)}$	$30.47 \times (5) \times (47) / (31)$		17.86											
	(28)	$\frac{h_p}{h_p + h_r}$	$1.45 \times (3) / (50)$		12.1	6.05	3.025	2.42	21.1	6.05	4.033	3.025	2.42			
	(29)	$\alpha$	(27) $\frac{1}{1 + (28)}$		1.026	0.621	0.476	0.4109	1.043	0.2803	0.4245	0.2803	0.2230			
	(30)	$\phi$	$\frac{h_p}{h_p + h_r}$		2.750	1.84	1.610	1.508	2.750	1.809	1.610	1.508	1.421			
(31)	$(h_{p1} - h_{p2})$	(4) - (37)		1031	1022	1014	1007	1001	995	989	983	977				
(32)	$(h_{p1} - h_{p2}) / \phi$	(61) / (30)		696	993	1110	1069	671	1013	1164	1244	1293				
(33)	$h_{p1} + h_{p2}$	(4) $\times$ (38) + (37)		21,750	30,808	7880	5408	4314	21,750	20,898	7821	24,328	4319			
(34)	Downstream exhaust-gas temperature	$[(61) + (62)] / [1 + (28)]$		1710	1681	1628	1646	1632	1711	1694	1667	1694	1641			
17	(35)	Downstream cooling-air temperature	(28) $[(4) - (61)] + (37)$	$t_{ca}$	2056	688	782	364	1046	670	593	407	345			
	(36)	Downstream exhaust-pipe temperature	(11) $\times$ (61) + (47) $\times$ (35)	$t_{pe}$	34.24	33.94	33.46	33.23	33.96	33.62	33.37	33.16	32.92			
18	(37)	Downstream exhaust-pipe temperature	(65) / (49)	$t_{pe}$	1693	1640	1574	1508	1461	1399	1349	1305	1265			

Values are carried in parentheses to indicate use in calculations.

INTERNAL SECURITY  
COMMITTEE FOR ASSASSINATIONS

TABLE 5 - Continued

CALCULATED FROM FOR GIVEN DESIGN - SWIRLING FLOW - Continued

Step No.	Quantity	Source	Symbol	Units			
19	Minimum diameter	Calculated from critical temperature plus one-half inch for safety margin in step 19	$d_c$	in	0.667	0.710	0.752
20	Cooling-air flow rate		$\dot{V}_a$	lb/min	1.28	1.94	2.37
(70)	Upstream cooling-air static pressure	$(69) (69)$ and error plotted against $\dot{V}_a$	$P_{s1}$	lb/in <sup>2</sup>	678	680	680
(71)	Upstream cooling-air temperature		$t_{s1}$	°F	-98	-37	-36.5
(72)	Downstream cooling-air temperature		$t_{s2}$	°F	580	110	568
(73)	Downstream cooling-air static pressure	$P_{s2} = P_{s1} = (10)$	$P_{s2}$	lb/in <sup>2</sup>	688.1		
(74)	Upstream cooling-air density	$0.00098 \times (70) / [(71) + 146]$	$\rho_{s1}$	slugs/ft <sup>3</sup>	0.000937	0.000937	0.000936
(75)	Downstream cooling-air density	$0.00098 \times (73) / [(72) + 146]$	$\rho_{s2}$	slugs/ft <sup>3</sup>	0.000974	0.000974	0.000974
(76)	$\left(1 + \frac{P_{s1}}{P_{s2}}\right)$	$1 + [(74)/(75)]$			3.907	3.303	3.117
(77)	$\dot{V}_a^{1.0}$	(69) and table 2			8.38	3.898	4.72
(78)	$(t_{s1} + t_{s2})^{1.0}$	$[(68) + (9)]$ and table 2			1.837	1.313	1.411
(79)	$(t_{s1} - t_{s2})^{1.0}$	$[(68) - (9)]$			0.00902	0.0160	0.00923
(80)	$\rho_{s1}^{0.8}$	(71) and table 13			0.0502	0.0502	0.0503
(81)	Relative pressure drop referred to standard density	$0.0577 \times (87) \times (76) \times (77) \times (80) / (78) \times (79)$	$\rho_{s1} \rho_{s2}$	lb/ft <sup>2</sup>	59.07	10.57	33.10
(82)	$\frac{P_{s1}}{P_{s2}} - 1$	$[8 \times (74)/(75)] - 1$			4.015	3.606	3.633
(83)	$\dot{V}_a^2$	(69) <sup>2</sup>			8.684	3.764	5.627
(84)	$(t_{s1} + t_{s2})^2$	$[(68) + (9)]^2$			1.866	1.368	1.469
(85)	$(t_{s1} - t_{s2})^2$	$[(68) - (9)]^2$			0.0436	0.0694	0.0863
(86)	Wetted and exiting pressure drop referred to standard density	$0.388 \times (80) \times (81) / [(82) \times (85)]$	$\rho_{s1} (\rho_{s1} + \rho_{s2})$	lb/ft <sup>2</sup>	68.68	21.30	47.80
(87)	Total pressure drop referred to standard density	$(81) + (86)$	$\rho_{s1} \Delta P$	lb/ft <sup>2</sup>	121.75	22.47	60.3
(88)	Cooling-air pressure drop in throat	$0.000978 \times (87) / (74)$	$\Delta P$	lb/ft <sup>2</sup>	399.0	934.7	807.1

\*Items are carried in parentheses to indicate use in calculations.

TABLE 4  
CALCULATION FORM FOR SHROUD DESIGN - COUNTERFLOW

Step	Item <sup>1</sup>	Quantity	Source	Symbol	Units	
Factors for design						
	(1)	Brake horsepower	Manufacturer	bhp	hp	
	(2)	Fuel-air ratio	Manufacturer	f		
1	(3)	Exhaust-gas-flow rate through engine	Manufacturer's data or equation (47)	$\dot{W}_e$	lb/sec	
2	(4)	Exhaust-gas temperature at shroud entrance	Manufacturer's data and equation (48) or analytical method	$t_{e1}$	$^{\circ}F$	
3	(5)	Exhaust-pipe diameter (outer)	Manufacturer	$d_p$	ft	
4	(6)	Velocity of airplane	Performance data	$V_o$	ft/sec	
	(7)	Altitude	Performance data		ft	
	(8)	Exhaust-pipe material	Manufacturer			
5	(9)	Design exhaust-gas temperature	Manufacturer	$t_{e2}$	$^{\circ}F$	
6	(10)	Design exhaust-pipe temperature	Manufacturer	$t_{p1}$	$^{\circ}F$	
7	(11)	Design shroud temperature	Manufacturer	$t_{s1}$	$^{\circ}F$	
Pressure drop available at shroud entrance						
8	(12)	Free-stream static pressure	(7) and reference 8	$P_o$	lb/ft <sup>2</sup>	
	(13)	Free-stream temperature	(7) and reference 8	$T_o$	$^{\circ}F$ abs	
	(14)	Free-stream density	(7) and reference 8	$\rho_o$	slugs/ft <sup>3</sup>	
	(15)	Free-stream dynamic pressure	(14) $\times$ (6) <sup>2</sup> $\times T_{o0}/2$	$q_{o0}$	lb/ft <sup>2</sup>	
9	(16)	Cooling-air-flow rate	Assumed (approximately 1/8 to 1/2 of (3))	$\dot{W}_a$	lb/sec	
10	(17)	Gross-sectional area of inlet-duct straight section	Area of straight section of assumed inlet duct	$A_1$	ft <sup>2</sup>	
	(18)	Length of inlet duct straight section	Length of straight section of assumed inlet duct	$L_1$	ft	
	(19)	Hydraulic diameter of inlet duct straight section	$4 \times (17) / \text{Perimeter of inlet duct straight section}$	$D_1$	ft	
	(20)	Dynamic pressure in straight section	$0.00048 \times [(15)/(17)]^2 / (14)$	$q_1$	lb/ft <sup>2</sup>	
	(21)	$\mu_{a0}$	$[(13) - 460]$ and figure 19	$\mu_{a0}$	$\frac{\text{slugs}}{(\text{sec})(ft)}$	
	(22)	$R_1$	$0.031 \times (16) \times (19) / [(17) \times (21)]$	$R_1$		
	(23)	Friction factor	(22) and reference 9	$f_1$		
	(24)	Friction pressure loss in straight-section inlet duct	$4 \times (18) \times (20) \times (23) / (19)$	$\Delta E_1$	lb/ft <sup>2</sup>	
	Where the inlet-duct contains more than one straight section, the calculations of items (16) to (24) are repeated to determine the pressure loss in each straight section. If the intake duct contains bends and/or diffusers, supplementary calculation forms will be needed to calculate the pressure losses in each bend and/or diffuser as given by the equation and method of step 10 of the single-segment design procedure.					
	(25)	Total pressure drop in inlet duct	$0.05 (15) + \sum (24) + \sum \text{Bend and diffuser losses}$	$\Delta E_{0-2}$	lb/ft <sup>2</sup>	
(26)	Pressure drop available at shroud entrance	(15) - (25)	$\Delta E_{\text{available}}$	lb/ft <sup>2</sup>		

<sup>1</sup>Items are carried in parentheses to indicate row used in calculations.

TABLE 4 - Continued

## CALCULATION FORM FOR SHROUD DESIGN - COUNTERFLOW - Continued

Step	Item <sup>1</sup>	Quantity	Source	Symbol	Units
Design variables					
11	(27)	Length of shroud segment	Assumed	$l$	ft
12	(28)	Shroud diameter	Assumed	$d_s$	ft
9	(29)	Cooling-air-flow rate	Assumed	$V_a$	lb/sec
Cooling-air conditions at shroud entrance					
13	(30)	Free-stream stagnation temperature	(13) + 0.000832 (6) <sup>2</sup>	$T_{o_0}$	°F abs
	(31)	Pressure drop available at shroud entrance	(29) and curve of $\Delta H_{available}$ for inlet duct selected by step (10)	$\Delta H_{available}$	lb/ft <sup>2</sup>
	(32)	Total pressure at shroud entrance	(12) + (31)	$H_{o_2}$	lb/ft <sup>2</sup>
	(33)	$d_s^2 - d_p^2$	(28) <sup>2</sup> - (5) <sup>2</sup>		
	(34)	$1.384 V_a \sqrt{\pi_{o_0}} / [(d_s^2 - d_p^2) \times H_{o_2}]$	$1.384 \times (29) \times (30)^{1/2} / [(32) \times (33)]$		
	(35)	$(H_{o_2} - P_{o_2}) / H_{o_2}$	(34) and figure 16		
	(36)	Cooling-air static pressure at shroud entrance	(32) [1 - (35)]	$P_{o_2}$	lb/ft <sup>2</sup>
14	(37)	Cooling-air temperature at shroud entrance	(30) [(36)/(32)] <sup>0.286</sup> - 460	$t_{o_2}$	°F
Downstream exhaust-gas temperature					
15	(38)	$V_g^{0.8}$	(3) and table 5		
	(39)	$d_p^{1.8}$	(5) and table 5		
	(40)	$k_g (Pr_g)^{0.4} / \mu_g^{0.8}$	(4) and figure 14		
	(41)	Heat-transfer coefficient on gas side	$0.001735 \times (38) \times (40)/(39)$	$h_g$	$\frac{\text{Btu}}{(\text{sec})(\text{ft}^2)(\text{°F})}$
	(42)	Factor depending on ratio of pipe diameters	(28)/(5) and figure 15	$\phi$	
	(43)	$\mu_g^{0.2}$	(37) and figure 13		
	(44)	$V_a^{0.8}$	(29) and table 5		
	(45)	$(d_s + d_p)^{0.8}$	[(28) + (5)] and table 5		
	(46)	$(d_s - d_p)$	(28) - (5)		
	(47)	Heat-transfer coefficient on air side	$\frac{0.01728 \times (42) \times (43) \times (44)}{(45) \times (46)}$	$h_a$	$\frac{\text{Btu}}{(\text{sec})(\text{ft}^2)(\text{°F})}$
(48)	$h_g t_{o_1} + h_a t_{o_2}$	(4) × (41) + (37) × (47)			
(49)	$h_g + h_a$	(41) + (47)			
(50)	Downstream exhaust-pipe temperature	(48)/(49)	$t_{p_2}$	°F	
8	(51)	Emissivity of exhaust pipe	(8) and literature	$\epsilon_p$	
15	(52)	$(t_{p_2} - t_{o_2})$	(50) - (37)		
	(53)	$(\frac{t_{p_2}}{100})^4$	$\{[(50) + 460]/100\}^4$		
	(54)	$(\frac{t_{o_2}}{100})^4$	$\{[(37) + 460]/100\}^4$		

<sup>1</sup>Items are carried in parentheses to indicate row used in calculations.

TABLE 4 - Continued

CALCULATION FORM FOR SHROUD DESIGN - COUNTERFLOW - Continued

Step	Item <sup>1</sup>	Quantity	Source	Symbol	Units
Downstream exhaust-gas temperature					
15	(55)	Radiant heat-transfer coefficient	$0.00048 \times (51) \times [(53) - (54)] / (52)$	$h_r$	$\frac{\text{Btu}}{(\text{sec})(\text{ft}^2)(^\circ\text{F})}$
	(56)	$\left(\frac{1}{h_a + h_r} + \frac{1}{h_o}\right)$	$\frac{1}{(47) + (55)} + \frac{1}{(41)}$		
	(57)	$\frac{2d_p^2}{\pi(\bar{v}_p \bar{v}_o)}$	$10.47 \times (5) \times (87) / (3)$		
	(58)	$\frac{\bar{v}_p \bar{v}_o}{\bar{v}_a \bar{v}_s}$	$1.25 \times (3) / (89)$	$\Sigma$	
	(59)	$\dagger$	$(57) [1 - (58)] / (56)$		
	(60)	$e^{\dagger}$	$e^{(59)}$		
	(61)	$t_{e2}(1 - e^{\dagger})$	$(37) [1 - (60)]$		
	(62)	$t_{e1}(1 - \Sigma)$	$(4) [1 - (58)]$		
	(63)	$\Sigma - e^{\dagger}$	$(58) - (60)$		
(64)	Downstream exhaust-gas temperature	$[(61) - (62)] / (63)$	$t_{e2}$	$^\circ\text{F}$	
Downstream cooling-air temperature					
16	(65)	Downstream cooling-air temperature	$(58) [(4) - (64)] + (37)$	$t_{a1}$	$^\circ\text{F}$
Upstream exhaust-pipe temperature					
17	(66)	$h_o t_{e1} + h_a t_{p1}$	$(4) \times (41) + (47) \times (65)$		
	(67)	Upstream exhaust-pipe temperature	$(66) / (49)$	$t_{p1}$	$^\circ\text{F}$
Cooling-air pressure drop in shroud					
18	(68)	Shroud diameter	Selected from critical temperature plots such that no limiting temperature is exceeded, as per instructions in step 18	$d_s$	ft
	(69)	Cooling-air-flow rate		$\dot{V}_a$	lb/sec
19	(70)	Upstream cooling-air static pressure	from (68), (69), and curves plotted against $\dot{V}_a$	$p_{s2}$	lb/ft <sup>2</sup>
	(71)	Upstream cooling-air temperature		$t_{a2}$	$^\circ\text{F}$
	(72)	Downstream cooling-air temperature		$t_{a1}$	$^\circ\text{F}$
	(73)	Downstream cooling-air static pressure		$p_{s1} = p_o - (32)$	$p_{s1}$
	(74)	Upstream cooling-air density	$0.00283 \times (70) / [(71) + 460]$	$\rho_{a2}$	slugs/ft <sup>3</sup>
	(75)	Downstream cooling-air density	$0.00283 \times (73) / [(72) + 460]$	$\rho_{a1}$	slugs/ft <sup>3</sup>
	(76)	$1 + \frac{\rho_{a2}}{\rho_{a1}}$	$1 + (74) / (75)$		
	(77)	$\dot{V}_a^{1.8}$	(69) and table 5		
	(78)	$(d_a + d_p)^{1.8}$	[(68) + (5)] and table 5		
	(79)	$(d_a - d_p)^3$	[(68) - (5)] <sup>3</sup>		
(80)	$\mu_a^{0.2}$	(71) and figure 13			
(81)	Friction pressure drop referred to standard density	$\frac{0.0879 \times (87) \times (76) \times (77) \times (80)}{(78) \times (79)}$	$\sigma_{e2} \Delta p_f$	lb/ft <sup>2</sup>	
(82)	$\Sigma \frac{\rho_{a2}}{\rho_{a1}} - 1$	$[\Sigma \times (74) / (75)] - 1$			
(83)	$\dot{V}_a^2$	(69) <sup>2</sup>			
(84)	$(d_a + d_p)^2$	[(68) + (5)] <sup>2</sup>			
(85)	$(d_a - d_p)^2$	[(68) - (5)] <sup>2</sup>			
(86)	Heating and cooling pressure drop referred to standard density	$0.3284 \times (82) \times (83) / [(84) \times (85)]$	$\sigma_{a2} (\Delta T_a + \Delta T_c)$	lb/ft <sup>2</sup>	
(87)	Total pressure drop referred to standard density	(81) + (86)	$\sigma_{e2} \Delta p$	lb/ft <sup>2</sup>	
(88)	Cooling-air pressure drop in shroud	$0.00278 (87) / (74)$	$\Delta p$	lb/ft <sup>2</sup>	

<sup>1</sup>Items are carried in parentheses to indicate row used in calculations.

TABLE 5

VALUES OF  $N$  RAISED TO THE 0.8 AND 1.8 POWERS

$N$	0	1	2	3	4	5	6	7	8	9
$N^{0.8}$										
0.2	0.2759	0.2869	0.2978	0.3086	0.3193	0.3299	0.3404	0.3508	0.3612	0.3715
.3	.3817	.3918	.4019	.4119	.4219	.4318	.4416	.4514	.4611	.4708
.4	.4804	.4900	.4996	.5091	.5185	.5279	.5373	.5466	.5559	.5651
.5	.5743	.5835	.5927	.6018	.6108	.6199	.6289	.6378	.6468	.6557
.6	.6645	.6734	.6822	.6910	.6998	.7085	.7172	.7259	.7345	.7432
.7	.7518	.7603	.7689	.7774	.7859	.7944	.8029	.8113	.8197	.8281
.8	.8365	.8449	.8532	.8615	.8698	.8781	.8863	.8946	.9028	.9110
.9	.9192	.9273	.9355	.9436	.9517	.9598	.9679	.9759	.9840	.9920
1.0	1.000	1.008	1.016	1.024	1.032	1.040	1.048	1.056	1.064	1.071
1.1	1.079	1.087	1.095	1.103	1.111	1.118	1.126	1.134	1.142	1.149
1.2	1.157	1.165	1.172	1.180	1.188	1.195	1.203	1.211	1.218	1.226
1.3	1.234	1.241	1.249	1.256	1.264	1.271	1.279	1.286	1.294	1.301
1.4	1.309	1.316	1.324	1.331	1.339	1.346	1.354	1.361	1.368	1.376
1.5	1.383	1.391	1.398	1.405	1.413	1.420	1.427	1.435	1.442	1.449
1.6	1.456	1.464	1.471	1.478	1.486	1.493	1.500	1.507	1.514	1.522
2.0	1.741	1.810	1.879	1.947	2.015	2.081	2.148	2.214	2.279	2.344
3.0	2.408	2.472	2.536	2.599	2.662	2.724	2.786	2.848	2.910	2.971
4.0	3.031	3.092	3.151	3.212	3.272	3.331	3.390	3.449	3.508	3.566
5.0	3.624	3.682	3.739	3.797	3.854	3.911	3.968	4.024	4.081	4.137
6.0	4.193	4.249	4.304	4.360	4.415	4.470	4.525	4.580	4.635	4.690
7.0	4.743	4.797	4.851	4.905	4.959	5.012	5.066	5.119	5.172	5.225
8.0	5.278	5.331	5.383	5.436	5.488	5.540	5.592	5.644	5.696	5.748
9.0	5.800	5.851	5.902	5.954	6.005	6.056	6.107	6.158	6.208	6.259
10.0	6.310	6.360	6.410	6.461	6.511	6.561	6.611	6.660	6.710	6.760
$N^{1.8}$										
0.2	0.05519	0.06026	0.06552	0.07098	0.07663	0.08247	0.08850	0.09472	0.10111	0.10777
.3	.1145	.1215	.1286	.1359	.1434	.1511	.1590	.1670	.1752	.1836
.4	.1922	.2009	.2098	.2189	.2281	.2376	.2472	.2569	.2668	.2769
.5	.2872	.2976	.3082	.3189	.3299	.3409	.3522	.3636	.3751	.3868
.6	.3987	.4108	.4230	.4353	.4478	.4605	.4733	.4863	.4995	.5128
.7	.5262	.5398	.5535	.5675	.5816	.5958	.6102	.6247	.6394	.6542
.8	.6692	.6843	.6996	.7151	.7306	.7464	.7622	.7783	.7945	.8108
.9	.8272	.8439	.8606	.8775	.8946	.9118	.9292	.9466	.9643	.9821
1.0	1.000	1.018	1.036	1.055	1.073	1.092	1.111	1.130	1.149	1.168
1.1	1.187	1.207	1.226	1.246	1.266	1.286	1.306	1.327	1.347	1.368
1.2	1.388	1.410	1.430	1.452	1.473	1.494	1.516	1.538	1.559	1.581
1.3	1.604	1.626	1.648	1.671	1.694	1.716	1.739	1.762	1.786	1.809
1.4	1.832	1.856	1.880	1.904	1.928	1.952	1.976	2.001	2.025	2.050
1.5	2.075	2.100	2.125	2.150	2.175	2.201	2.227	2.252	2.278	2.304
1.6	2.330	2.357	2.383	2.410	2.436	2.463	2.490	2.517	2.544	2.572
2.0	3.482	3.802	4.134	4.478	4.835	5.204	5.584	5.977	6.381	6.797
3.0	7.225	7.664	8.115	8.577	9.050	9.535	10.031	10.538	11.056	11.586
4.0	12.126	12.877	13.639	13.812	14.395	14.989	15.594	16.210	16.836	17.472
5.0	18.119	18.777	19.445	20.123	20.812	21.511	22.220	22.939	23.669	24.408
6.0	25.158	25.918	26.687	27.467	28.257	29.057	29.866	30.686	31.515	32.354
7.0	33.203	34.062	34.930	35.808	36.696	37.594	38.500	39.417	40.344	41.279
8.0	42.224	43.179	44.143	45.117	46.100	47.093	48.095	49.106	50.126	51.157
9.0	52.196	53.244	54.302	55.359	56.446	57.531	58.626	59.730	60.842	61.965
10.0	63.096	64.236	65.386	66.554	67.711	68.888	70.073	71.267	72.471	73.683

TABLE 6

VARIATION OF KEROSENE-GAS ENTHALPY REFERRED TO 0° ABSOLUTE WITH KEROSENE-GAS TEMPERATURE, FUEL-AIR RATIO, AND HYDROGEN-CARBON RATIO

$\tau$ , °F	0.01	0.02	0.03	0.04	0.05	0.06	0.07	0.08	0.09	0.10	0.11	0.12
(Btu/lb)												
$\frac{H}{C} = 0.10$												
440	217.0	217.6	218.2	218.8	219.4	220.0	221.6	223.2	224.8	226.4	228.0	229.7
620	228.2	228.8	229.4	229.9	230.5	231.1	231.7	232.3	232.9	233.5	234.1	234.7
800	308.3	309.8	311.2	312.6	314.0	315.4	316.8	318.2	319.6	321.0	322.4	323.8
980	375.6	377.6	379.5	381.4	383.3	385.2	387.1	389.0	390.9	392.8	394.7	396.6
1160	403.9	406.4	408.8	411.2	413.6	415.9	418.3	420.7	423.1	425.5	427.9	430.3
1340	423.2	426.2	429.2	432.2	435.1	438.0	440.9	443.8	446.7	449.6	452.5	455.4
1520	433.3	437.0	440.6	444.2	447.8	451.4	455.0	458.6	462.2	465.8	469.4	473.0
1700	434.1	438.8	443.4	448.0	452.6	457.2	461.8	466.4	471.0	475.6	480.2	484.8
1880	425.2	430.8	436.4	442.0	447.6	453.2	458.8	464.4	470.0	475.6	481.2	486.8
2060	397.7	403.3	408.9	414.5	420.1	425.7	431.3	436.9	442.5	448.1	453.7	459.3
2240	310.4	316.8	323.1	329.3	335.5	341.7	347.9	354.1	360.3	366.5	372.7	378.9
$\frac{H}{C} = 0.12$												
440	217.3	218.2	219.1	220.0	220.9	221.7	222.6	223.5	224.4	225.3	226.2	227.1
620	228.5	229.4	230.3	231.2	232.1	233.0	233.9	234.8	235.7	236.6	237.5	238.4
800	308.8	310.7	312.5	314.3	316.1	317.8	319.6	321.4	323.2	325.0	326.8	328.6
980	376.1	378.5	380.9	383.3	385.7	388.1	390.5	392.9	395.3	397.7	400.1	402.5
1160	404.5	407.5	410.5	413.5	416.5	419.5	422.5	425.5	428.5	431.5	434.5	437.5
1340	423.8	427.3	430.8	434.3	437.8	441.3	444.8	448.3	451.8	455.3	458.8	462.3
1520	434.0	438.3	442.6	446.9	451.2	455.5	459.8	464.1	468.4	472.7	477.0	481.3
1700	434.9	439.8	444.7	449.6	454.5	459.4	464.3	469.2	474.1	479.0	483.9	488.8
1880	426.0	431.8	437.6	443.4	449.2	455.0	460.8	466.6	472.4	478.2	484.0	489.8
2060	398.7	404.5	410.3	416.1	421.9	427.7	433.5	439.3	445.1	450.9	456.7	462.5
2240	311.4	318.8	326.1	333.4	340.7	348.0	355.3	362.6	369.9	377.2	384.5	391.8
$\frac{H}{C} = 0.14$												
440	217.6	218.8	220.0	221.2	222.3	223.4	224.6	225.8	227.0	228.2	229.4	230.6
620	228.9	229.8	230.7	231.6	232.5	233.4	234.3	235.2	236.1	237.0	237.9	238.8
800	309.2	311.5	313.7	315.9	318.1	320.2	322.4	324.5	326.7	328.8	330.9	333.0
980	376.6	379.5	382.3	385.2	388.1	391.0	393.9	396.8	399.7	402.6	405.5	408.4
1160	405.0	408.6	412.1	415.5	418.9	422.3	425.7	429.1	432.5	435.9	439.3	442.7
1340	424.4	428.7	433.0	437.3	441.6	445.9	450.2	454.5	458.8	463.1	467.4	471.7
1520	434.6	439.7	444.8	449.9	455.0	460.1	465.2	470.3	475.4	480.5	485.6	490.7
1700	435.7	441.5	447.2	452.9	458.6	464.3	470.0	475.7	481.4	487.1	492.8	498.5
1880	426.8	433.5	440.2	446.9	453.6	460.3	467.0	473.7	480.4	487.1	493.8	500.5
2060	399.6	405.3	411.0	416.7	422.4	428.1	433.8	439.5	445.2	450.9	456.6	462.3
2240	312.4	320.8	329.0	337.1	345.2	353.3	361.4	369.5	377.6	385.7	393.8	401.9
$\frac{H}{C} = 0.16$												
440	217.9	219.4	220.8	222.3	223.7	225.0	226.4	227.8	229.2	230.6	232.0	233.4
620	229.2	229.9	230.6	231.3	232.0	232.7	233.4	234.1	234.8	235.5	236.2	236.9
800	309.6	312.5	315.3	318.1	320.9	323.7	326.5	329.3	332.1	334.9	337.7	340.5
980	377.0	380.5	384.0	387.5	391.0	394.5	398.0	401.5	405.0	408.5	412.0	415.5
1160	405.5	409.6	413.6	417.5	421.4	425.3	429.2	433.1	437.0	440.9	444.8	448.7
1340	424.9	429.8	434.7	439.6	444.5	449.4	454.3	459.2	464.1	469.0	473.9	478.8
1520	435.3	441.0	446.7	452.4	458.1	463.8	469.5	475.2	480.9	486.6	492.3	498.0
1700	436.4	443.0	449.6	456.2	462.8	469.4	476.0	482.6	489.2	495.8	502.4	509.0
1880	428.6	436.2	443.8	451.4	459.0	466.6	474.2	481.8	489.4	497.0	504.6	512.2
2060	400.4	406.8	413.2	419.6	426.0	432.4	438.8	445.2	451.6	458.0	464.4	470.8
2240	313.4	322.7	331.8	340.9	349.9	358.9	367.9	376.9	385.9	394.9	403.9	412.9
$\frac{H}{C} = 0.18$												
440	218.2	219.9	221.7	223.3	225.0	226.6	228.2	229.9	231.5	233.2	234.8	236.5
620	229.5	229.9	230.3	230.7	231.1	231.5	231.9	232.3	232.7	233.1	233.5	233.9
800	310.0	313.0	316.0	319.0	322.0	325.0	328.0	331.0	334.0	337.0	340.0	343.0
980	377.5	381.3	385.0	388.7	392.4	396.1	399.8	403.5	407.2	410.9	414.6	418.3
1160	406.0	410.6	415.1	419.5	423.9	428.3	432.7	437.1	441.5	445.9	450.3	454.7
1340	425.6	431.0	436.3	441.6	446.9	452.2	457.5	462.8	468.1	473.4	478.7	484.0
1520	436.0	442.5	449.0	455.5	462.0	468.5	475.0	481.5	488.0	494.5	501.0	507.5
1700	437.1	444.5	451.9	459.3	466.7	474.1	481.5	488.9	496.3	503.7	511.1	518.5
1880	429.4	438.0	446.6	455.2	463.8	472.4	481.0	489.6	498.2	506.8	515.4	524.0
2060	401.3	407.8	414.3	420.8	427.3	433.8	440.3	446.8	453.3	459.8	466.3	472.8
2240	314.3	324.5	334.5	344.4	354.3	364.2	374.1	384.0	393.9	403.8	413.7	423.6
$\frac{H}{C} = 0.20$												
440	218.5	220.3	222.5	224.4	226.3	228.2	230.0	231.8	233.6	235.4	237.2	239.0
620	229.9	229.9	229.9	229.9	229.9	229.9	229.9	229.9	229.9	229.9	229.9	229.9
800	310.3	313.8	317.1	320.4	323.7	327.0	330.3	333.6	336.9	340.2	343.5	346.8
980	377.9	382.1	386.3	390.5	394.7	398.9	403.1	407.3	411.5	415.7	419.9	424.1
1160	406.5	411.6	416.7	421.8	426.9	432.0	437.1	442.2	447.3	452.4	457.5	462.6
1340	426.1	432.4	438.7	445.0	451.3	457.6	463.9	470.2	476.5	482.8	489.1	495.4
1520	436.6	444.0	451.4	458.8	466.2	473.6	481.0	488.4	495.8	503.2	510.6	518.0
1700	437.8	446.1	454.4	462.7	471.0	479.3	487.6	495.9	504.2	512.5	520.8	529.1
1880	429.9	439.6	449.3	459.0	468.7	478.4	488.1	497.8	507.5	517.2	526.9	536.6
2060	401.9	408.4	414.9	421.4	427.9	434.4	440.9	447.4	453.9	460.4	466.9	473.4
2240	315.2	326.3	337.2	348.1	359.0	369.9	380.8	391.7	402.6	413.5	424.4	435.3

TABLE 7

CONSTANTS FOR THE CALCULATION OF ABSOLUTE  
VISCOSITY OF EXHAUST GAS

Temperature (°F)	$\mu_a$	$a_1$	$b_1$	$C_1$	$D_1$	$E_1$	$\phi_1$
	(mlugs/(sec)(ft) $\times 10^6$ )						
500	0.587	0.0223	-0.0112	0.726	0.0493	0.202	-0.133
700	.663	.0399	-.0116	.783	.0537	.234	-.159
900	.732	.0580	-.0121	.854	.0591	.270	-.197
1100	.800	.0756	-.0121	.903	.0632	.300	-.223
1300	.864	.0945	-.0124	.955	.0672	.331	-.255
1500	.928	.1116	-.0128	1.008	.0712	.362	-.286
1700	.977	.1280	-.0131	1.046	.0741	.387	-.308
1900	1.028	.1443	-.0133	1.088	.0774	.414	-.332
2100	1.077	.1602	-.0135	1.130	.0806	.440	-.358
2300	1.125	.1753	-.0138	1.169	.0837	.465	-.380

TABLE 8

CONSTANTS FOR THE CALCULATION OF THERMAL  
CONDUCTIVITY OF EXHAUST GAS

Temperature (°F)	$k_a$	$a_2$	$b_2$	$C_2$	$D_2$	$E_2$	$\phi_2$
	(Btu/(sec)(sq ft)(°F/ft) $\times 10^5$ )						
500	0.695	0.0921	-0.0127	0.861	0.0590	0.306	4.08
700	.814	.1315	-.0118	.919	.0648	.360	4.39
900	.928	.1748	-.0118	1.014	.0727	.426	4.84
1100	1.045	.2214	-.0111	1.078	.0787	.489	5.35
1300	1.164	.2772	-.0099	1.153	.0861	.563	5.87
1500	1.281	.3333	-.0093	1.231	.0933	.639	6.32
1700	1.392	.3947	-.0085	1.271	.0974	.710	6.94
1900	1.500	.4597	-.0078	1.345	.1043	.793	7.48
2100	1.607	.5293	-.0068	1.415	.1111	.880	8.01
2300	1.707	.6033	-.0051	1.472	.1175	.968	8.60

TABLE 9

VARIATIONS OF EXHAUST-GAS BRANDEL NUMBER WITH EXHAUST-GAS TEMPERATURE,  
FUEL-AIR RATIO, AND HYDROGEN-CARBON RATIO

$\frac{z}{t, \text{ }^\circ\text{F}}$	0.01	0.02	0.03	0.04	0.05	0.06	0.07	0.08	0.09	0.10	0.11	0.12
$\frac{H}{C} = 0.10$												
500	0.679	0.683	0.685	0.689	0.692	0.695	0.699	0.698	0.695	0.698	0.703	0.706
700	.672	.676	.679	.683	.685	.689	.693	.692	.689	.692	.697	.700
900	.665	.670	.674	.678	.682	.685	.688	.687	.684	.687	.692	.695
1100	.658	.662	.666	.670	.673	.677	.681	.680	.677	.680	.685	.688
1300	.656	.660	.664	.668	.672	.676	.679	.678	.675	.678	.683	.686
1500	.650	.654	.658	.662	.666	.670	.673	.672	.669	.672	.677	.680
1700	.644	.647	.651	.655	.659	.663	.665	.664	.661	.664	.669	.672
1900	.636	.640	.644	.647	.652	.656	.657	.656	.653	.656	.661	.664
2100	.627	.631	.635	.639	.643	.647	.648	.647	.644	.647	.652	.655
2300	.619	.623	.627	.630	.634	.638	.639	.637	.634	.637	.642	.645
$\frac{H}{C} = 0.12$												
500	0.679	0.683	0.687	0.691	0.695	0.699	0.698	0.697	0.695	0.698	0.703	0.706
700	.672	.676	.680	.684	.688	.693	.692	.691	.689	.692	.697	.700
900	.667	.671	.675	.679	.683	.688	.687	.686	.684	.687	.692	.695
1100	.662	.667	.671	.675	.679	.684	.683	.682	.680	.683	.688	.691
1300	.656	.660	.665	.670	.674	.679	.678	.677	.675	.678	.683	.686
1500	.650	.654	.658	.664	.669	.673	.672	.671	.669	.672	.677	.680
1700	.644	.648	.653	.657	.661	.666	.665	.664	.662	.665	.670	.673
1900	.636	.641	.645	.649	.654	.658	.657	.656	.654	.657	.662	.665
2100	.627	.632	.637	.641	.645	.650	.649	.648	.646	.649	.654	.657
2300	.620	.624	.628	.632	.636	.640	.639	.638	.636	.639	.644	.647
$\frac{H}{C} = 0.14$												
500	0.679	0.684	0.689	0.693	0.698	0.703	0.698	0.697	0.695	0.698	0.703	0.706
700	.673	.677	.682	.687	.692	.697	.696	.695	.693	.696	.701	.704
900	.667	.672	.677	.682	.687	.692	.691	.690	.688	.691	.696	.700
1100	.662	.667	.672	.677	.682	.687	.686	.685	.683	.686	.691	.694
1300	.656	.661	.666	.671	.676	.681	.680	.679	.677	.680	.685	.688
1500	.651	.655	.660	.665	.670	.675	.674	.673	.671	.674	.679	.682
1700	.644	.649	.654	.659	.664	.669	.668	.667	.665	.668	.673	.676
1900	.637	.642	.647	.651	.656	.661	.660	.659	.657	.660	.665	.668
2100	.628	.633	.638	.643	.648	.653	.652	.651	.649	.652	.657	.660
2300	.621	.625	.630	.634	.638	.643	.642	.641	.639	.642	.647	.650
$\frac{H}{C} = 0.16$												
500	0.679	0.685	0.690	0.696	0.701	0.707	0.697	0.696	0.694	0.697	0.702	0.706
700	.673	.678	.683	.689	.694	.700	.690	.689	.687	.690	.695	.699
900	.667	.672	.678	.684	.689	.695	.685	.684	.682	.685	.690	.694
1100	.663	.668	.674	.680	.685	.690	.680	.679	.677	.680	.685	.689
1300	.656	.662	.668	.674	.679	.684	.674	.673	.671	.674	.679	.683
1500	.651	.657	.662	.668	.673	.678	.668	.667	.665	.668	.673	.677
1700	.645	.650	.655	.661	.666	.671	.661	.660	.658	.661	.666	.670
1900	.637	.642	.648	.653	.658	.663	.653	.652	.650	.653	.658	.662
2100	.629	.634	.640	.645	.650	.655	.645	.644	.642	.645	.650	.654
2300	.622	.626	.631	.636	.640	.645	.635	.634	.632	.635	.640	.644
$\frac{H}{C} = 0.18$												
500	0.680	0.685	0.692	0.698	0.704	0.711	0.697	0.696	0.694	0.697	0.702	0.706
700	.673	.679	.685	.691	.697	.703	.693	.692	.690	.693	.698	.702
900	.667	.674	.680	.686	.692	.698	.688	.687	.685	.688	.693	.697
1100	.663	.669	.675	.681	.687	.693	.683	.682	.680	.683	.688	.692
1300	.657	.663	.669	.675	.681	.687	.677	.676	.674	.677	.682	.686
1500	.652	.658	.664	.670	.676	.682	.672	.671	.669	.672	.677	.681
1700	.645	.651	.657	.663	.669	.675	.665	.664	.662	.665	.670	.674
1900	.638	.644	.650	.656	.662	.668	.658	.657	.655	.658	.663	.667
2100	.630	.636	.641	.647	.653	.659	.649	.648	.646	.649	.654	.658
2300	.623	.628	.633	.639	.644	.649	.640	.639	.637	.640	.645	.649
$\frac{H}{C} = 0.20$												
500	0.680	0.687	0.694	0.700	0.707	0.714	0.697	0.696	0.694	0.697	0.702	0.706
700	.673	.680	.686	.693	.699	.706	.696	.695	.693	.696	.701	.705
900	.668	.675	.681	.688	.695	.701	.691	.690	.688	.691	.696	.700
1100	.663	.670	.676	.683	.690	.696	.686	.685	.683	.686	.691	.695
1300	.658	.664	.671	.677	.684	.691	.681	.680	.678	.681	.686	.690
1500	.652	.658	.665	.671	.678	.685	.675	.674	.672	.675	.680	.684
1700	.646	.652	.659	.665	.671	.677	.667	.666	.664	.667	.672	.676
1900	.639	.645	.651	.657	.663	.670	.660	.659	.657	.660	.665	.669
2100	.631	.637	.643	.649	.655	.660	.650	.649	.647	.650	.655	.659
2300	.624	.629	.634	.639	.644	.649	.640	.639	.637	.640	.645	.649

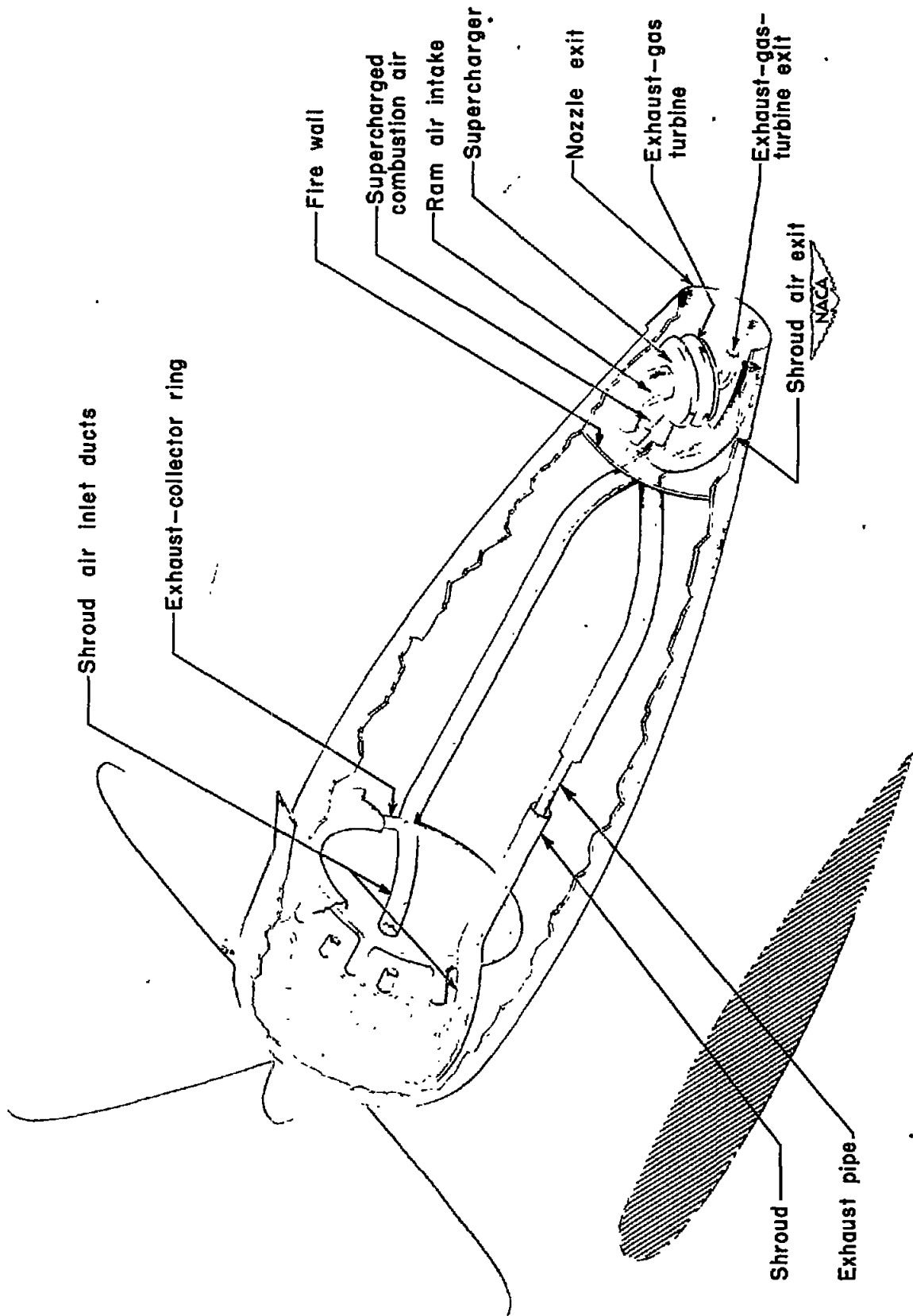
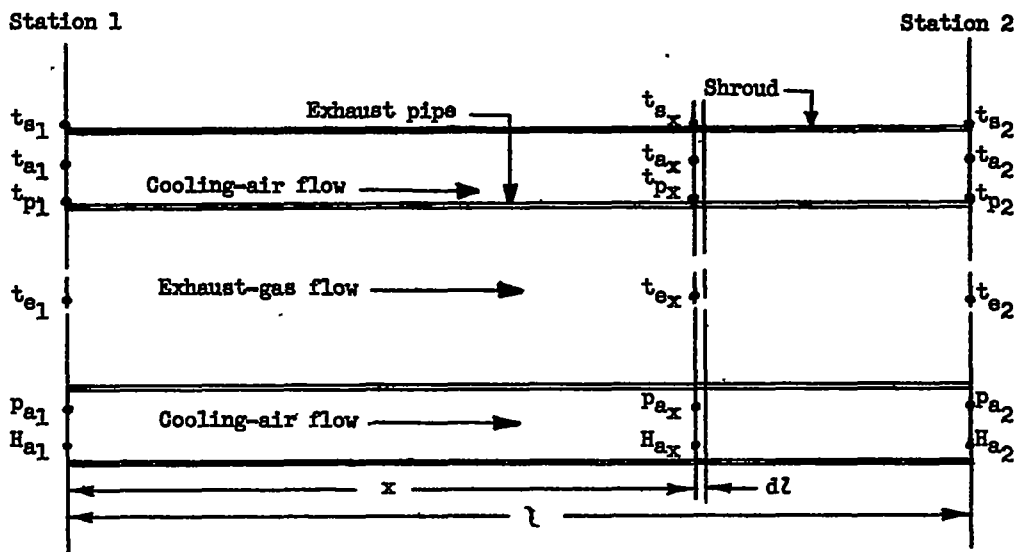
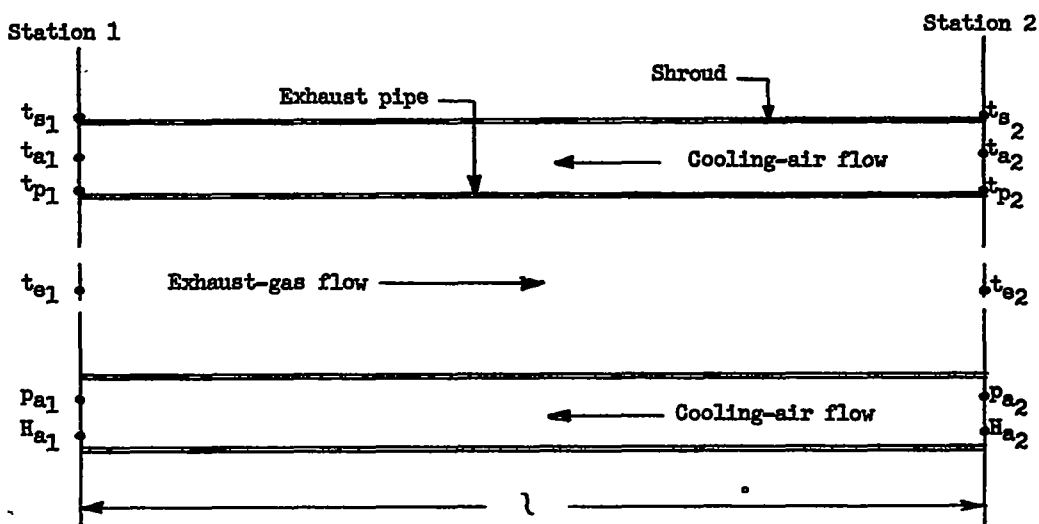


Figure 1.- Illustration of a shrouded exhaust-pipe system in an airplane.



(a) Parallel flow.



(b) Counter flow.

NATIONAL ADVISORY  
COMMITTEE FOR AERONAUTICS

Figure 2.- Illustration of symbols defined for a shrouded exhaust-pipe system.

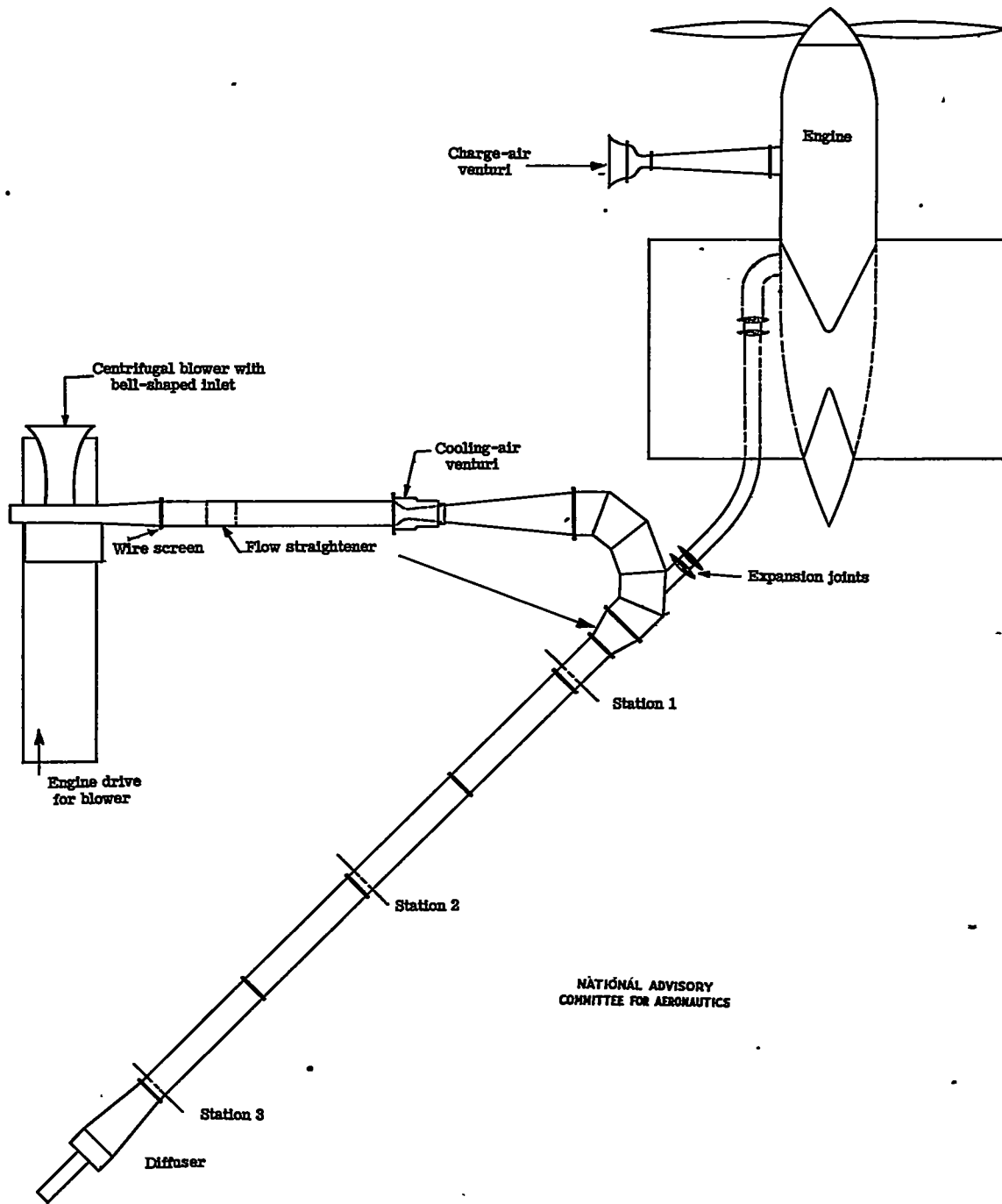
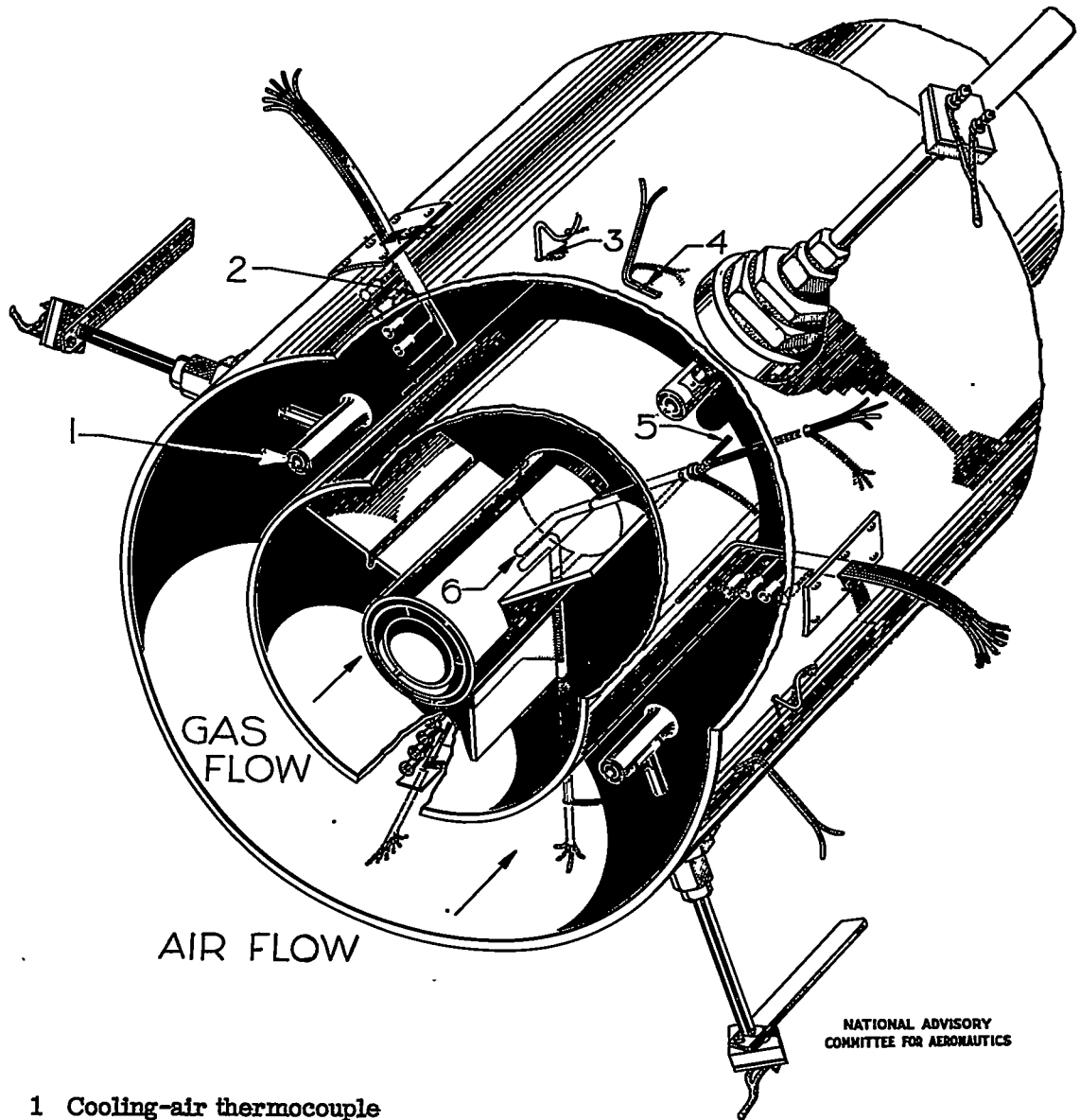
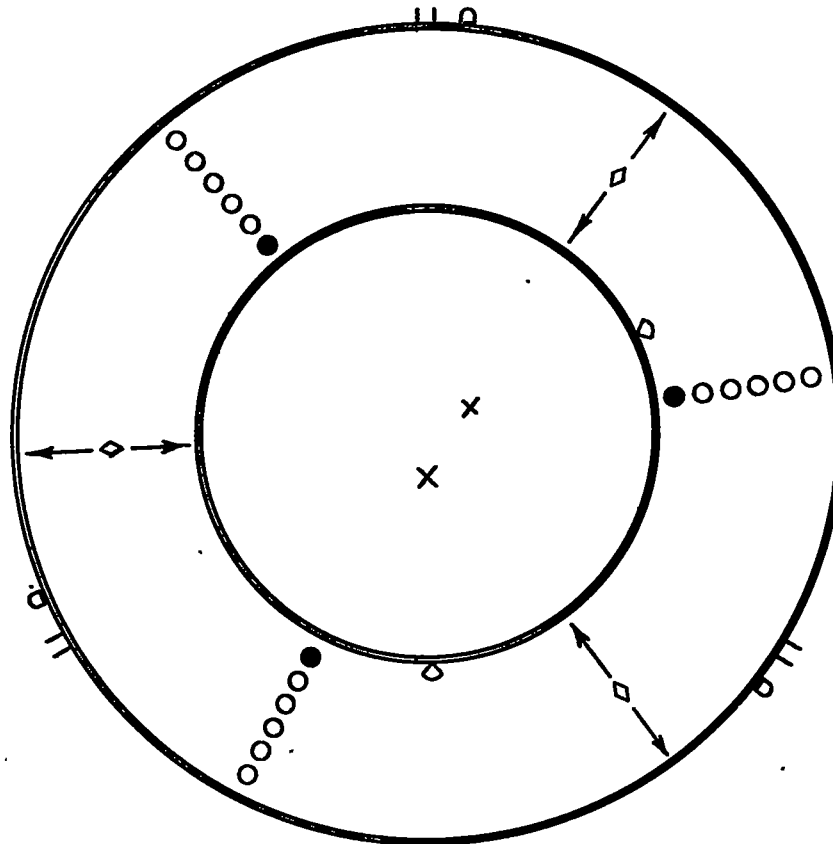


Figure 3.- Schematic diagram of experimental exhaust-pipe-shroud test setup.



- 1 Cooling-air thermocouple
- 2 Pressure rake consisting of one static-pressure tube, one unshielded and four shielded total-pressure tubes
- 3 Wall static-pressure orifice
- 4 Shroud thermocouple
- 5 Exhaust-pipe thermocouple
- 6 Exhaust-gas thermocouple

Figure 4.- Sketch of typical instrument station showing temperature- and pressure-measuring devices.



NATIONAL ADVISORY  
COMMITTEE FOR AERONAUTICS

Symbols

- Total-pressure-tube position
- Static-pressure-tube position
- || Wall-static-orifice position
- X Exhaust-gas thermocouple position
- ◇ Exhaust-pipe-thermocouple position
- ◇ Cooling-air-thermocouple position  
(← → indicates direction  
of traverse)
- Shroud-thermocouple position

Figure 5.- Sketch of typical instrument station showing relative location of instruments.

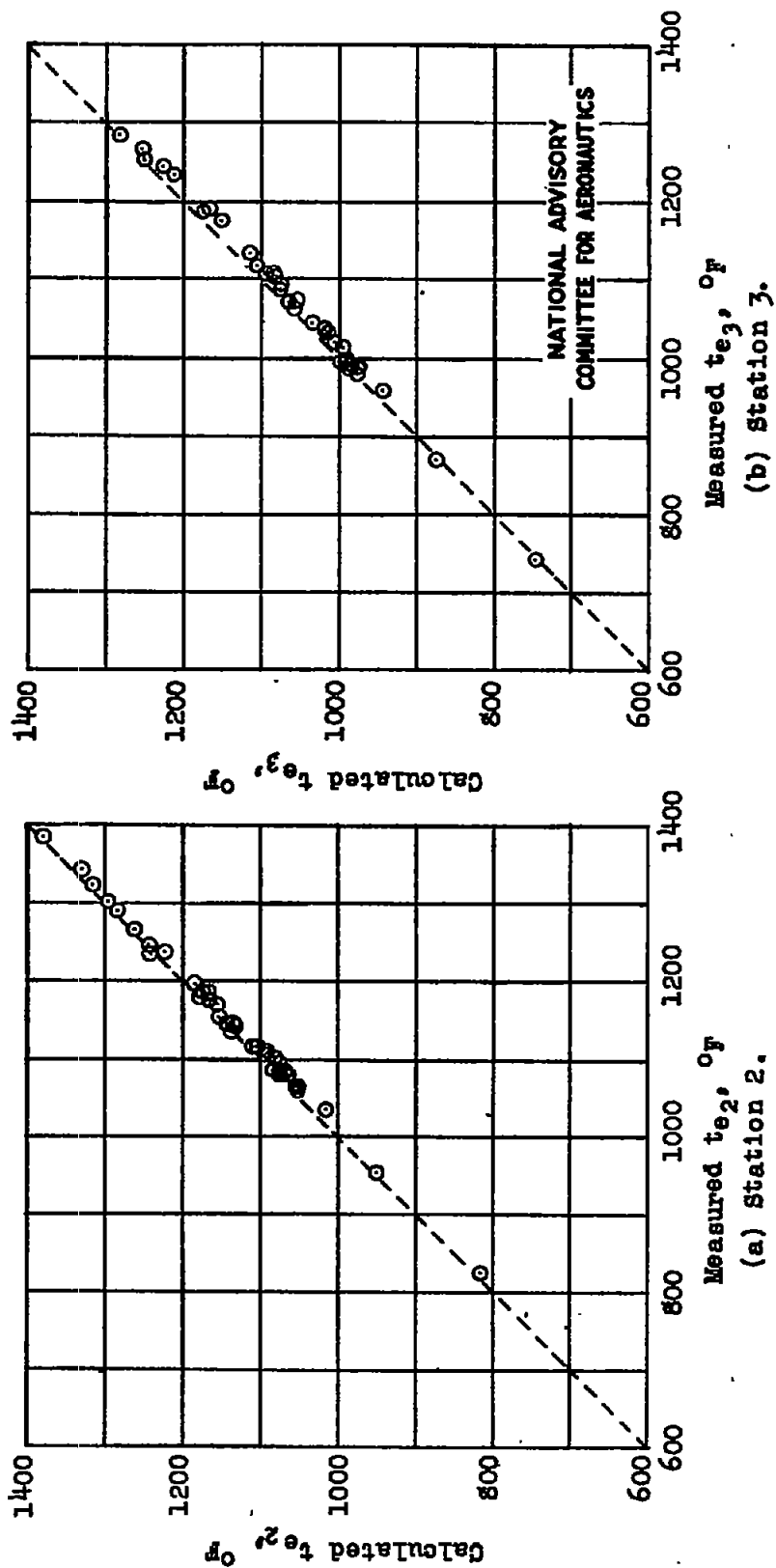
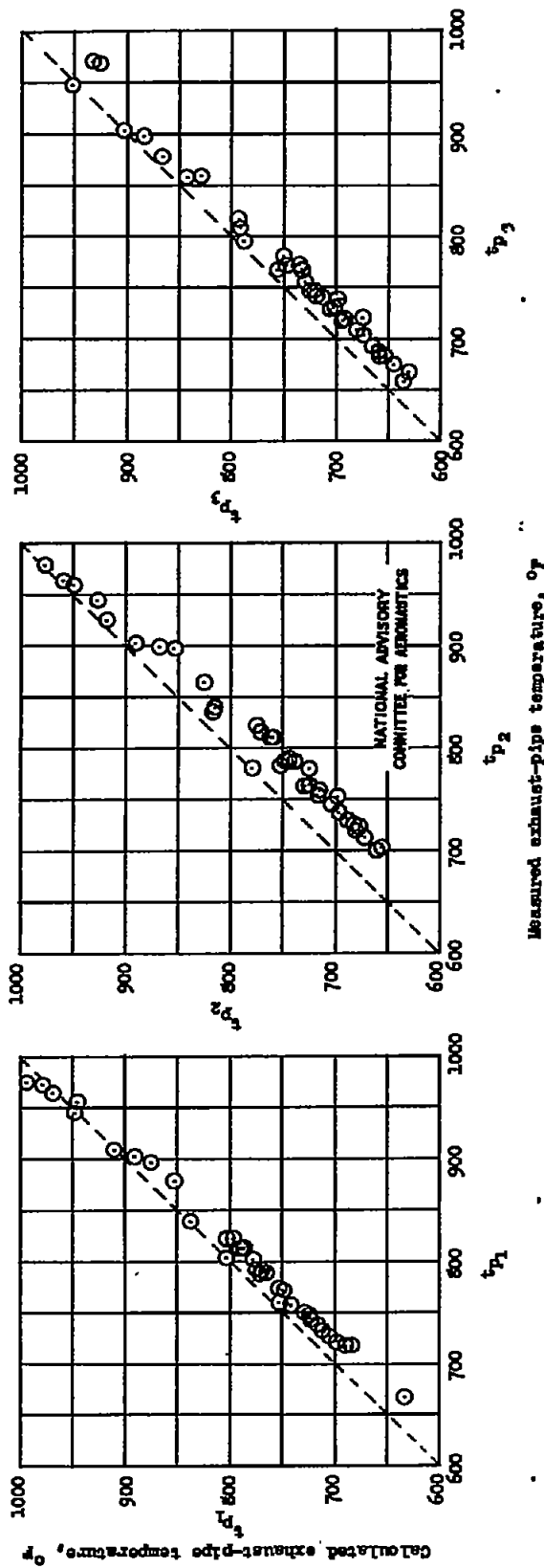


Figure 6.- Comparison of calculated with measured downstream exhaust-gas temperatures. (Calculated temperatures based on air properties and corrected arithmetic mean air temperatures.)



(a) Station 1.

(b) Station 2.

(c) Station 3.

Figure 7.- Comparison of calculated with measured exhaust-pipe temperatures. (Calculated temperatures based on air properties and corrected arithmetic mean air temperatures.)

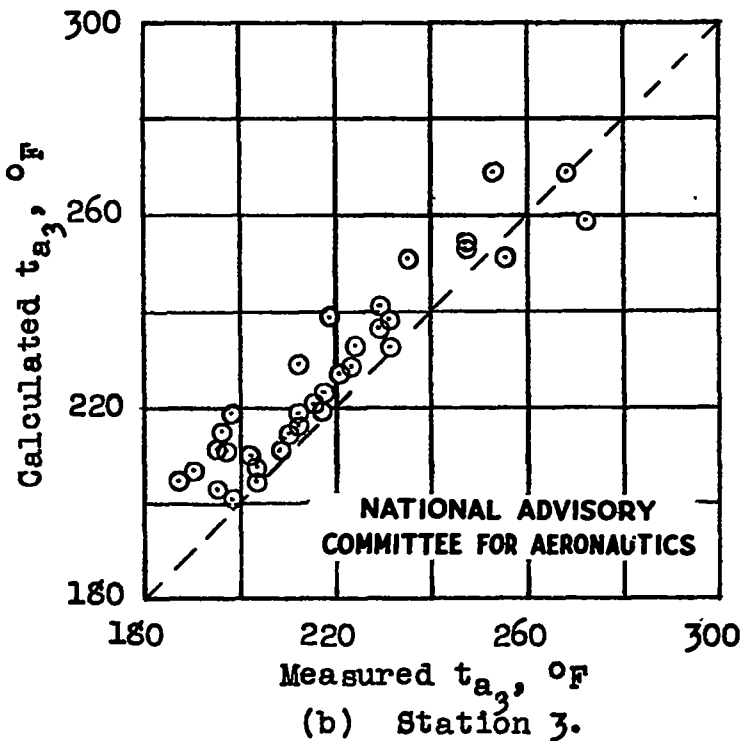
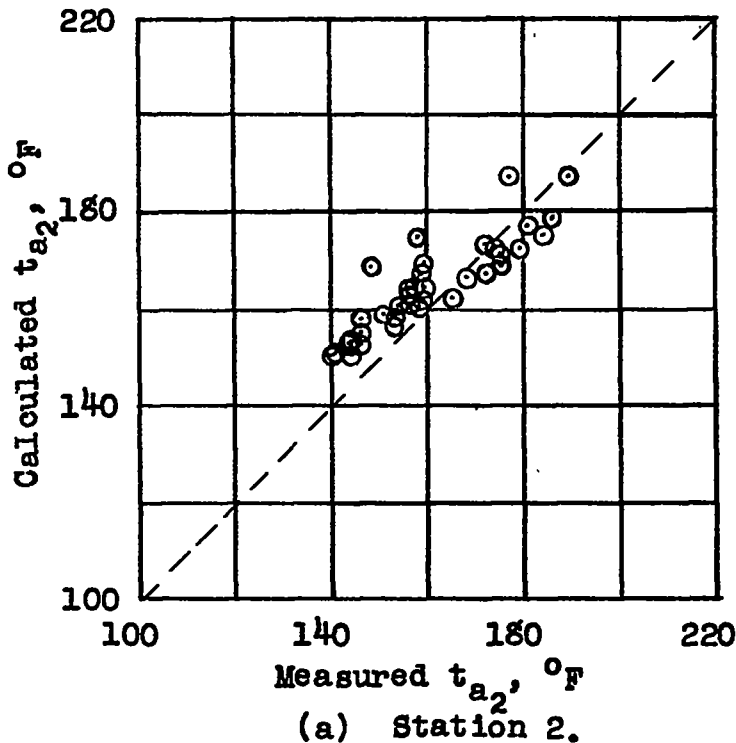
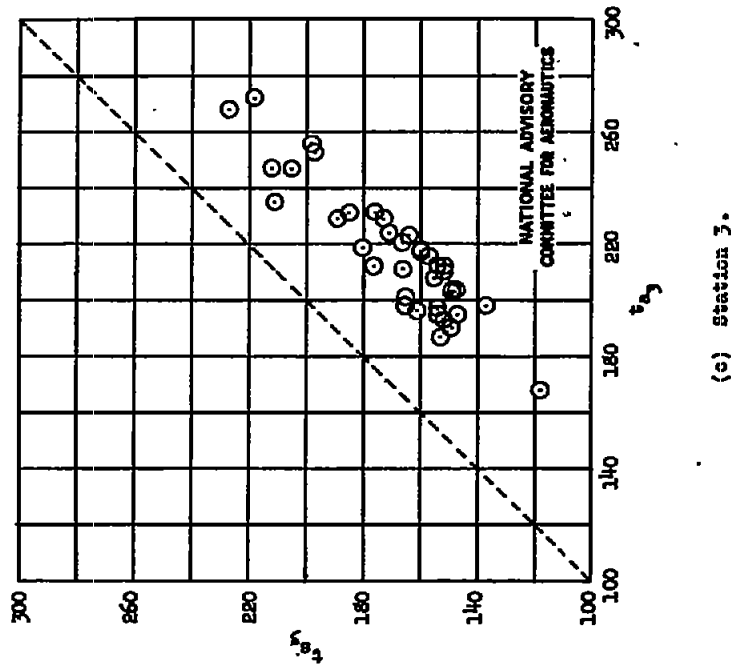
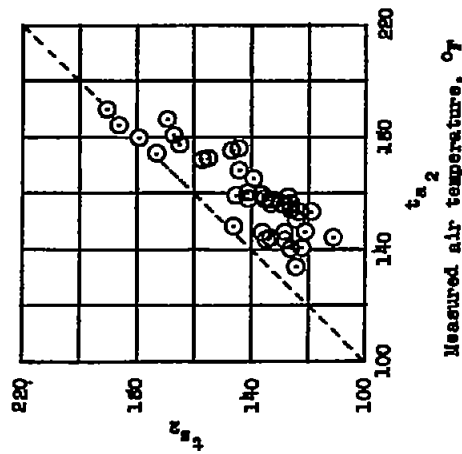


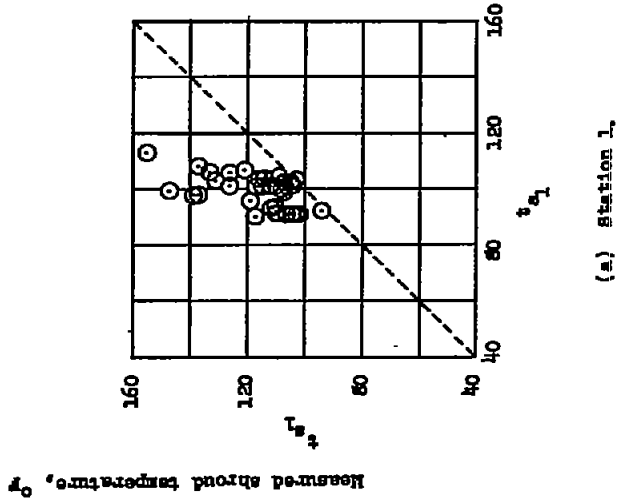
Figure 8.- Comparison of calculated with measured downstream cooling-air temperatures. (Calculated temperatures based on air properties and corrected arithmetic mean air temperatures. Measured temperatures are corrected arithmetic means.)



(c) Station 3.



(b) Station 2.



(a) Station 1.

Figure 9.- Relation of the measured shroud temperature to the measured cooling-air temperature.

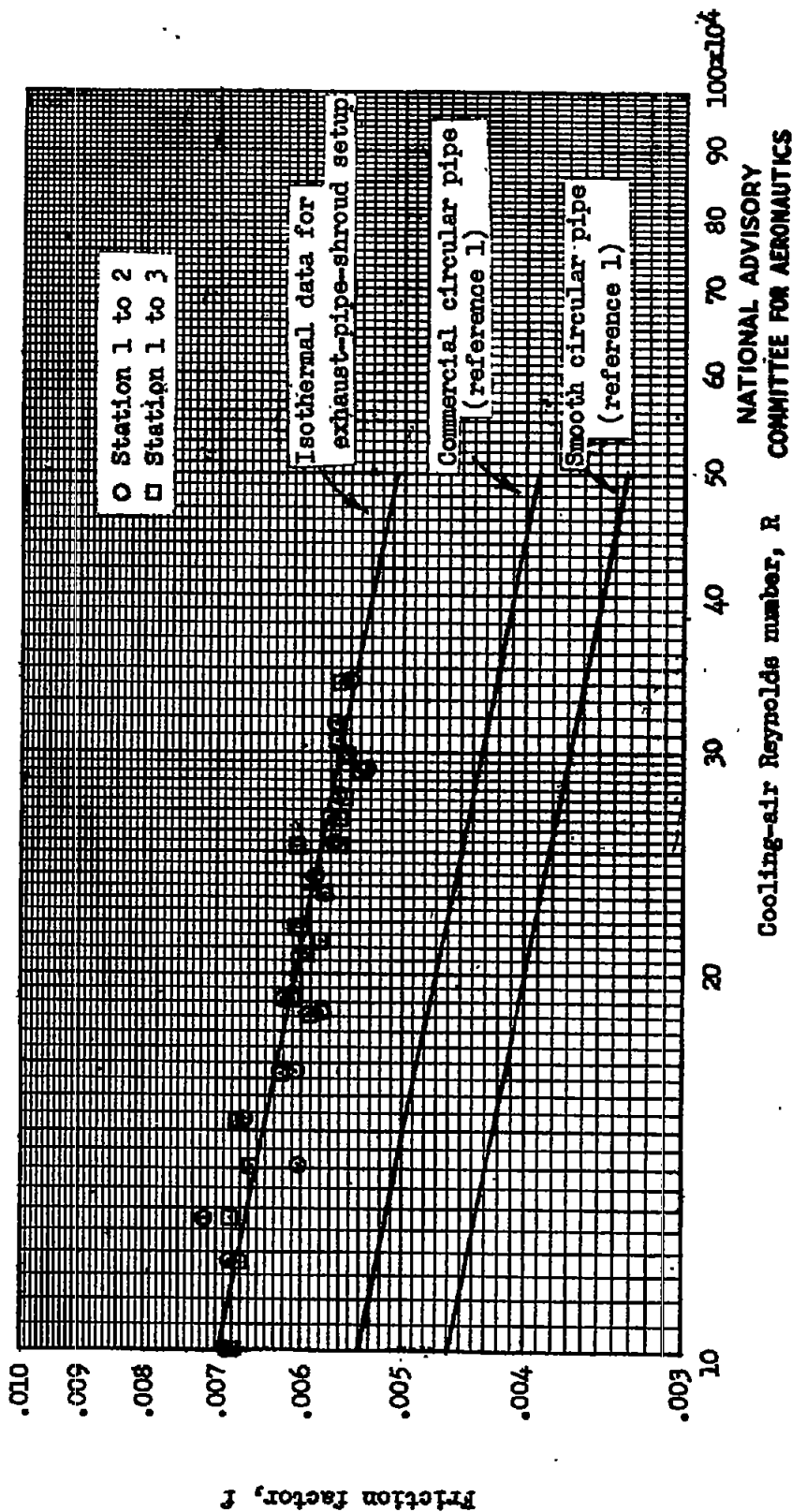
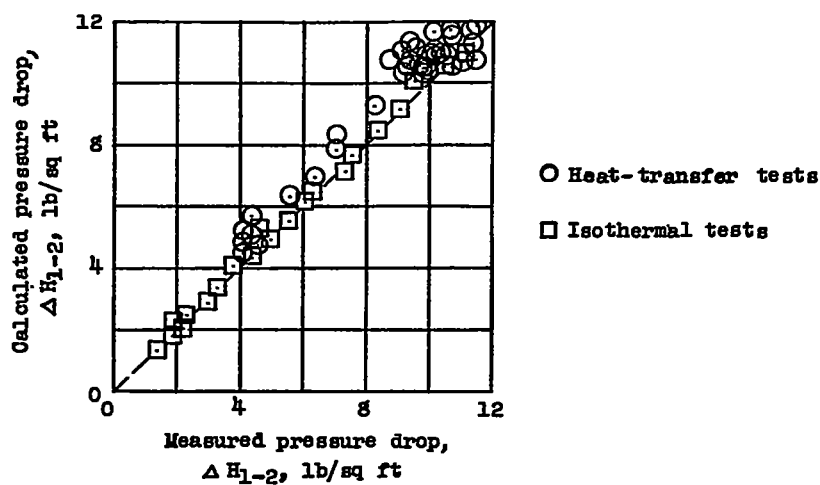
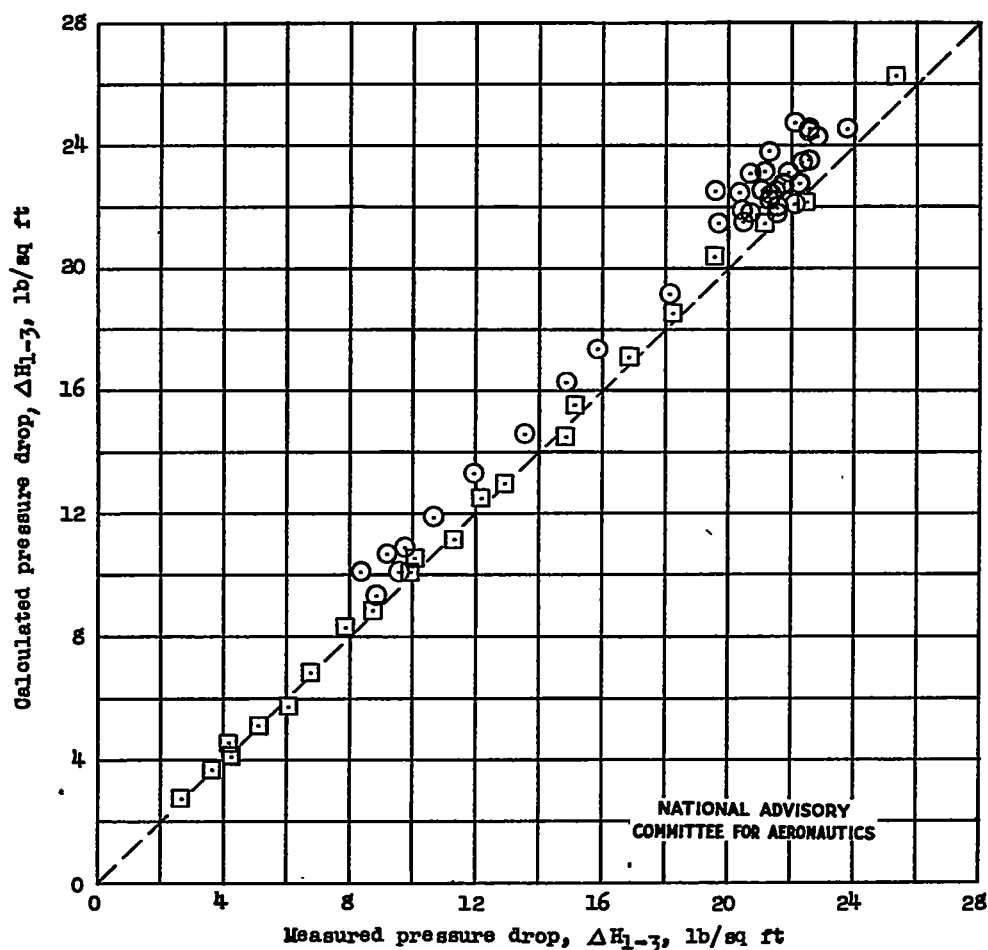


Figure 10.- Variation of friction factors for the exhaust-pipe-shroud setup and for commercial and smooth circular pipes with cooling-air Reynolds number.



(a) Station 1 to 2.



(b) Station 1 to 3.

Figure 11.- Comparison of calculated with measured total-pressure losses for the isothermal and heat-transfer tests. (Calculated pressure losses based on arithmetic mean pressures and calculated downstream air temperatures based on air properties and corrected arithmetic mean air temperatures.)

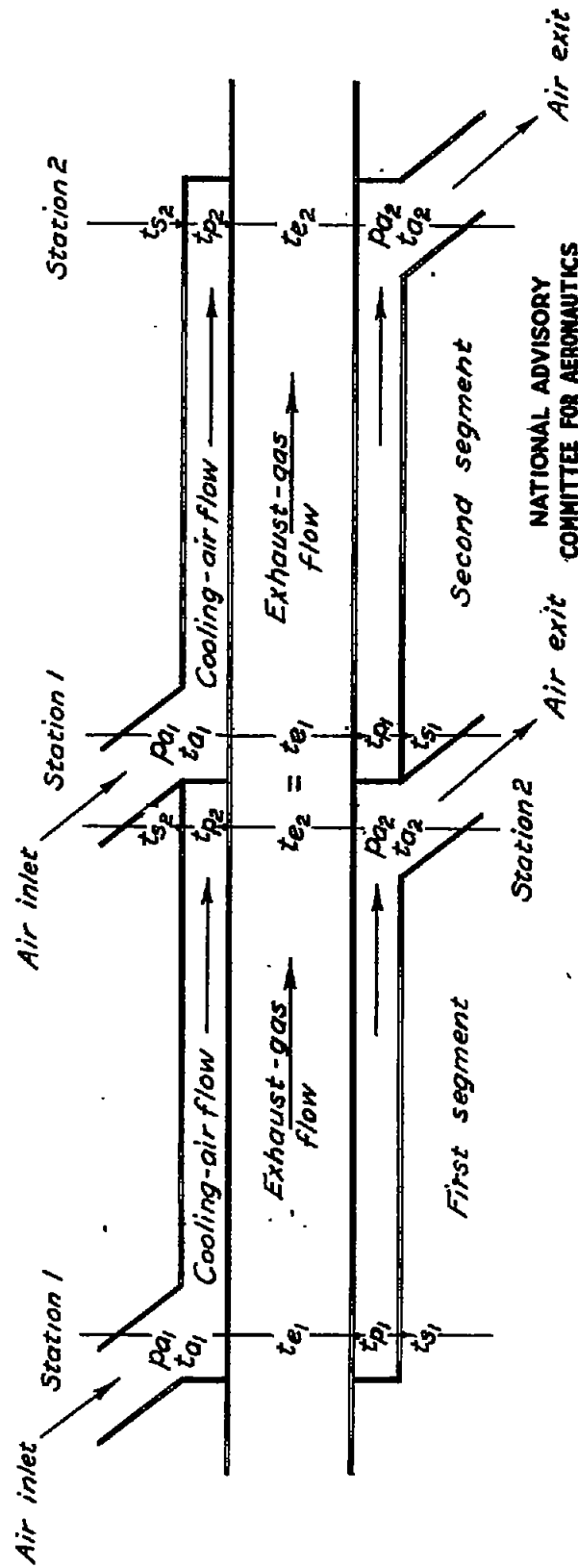


Figure 12.- Diagrammatic sketch of a multisegment exhaust-pipe-shroud system for parallel flow.

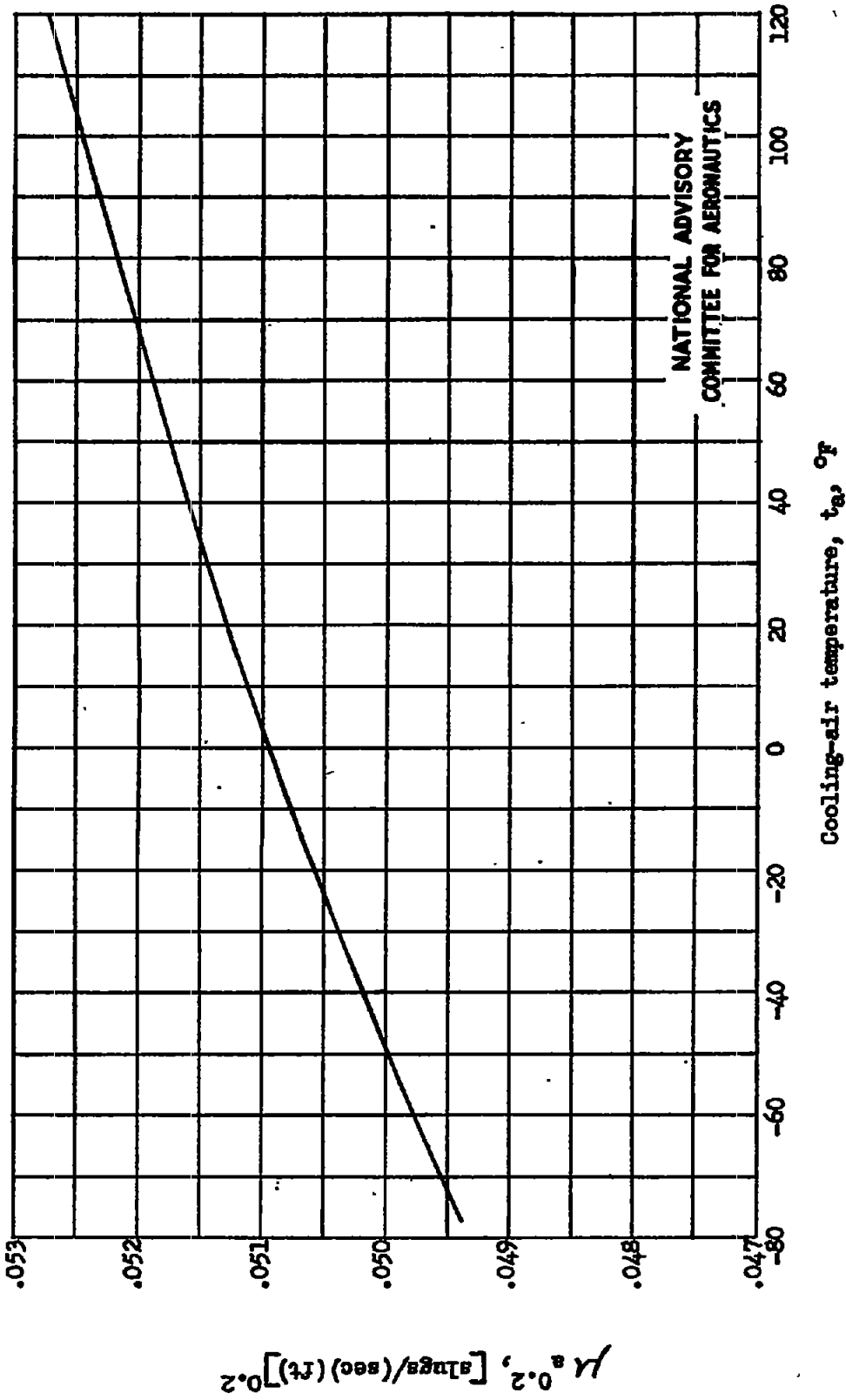


Figure 13.- Variation of  $\mu_a^{0.2}$  with cooling-air temperature.

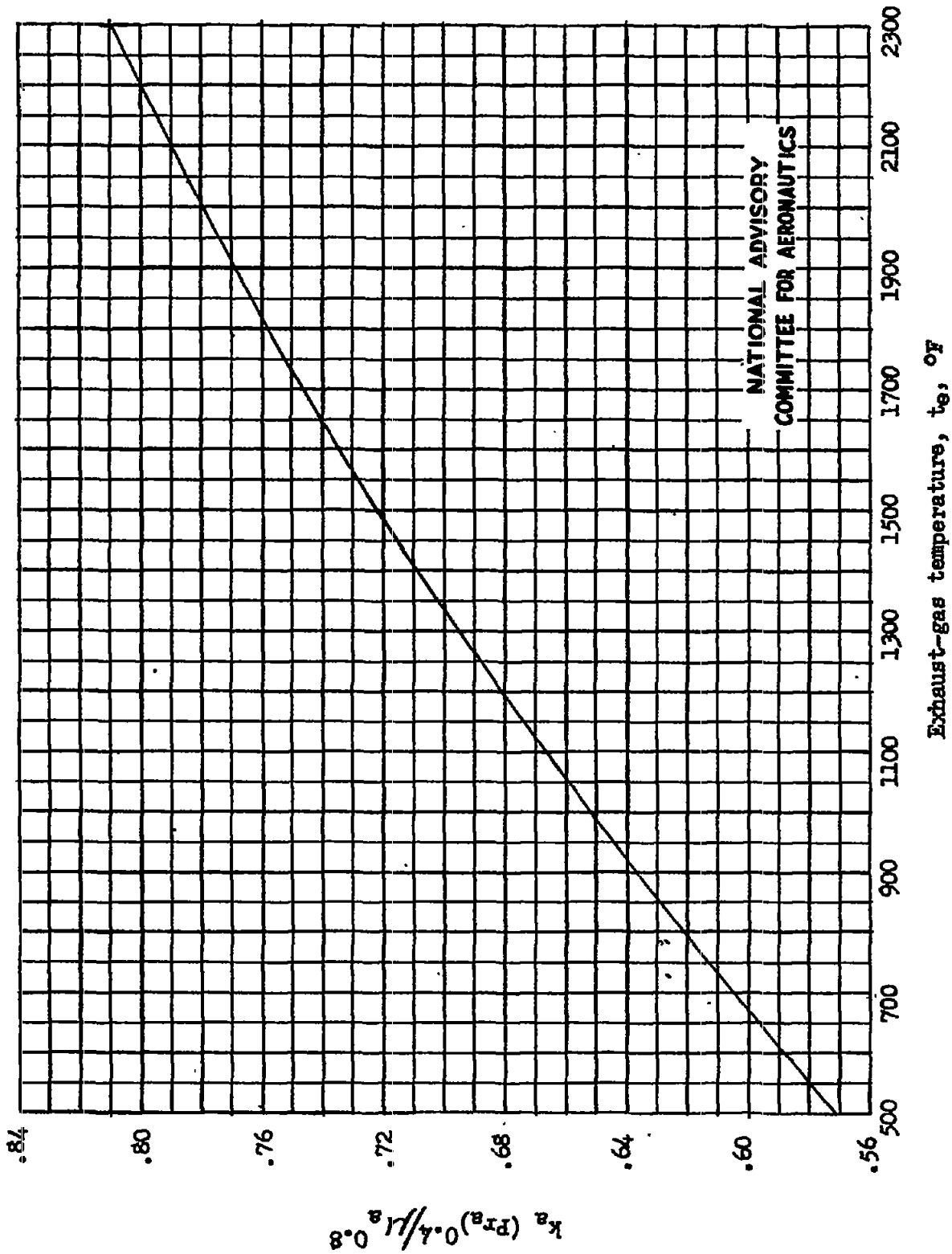


Figure 14.- Variation of the factor  $k_a (Pr_a)^{0.4} / \mu_a$  with exhaust-gas temperature.

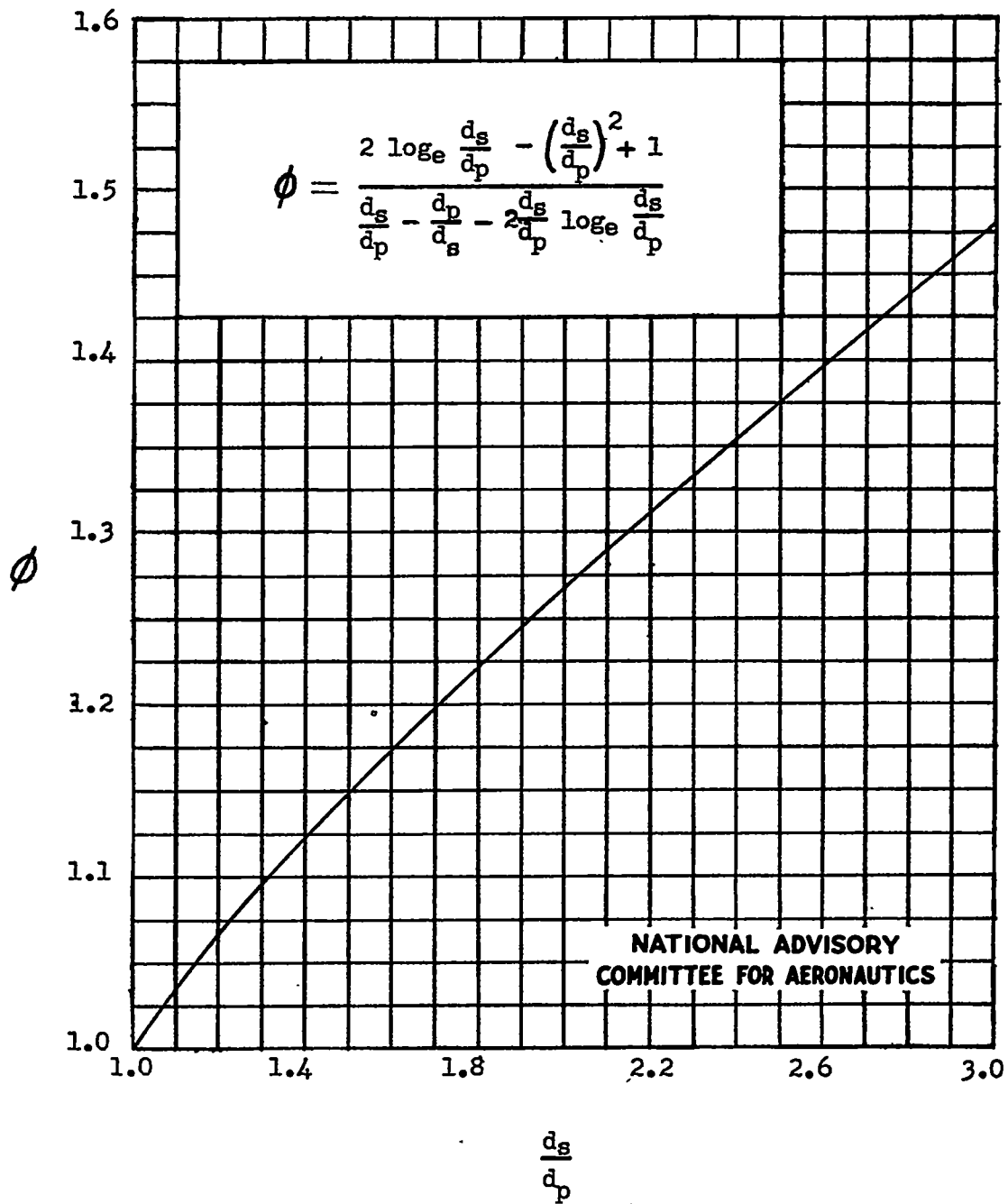
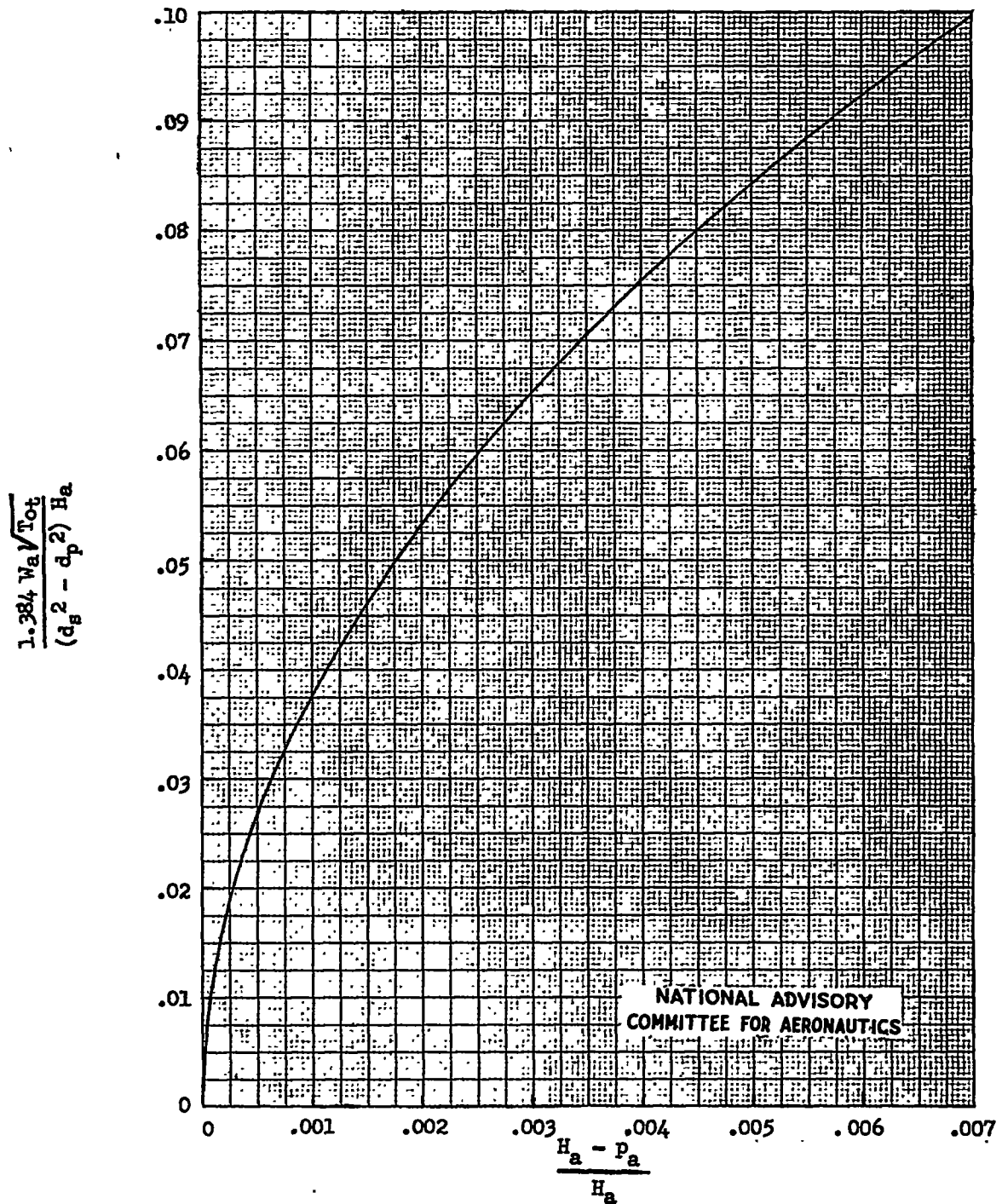
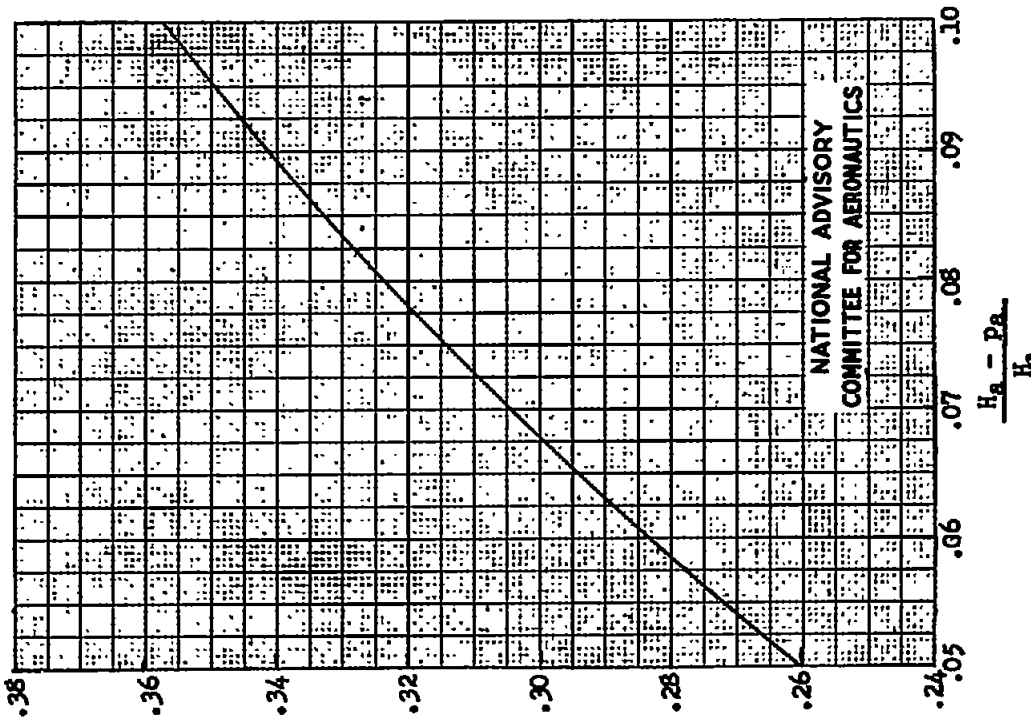


Figure 15.- Variation of the factor  $\phi$  with diameter ratio.

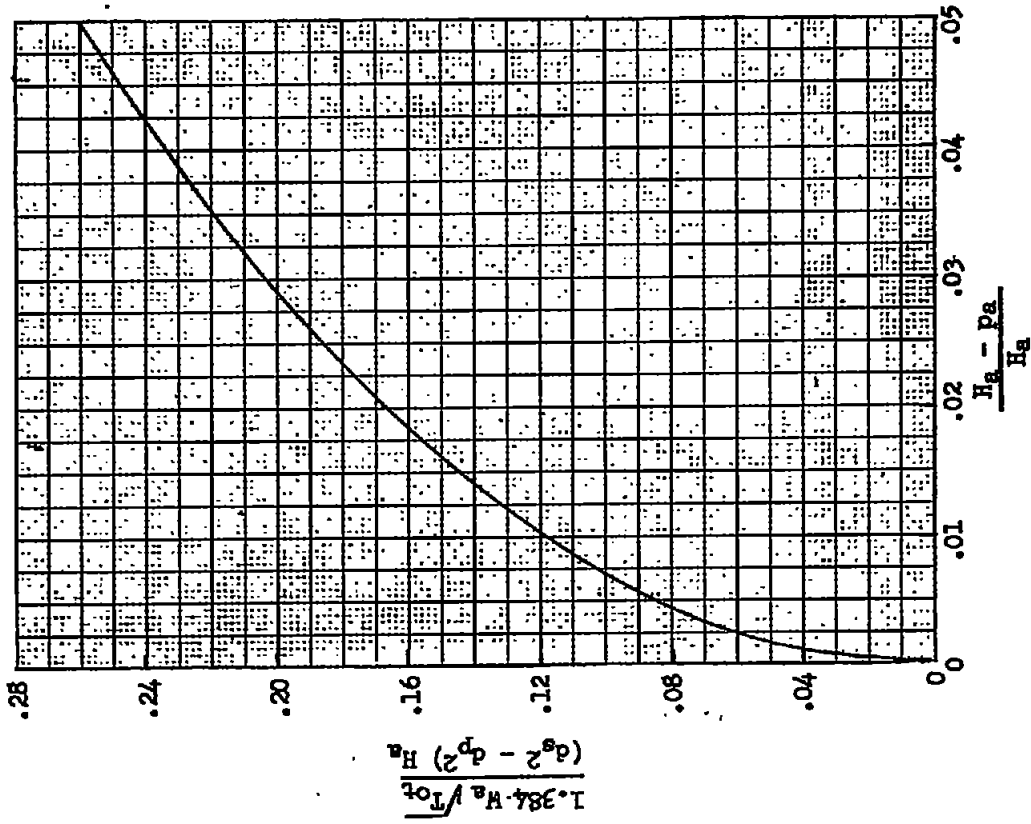


(a) Range of  $\frac{H_a - p_a}{H_a}$  from 0 to 0.007.

Figure 16.- Variation of the choke factor  $\frac{1.384 W_a \sqrt{T_{0t}}}{(d_s^2 - d_p^2) H_a}$  with  $\frac{H_a - p_a}{H_a}$ .

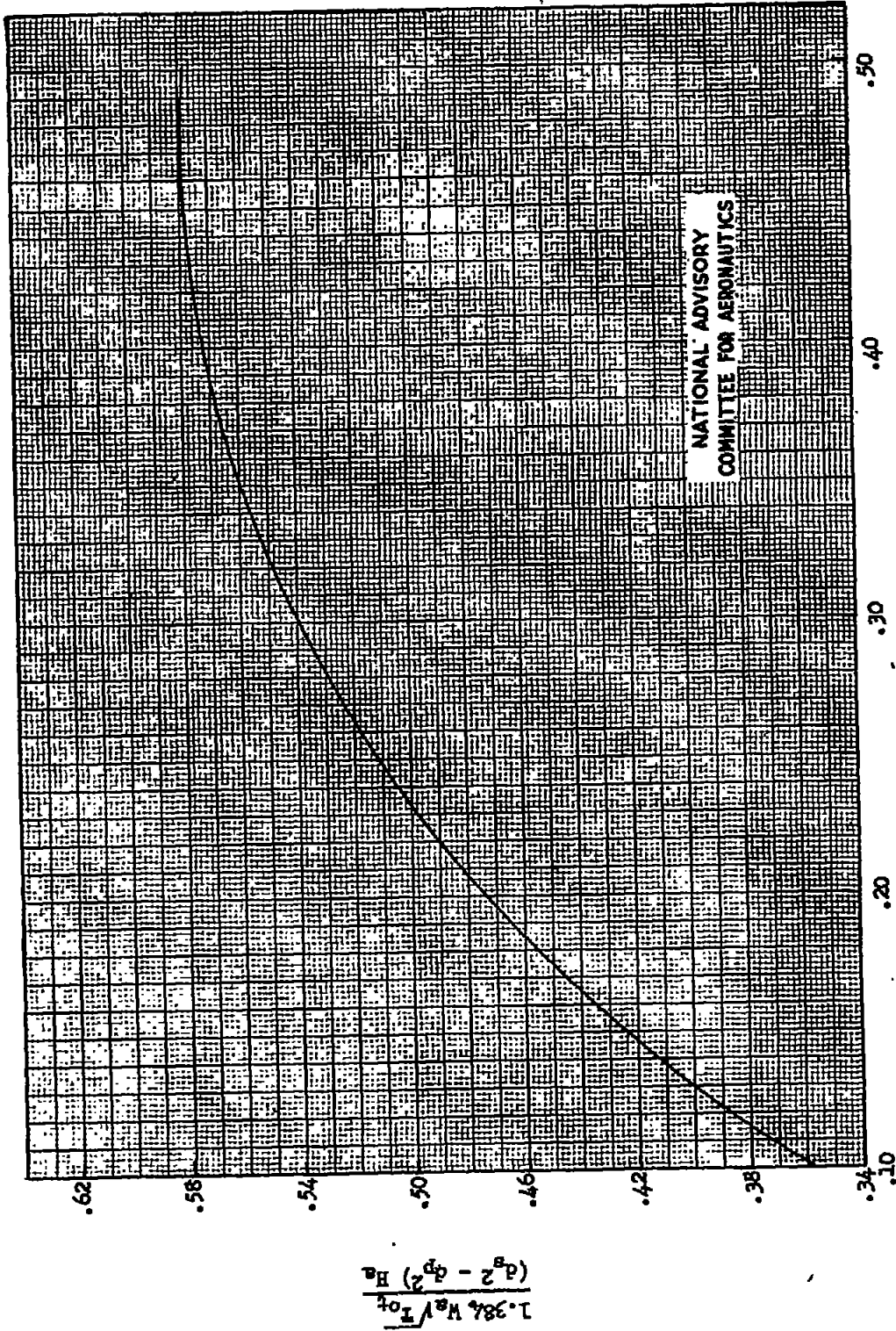


(c) Range of  $\frac{H_a - p_a}{H_a}$  from 0.05 to 0.10.



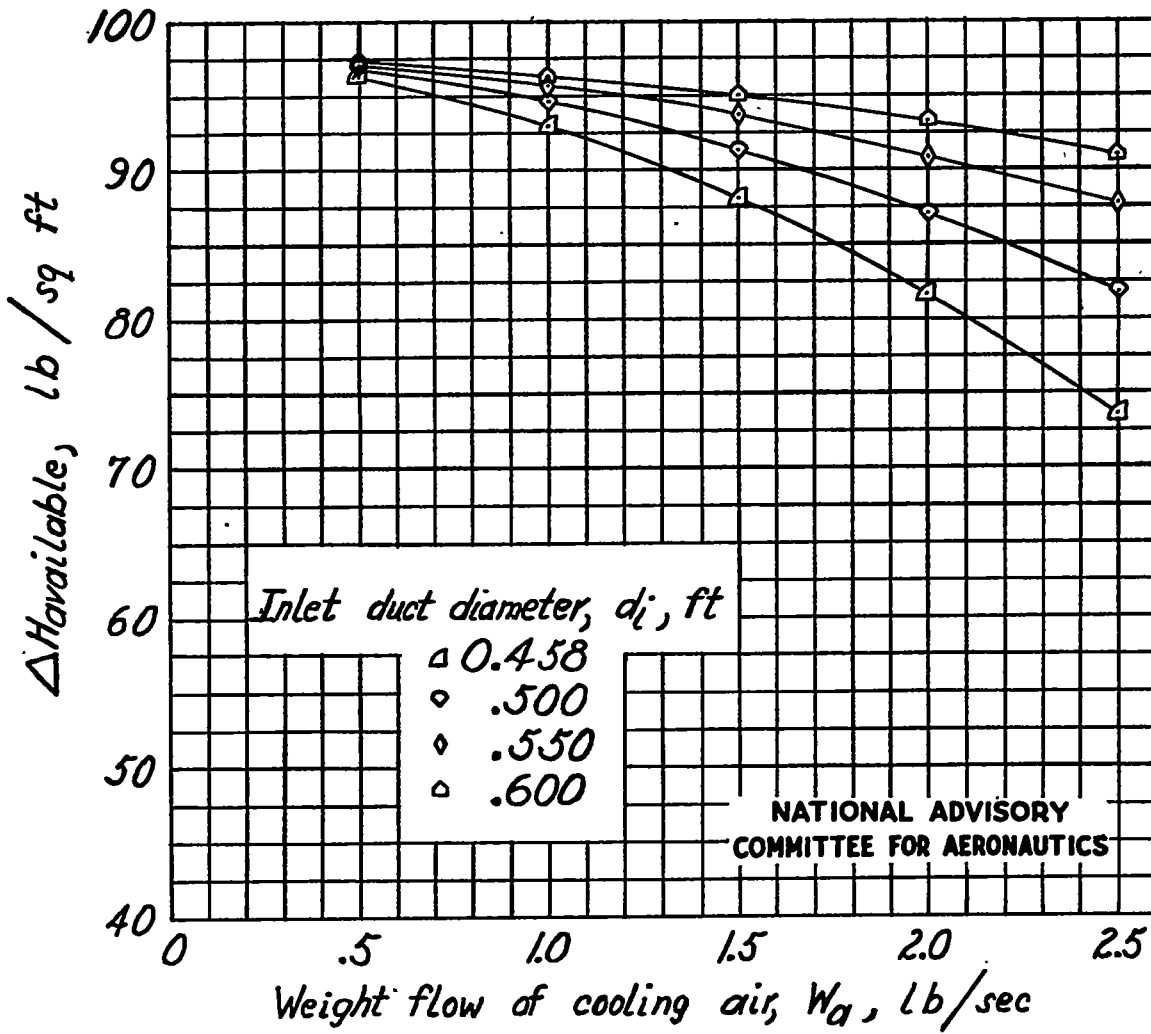
(b) Range of  $\frac{H_a - p_a}{H_a}$  from 0 to 0.05.

Figure 16.- Continued.



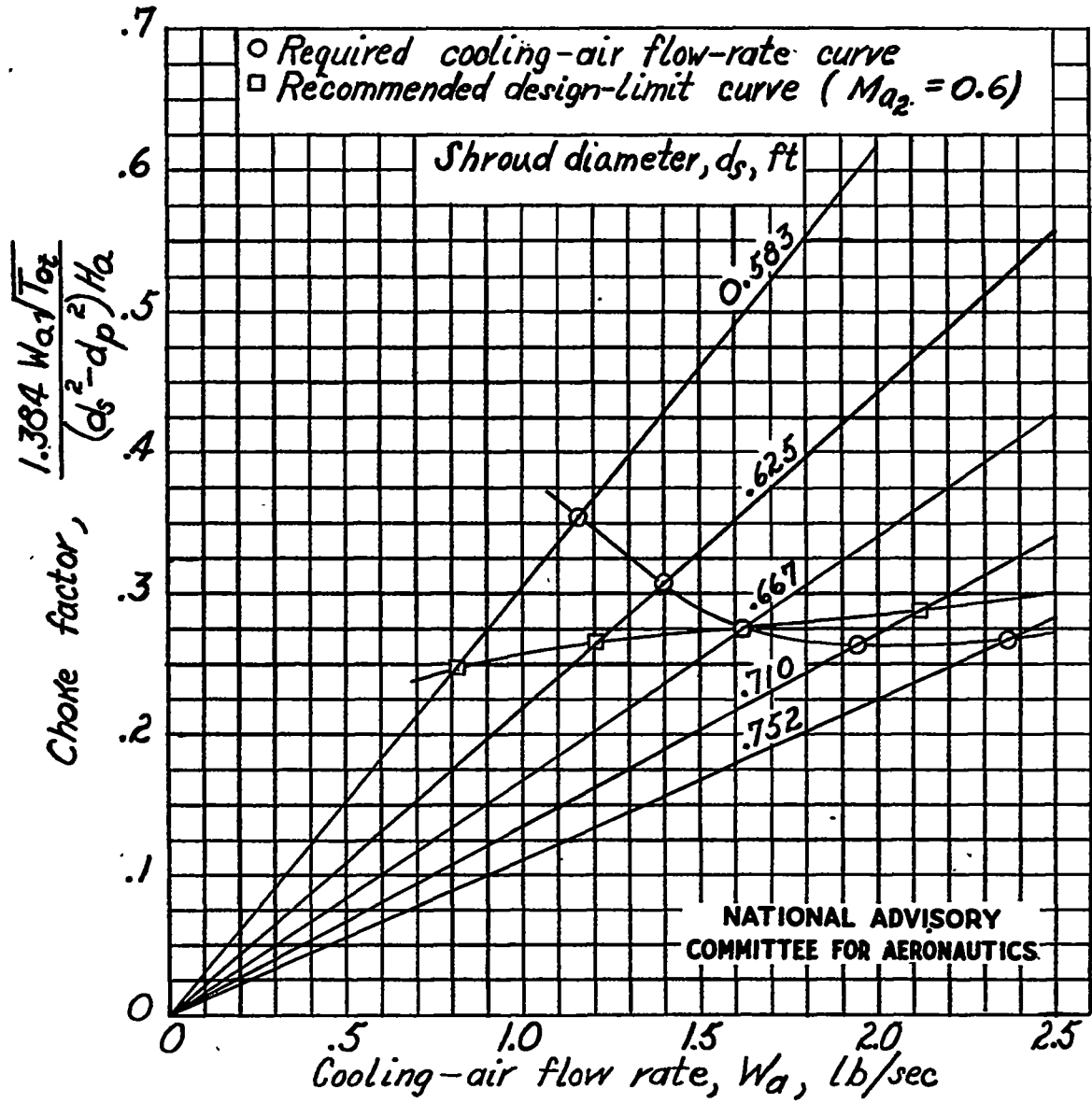
(d) Range of  $\frac{H_a - P_a}{H_a}$  from 0.10 to 0.50.

Figure 16.- Concluded.



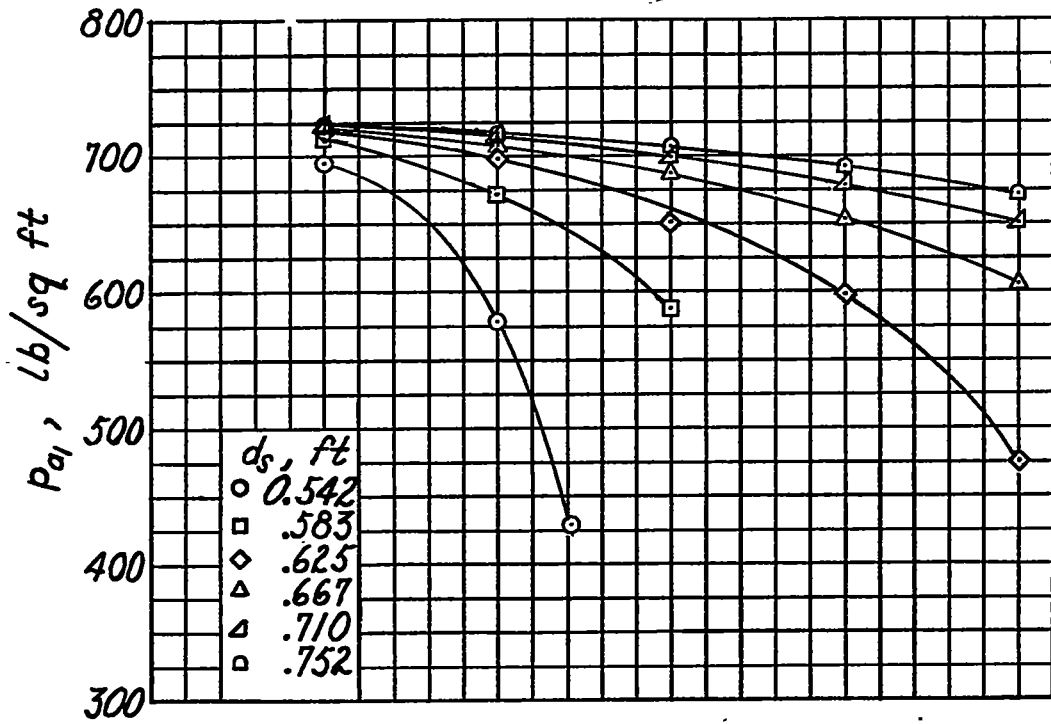
(a) Cooling-air pressure drop available at shroud entrance.

Figure 17.- Curves determined and used in the application of the design methods to the example.

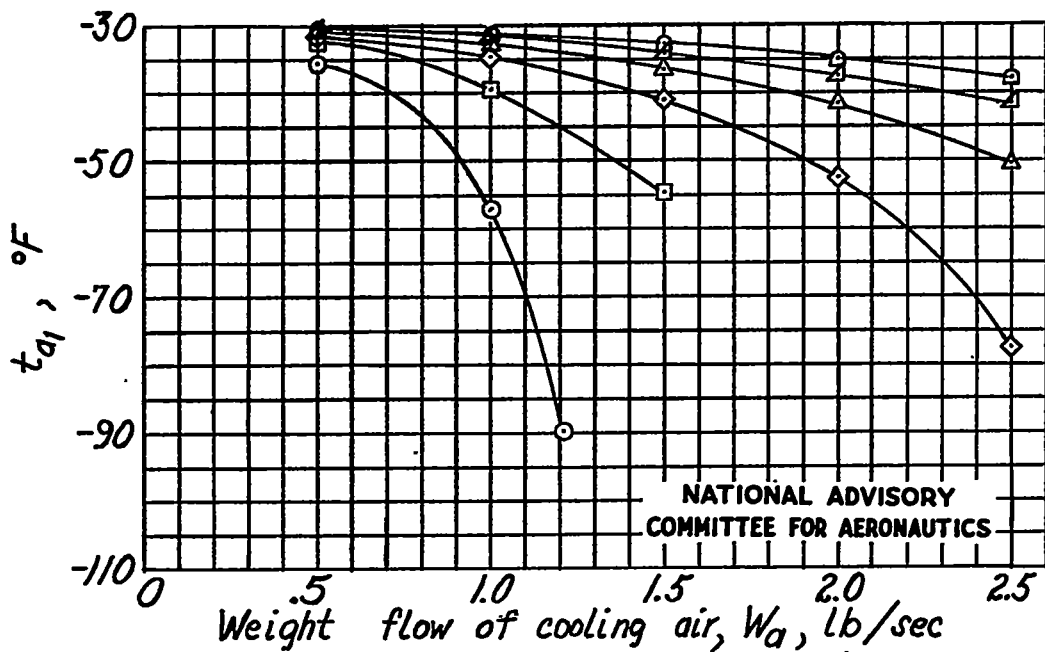


(b) Variation of choke factor with cooling-air flow rate.

Figure 17.- Continued.

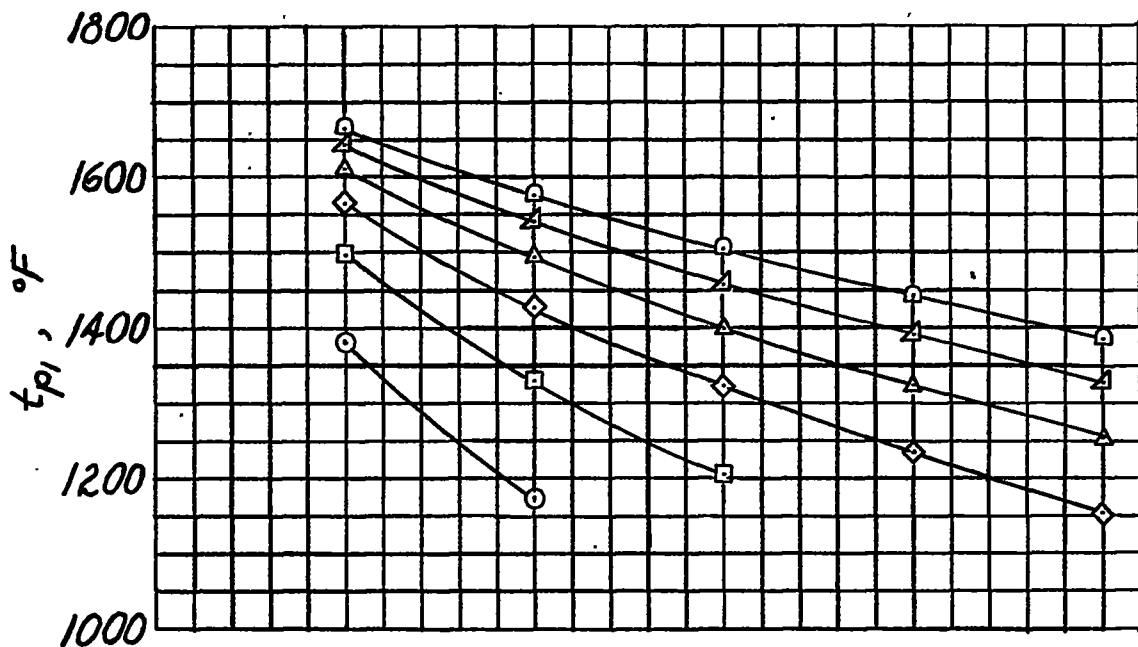


(c) Cooling-air static pressure at shroud entrance.

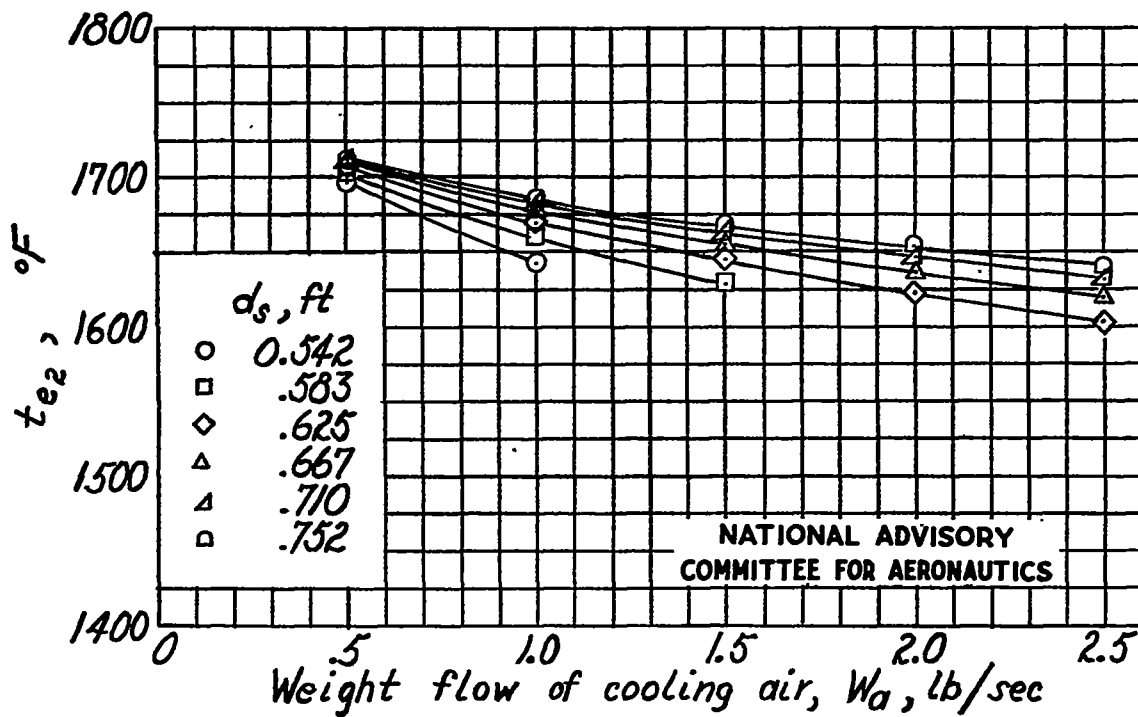


(d) Cooling-air temperature at shroud entrance.

Figure 17.- Continued.

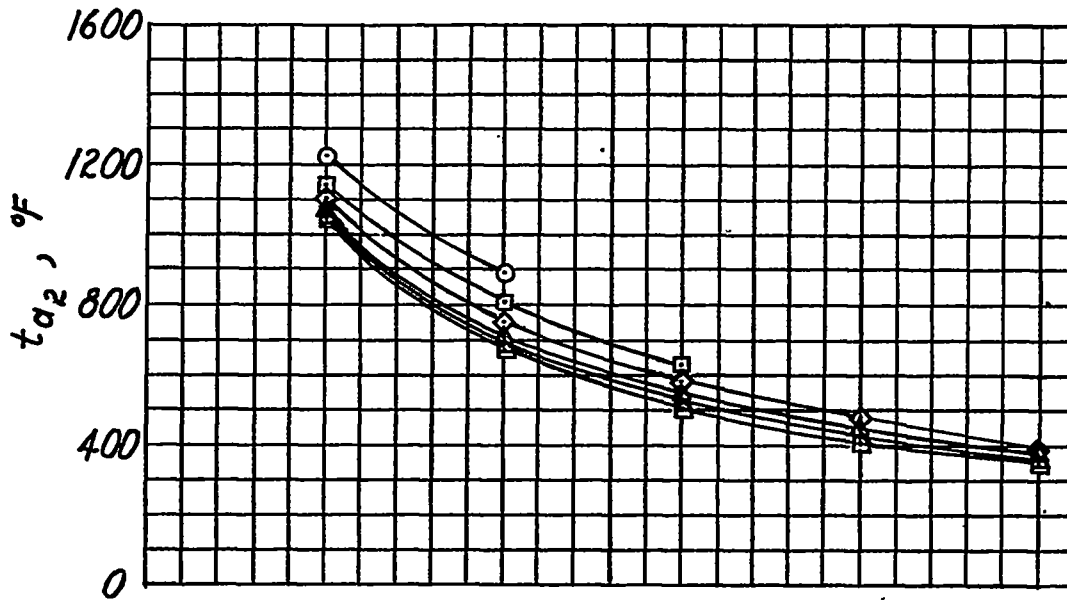


(e) Upstream exhaust-pipe temperature.

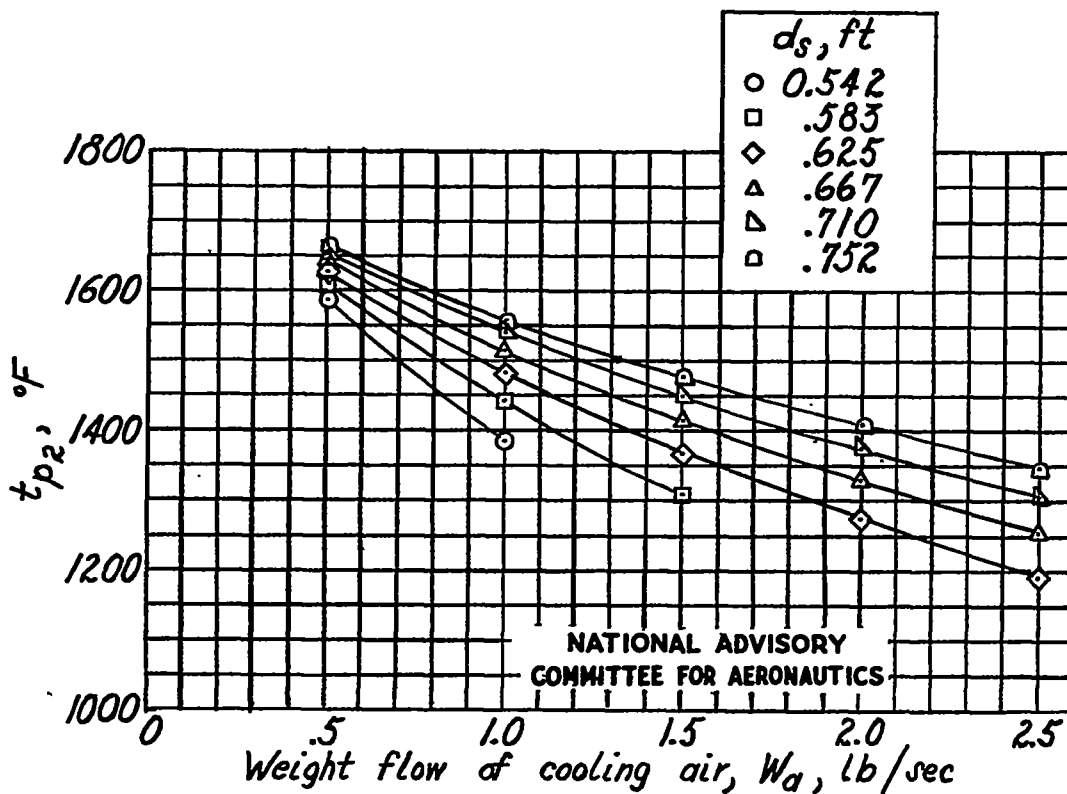


(f) Downstream exhaust-gas temperature.

Figure 17.- Continued.

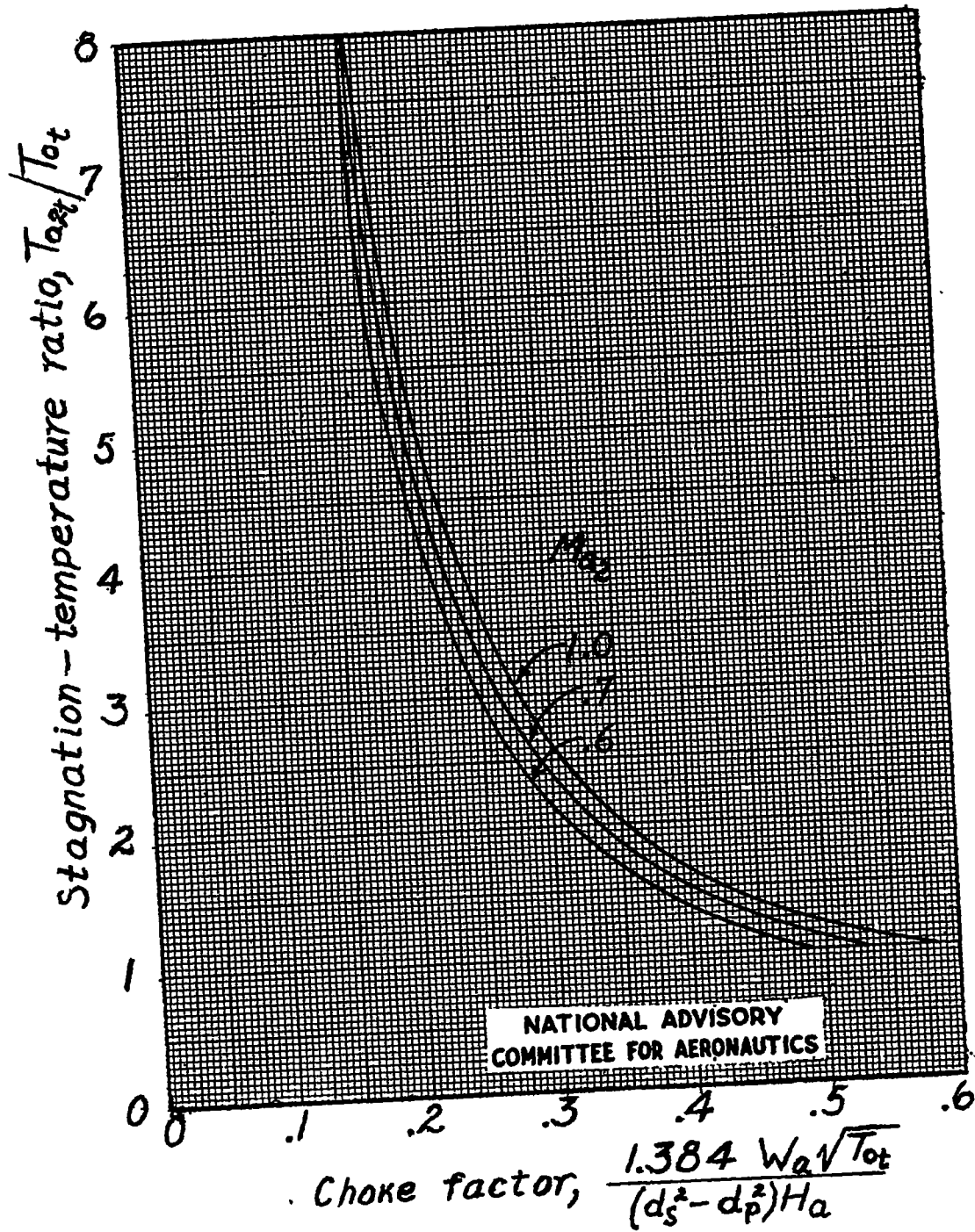


(g) Downstream cooling-air temperature.



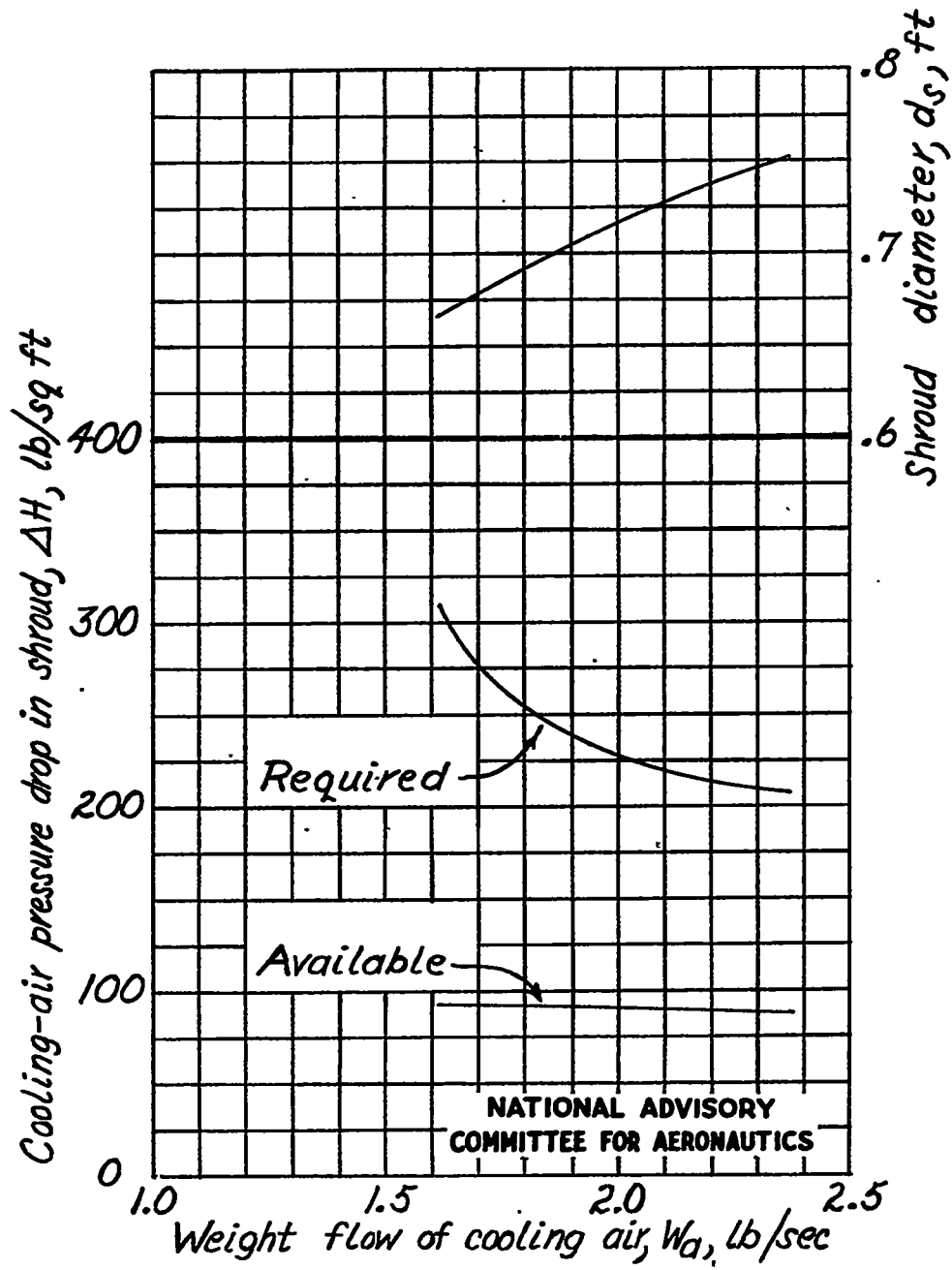
(h) Downstream exhaust-pipe temperature.

Figure 17.- Continued.



(i) Curve for determination of choke factor.

Figure 17.- Continued.



- (j) Cooling-air pressure drop required and available in shroud for required cooling.

Figure 17.- Concluded.

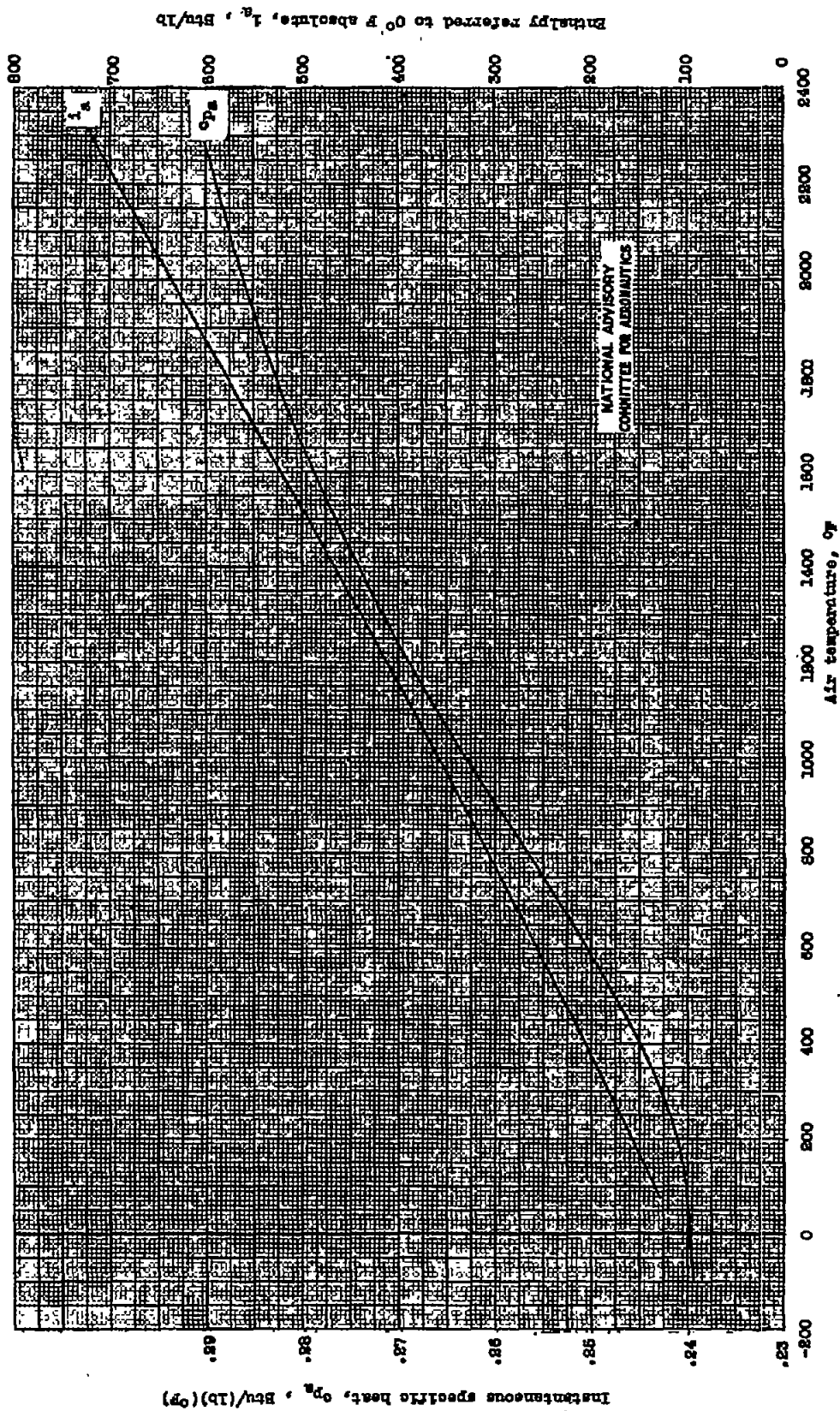


Figure 18.- Variation of instantaneous specific heat and enthalpy with air temperature.

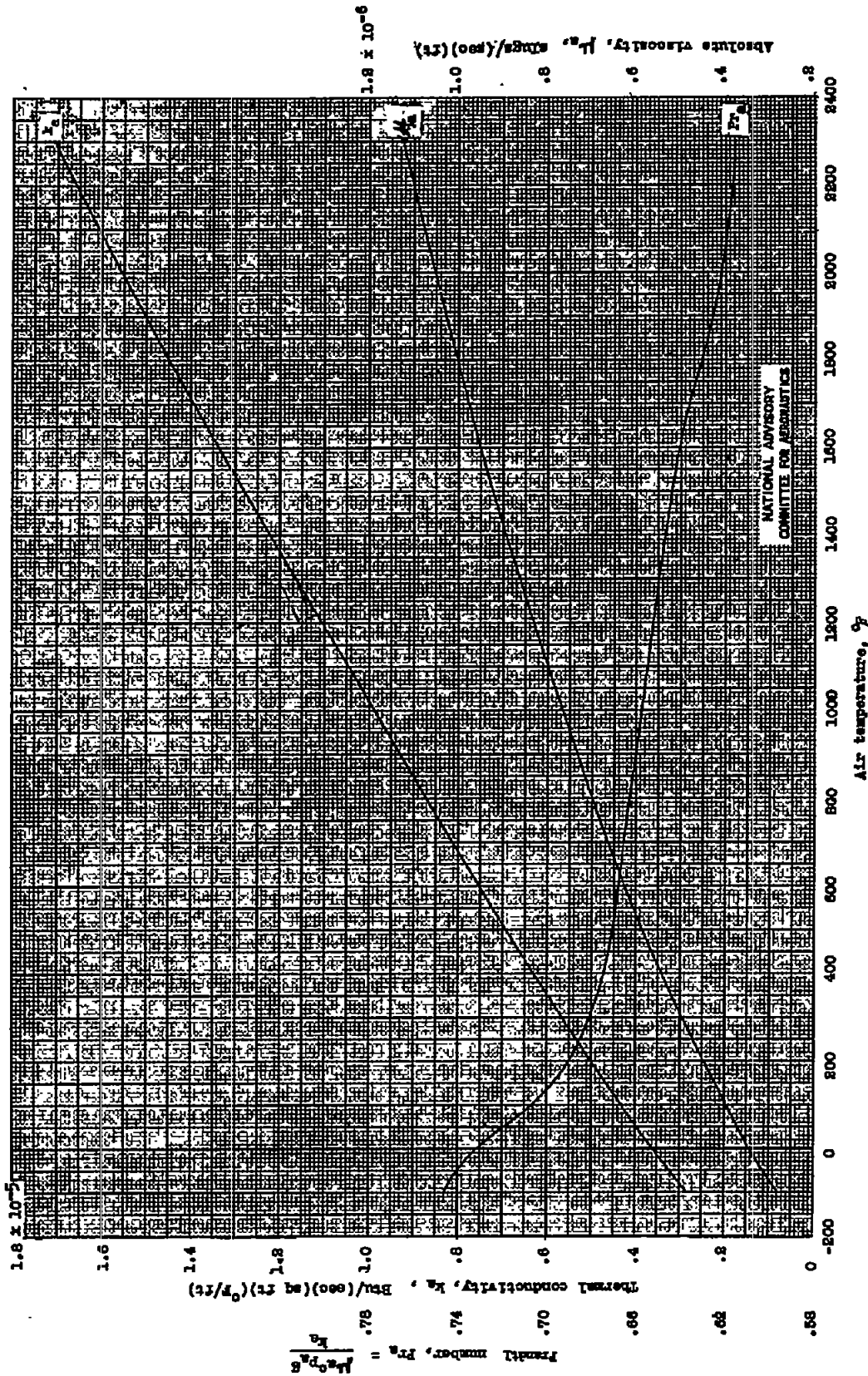


Figure 19.- Variation of thermal conductivity, Prandtl number, and absolute viscosity with air temperature.

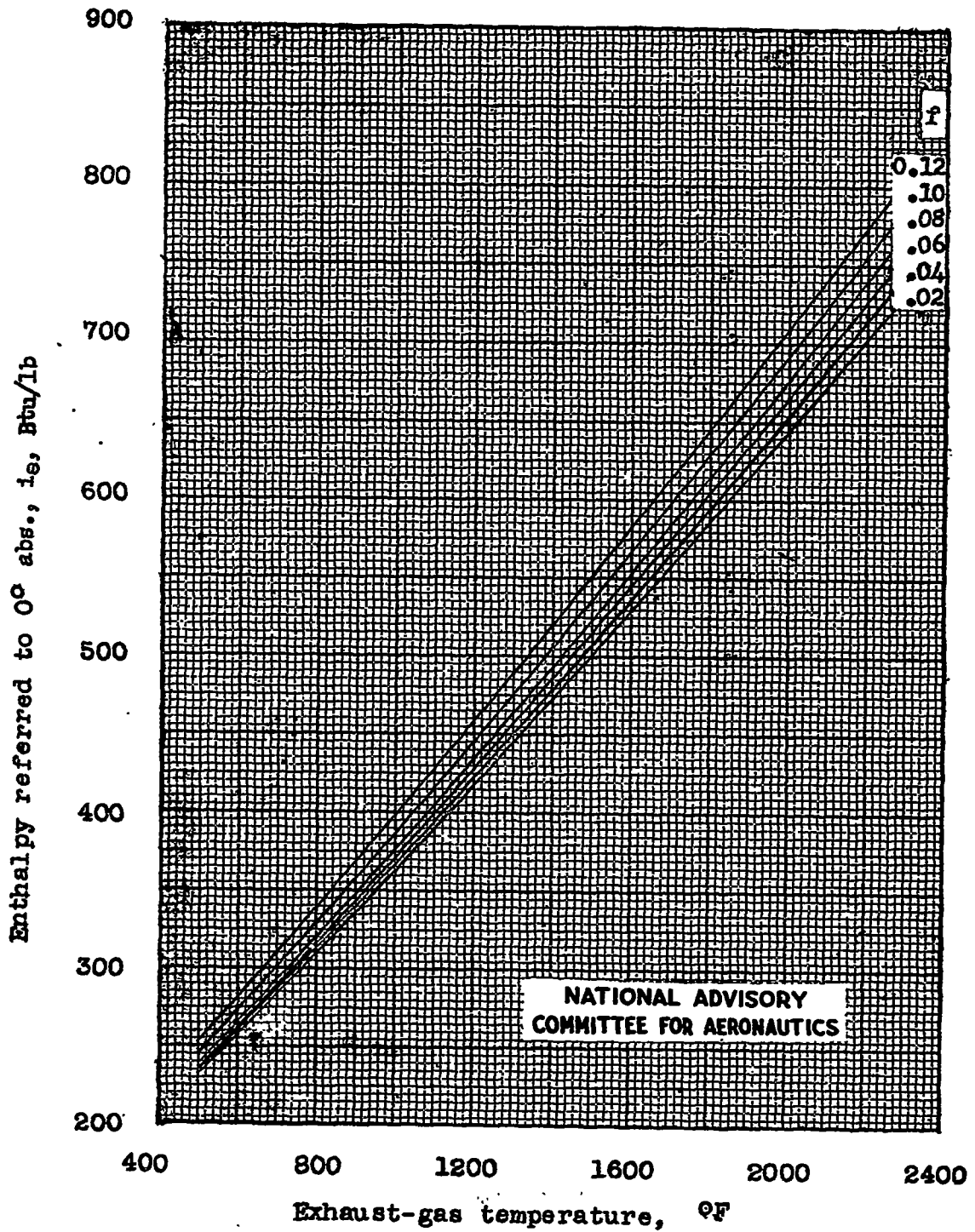
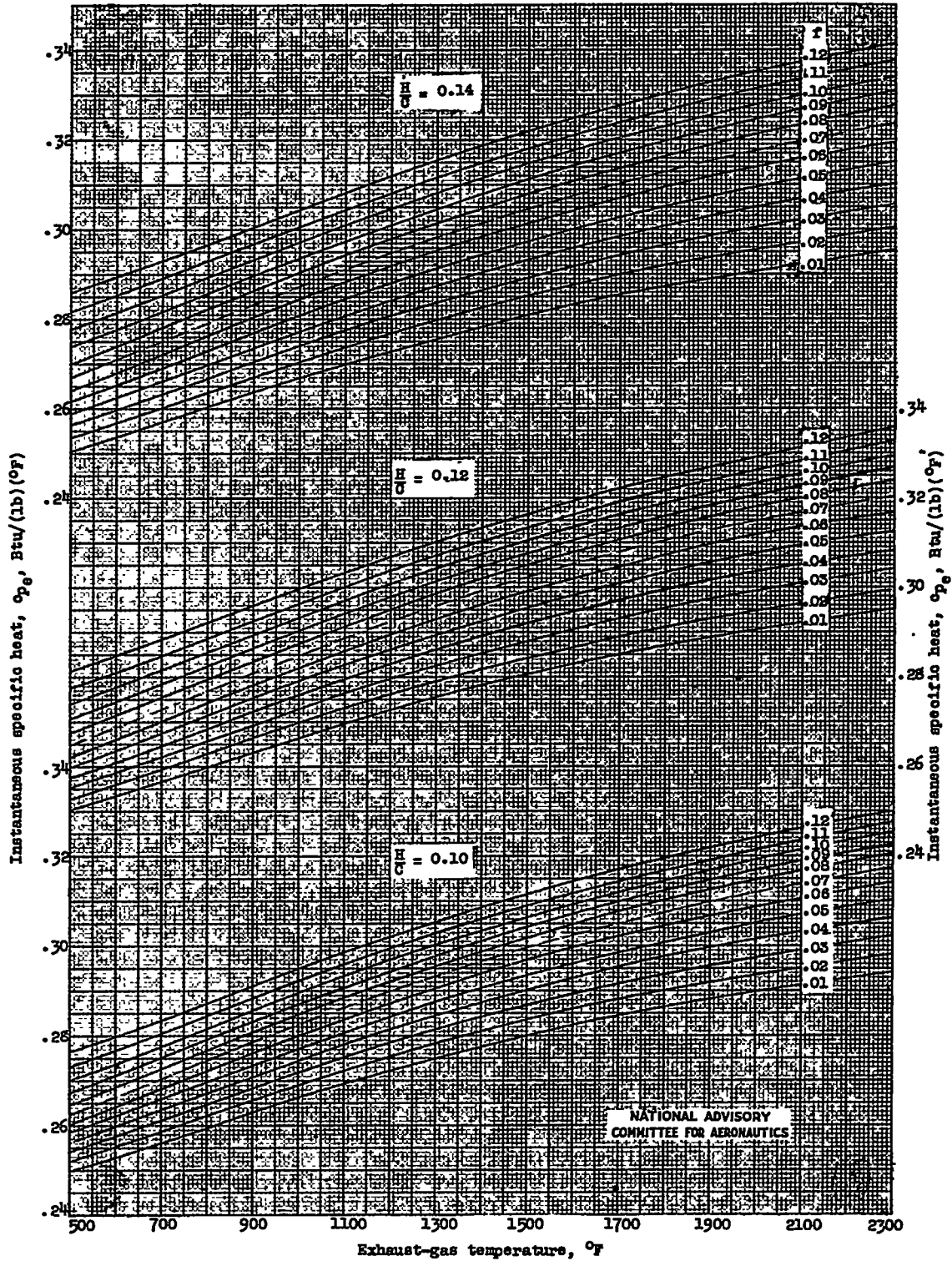
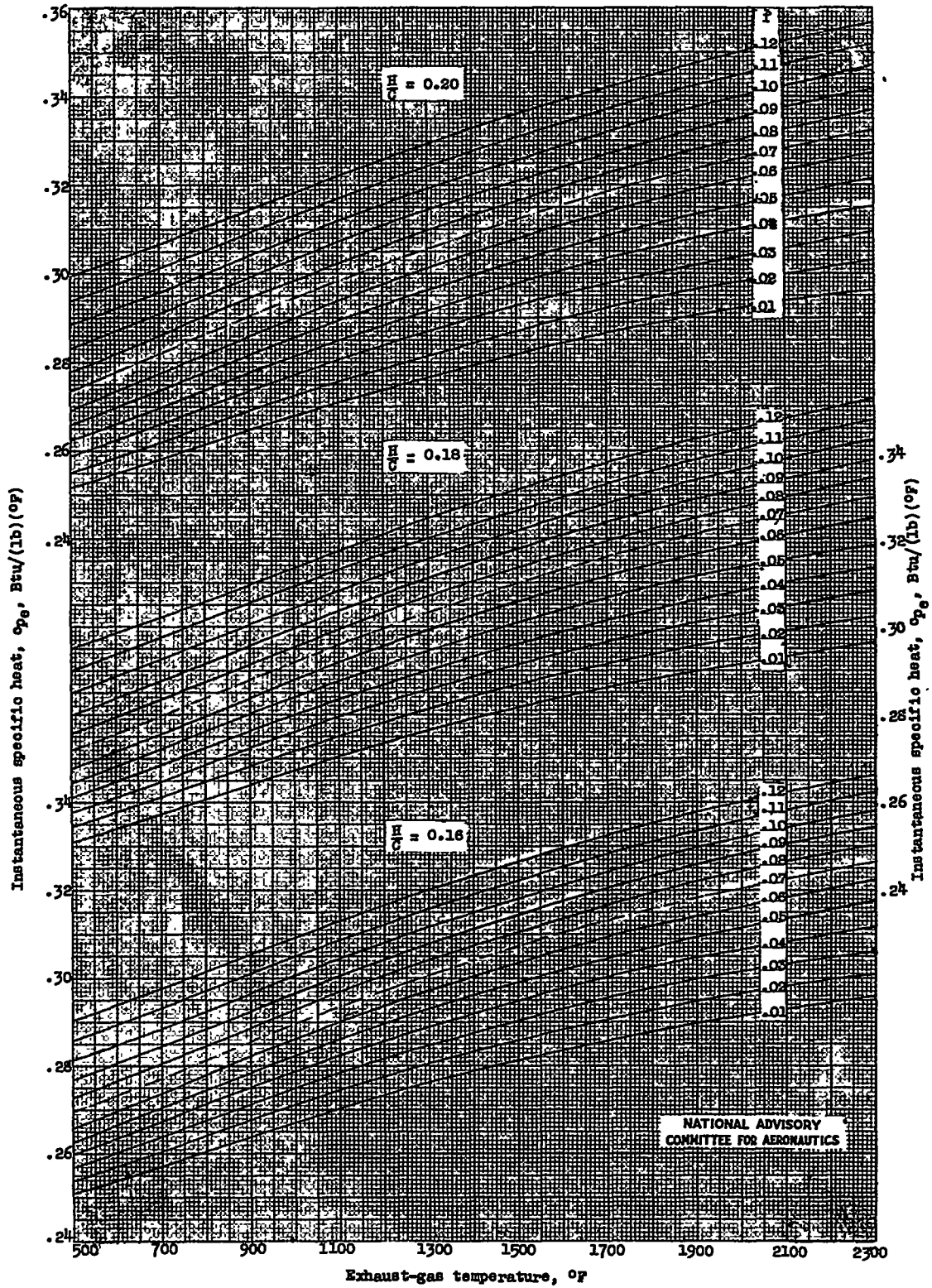


Figure 20.- Variation of enthalpy, referred to 0° absolute with exhaust-gas temperature for 0.10 hydrogen-carbon ratio.



(a) H/C : 0.10, 0.12, 0.14.

Figure 21.- Variation of instantaneous specific heat with exhaust-gas temperature for practical fuel-air and hydrogen-carbon ratios.



(b)  $H/C$  : 0.16, 0.18, 0.20.

Figure 21.- Concluded.

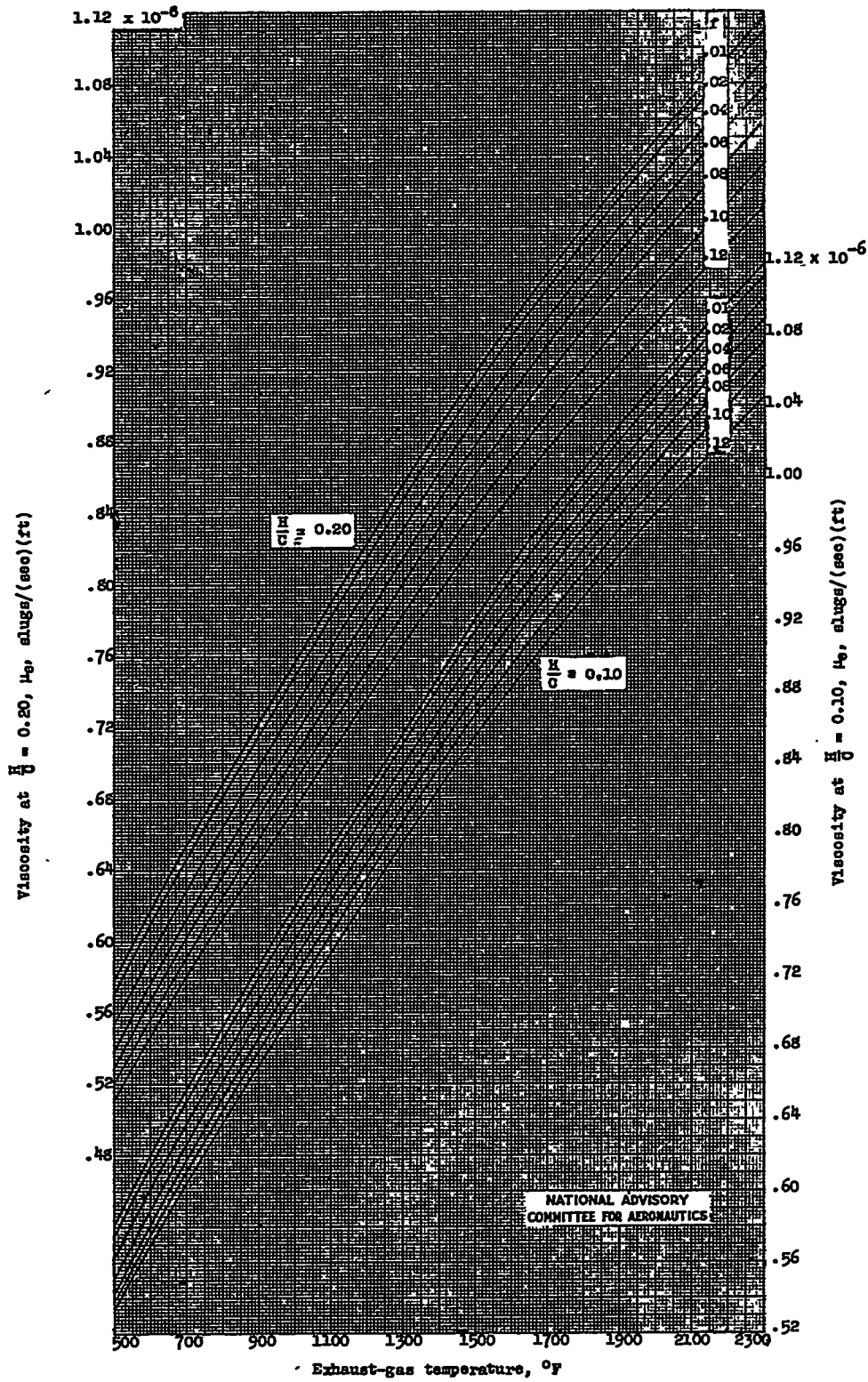
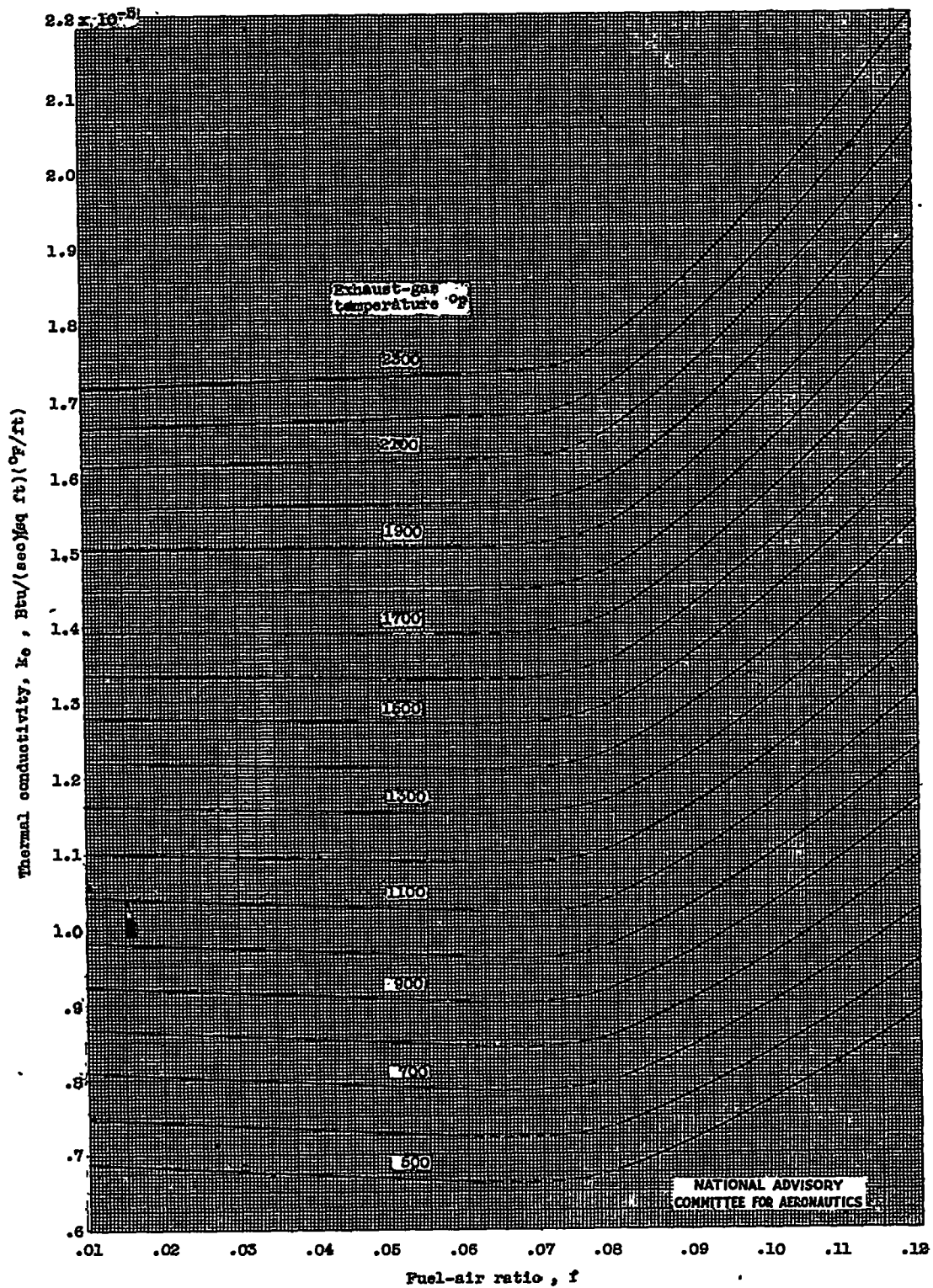
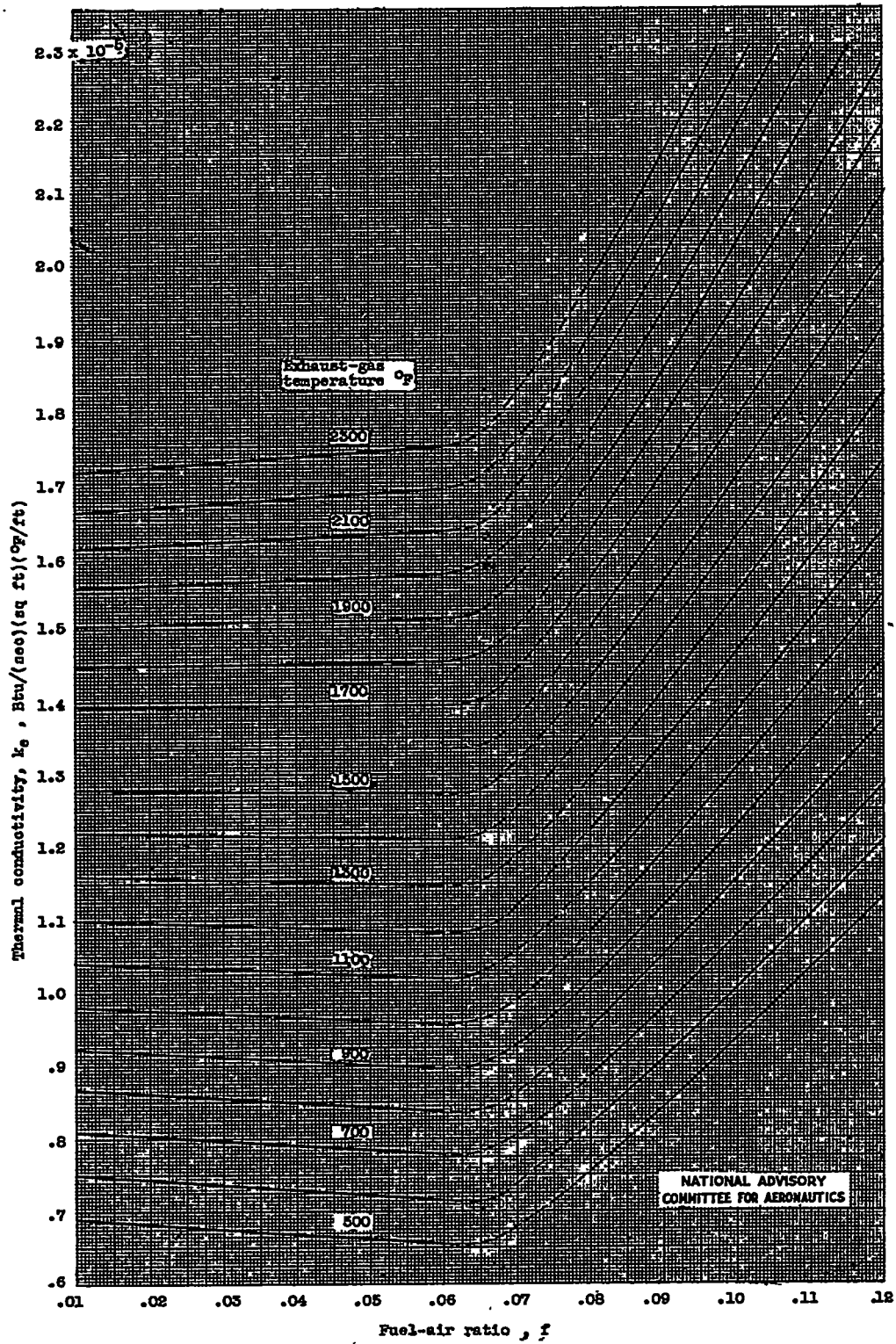


Figure 22.- Variation of exhaust-gas viscosity with temperature for 0.10 and 0.20 hydrogen-carbon ratios and various fuel-air ratios.



(a) H/C : 0.10.

Figure 23.- Variation of thermal conductivity with fuel-air ratio for various exhaust-gas temperatures.



(b) H/C : 0.20.

Figure 23.- Concluded.

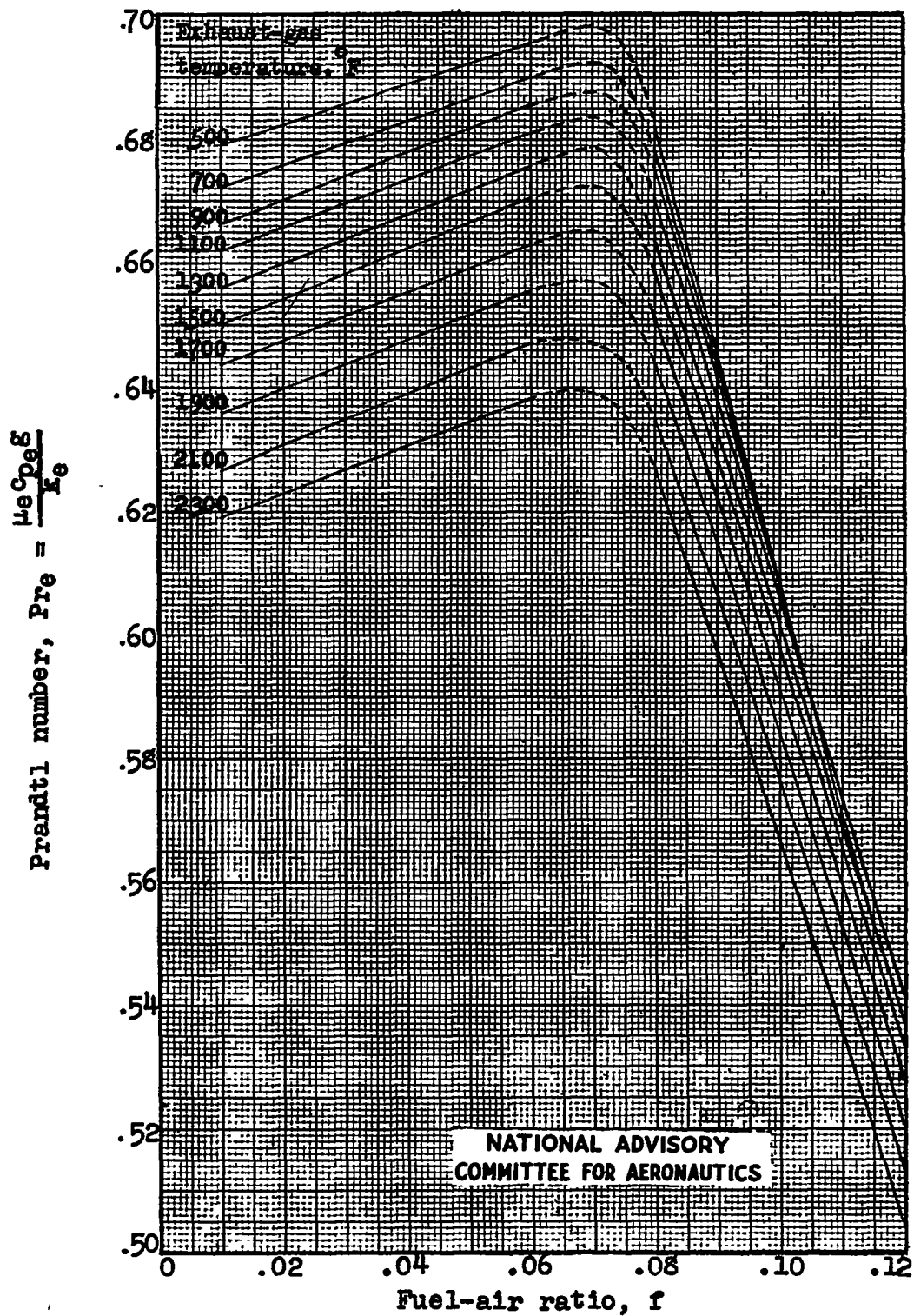


Figure 24.- Variation of Prandtl number with fuel-air ratio for various exhaust-gas temperatures and hydrogen-carbon ratio of 0.10.